THE INFLUENCE OF LOSS OF BOND ON THE FAILURE MECHANISM OF REINFORCED CONCRETE BEAMS

THE INFLUENCE OF LOSS OF BOND ON THE FAILURE MECHANISM OF REINFORCED CONCRETE BEAMS

By

HENRY H. H. HO, B.Sc.

A Thesis

Submitted to the Faculty of Graduate Studies

in Partial Fulfilment of the Requirements

for the Degree

Master of Engineering

McMaster University

May 1966

MASTER OF ENGINEERING (1966)
(Civil Engineering)

McMASTER UNIVERSITY
Hamilton, Ontario

TITLE: The Influence of Loss of Bond on the Failure Mechanism of Reinforced Concrete Beams.

AUTHOR: Henry H. H. Ho, B.Sc. (Oklahoma State University)

SUPERVISOR: Dr. H. Robinson

NUMBER OF PAGES: ix, 99

SCOPE AND CONTENTS: Consideration of the reinforced concrete beam as a composite beam with incomplete interaction, the effect of the principal strains in the shear span is studied. The influence of bond slip on the formation of cracks is studied both analytically and experimentally.

ACKNOWLEDGEMENTS

The author wishes to express sincere gratitude to Dr. H. Robinson for his advice and encouragement throughout the course of this study.

Thanks are also due to the National Research Council for financial support.

TABLE OF CONTENTS

List of Figures

List of Tables

CHAPTER 1

Introduction

1.1 Introduction

A beam composed of a concrete slab and a steel I-beam inter-connected by shear connectors in such a manner that they act as a unit is a well defined composite member. By the same analogy, a reinforced concrete beam consisting of a rectangular concrete section and reinforcing steel which act together through the inter-connection of bond can be considered as a composite member with incomplete interaction, a deviation from the conventional concept.

In the light of his investigation Robinson[1] suggested that a reinforced concrete beam may well be considered as a composite beam with incomplete interaction. He further illustrated that owing to the influence of breakdown of interaction in a reinforced concrete beam, a reduction in mid-height strain and an increase in the lower strain along reinforcement would result. A reduction in mid-height strain has been observed experimentally by Plowman[2]. By considering the reinforced concrete beam as a composite beam with incomplete interaction, it is hoped that a rational explanation of the occurrence of the diagonal cracking in the shear span, can be achieved.

1.2 Literature Survey

The so-called "shear-failure" in reinforced concrete beams has been an intriguing problem. In the early 1900's, the widely-used nominal shearing stress equation $v = \frac{V}{bjd}$ had been developed by Morsch. He further explained and argued that shear failure in beams was due to diagonal tension, not horizontal shear.

With the acceptance of Morsch's proposed tensile phenomenon, design specifications were adopted in the United States. This nominal shearing stress, related to the cylinder strength of concrete, was considered to be a measure of the diagonal tension in reinforced concrete beams. Talbot[3], however, as early as1909 suggested that the value of nominal shearing stress would vary with the amount of reinforcement, the length-to-depth ratio and other factors which affect the stiffness of the beam.

Since 1950, after Clark[3] introduced Talbot's notion by a mathematical equation which involves variables such as percentage of reinforcement, length-to depth ratio and concrete strength, research workers have attempted to explore the failure mechanism of reinforced concrete members in this respect.

In recent years, the research group at the University of Illinois[4] reported significant contributions to the so-called "shear-failure" problem. They described diagonal tension failure as diagonal tension cracking, followed by a redistribution of internal stresses, usually associated with increasing load and with a final failure in

bending under special conditions that have been termed as a shear-compression failure.

Although there is a trend to design for bending according to the ultimate load method, the working stress design is still used for shear. For this reason it is an urgent necessity to estimate the shear failure load more precisely, as for bending. The subject of shear failure of reinforced concrete beams has drawn the attention of many research workers.

The ACI-ASCE Committee 326[3,5] reported the investigations into this unsolved problem over the last 50 years, and proposed a new empirical design procedure. They indicated that the problems of shear and diagonal tension have not been fundamentally and conclusively solved and further research work is encouraged for the establishing of a more rational theory to describe the effects of shear and diagonal tension on the behaviour of reinforced concrete members.

Kani[6] in his paper "The Mechanism of the so-called Shear Failure" used the "concrete teeth" concept to explain the mechanism of failure and suggested that the so-called shear failure is a problem of diagonal compression failure, a deviation from earlier diagonal tension failure concept. In his next paper "The Riddle of Shear Failure and Its Solution",[7] he further emphasized the process of transformation of a reinforced concrete beam into a tied arch due to redistribution of internal stresses, to explain the mechanism of shear and diagonal failure.

Leonhardt and Walther[8] pointed out that for failure of the concrete, the principal tensile stresses govern the crack formation of the brittle concrete. These principal tensile stresses depend on the combination of moment and shear force, and the shear stress is neither decisive for the crack formation nor for the carrying capacity.

Ferguson[4] described the failure pattern in terms of the conventional theory of combined stresses. He further emphasized the possibility of applying the theory of combined stresses more constructively in connection with diagonal tension so that a more rational solution could be attained.

It has been well known that diagonal tension is a combined stress problem. The location and inclination of diagonal tension cracks indicate that the principal tensile stress exceeds the tensile strength of the concrete. However, by using the principal stress equation:

$$\tau_{1,2} = \frac{\sigma_x}{2} \pm \sqrt{\left(\frac{\sigma_x}{2}\right)^2 + \tau_{xy}^2} \qquad (1\text{-}1)$$

difficulties arise in expressing both the bending stress and the shear stress in reinforced concrete members. Owing to cracks occurring in the tensile zone, there will be a redistribution of interior stresses, at different sections, that depend on the crack pattern, the tensile reinforcement and the condition of loading. Without knowing the redistribution of these internal stresses, any theoretical treatment of this problem is a rough approximation. The analysis is thus limited to a certain extent.

In his preliminary investigation on composite beams having a cellular zone between the concrete slab and steel I-beam, Robinson[1,9] discovered that in spite of the fact that there was no distinct interfacial plane between the concrete slab and the steel beam, the strain distribution at any section had been observed to be essentially linear in the elastic range. He further suggested that the total slip between the concrete slab and the steel beam could be considered to consist of an interfacial slip between the lower part of the cellular zone and the steel beam and a larger slip, particularly after cracking, due to the rotation of the concrete ribs formed by the cells. This could be considered to be analogous to the rotation of the cantilever or teeth referred to by Moe[10] and Kani[7].

Wong[11] in his analytical study stated that in spite of the fact that a cracked reinforced concrete beam does not have a distinct interfacial plane between concrete and steel, through a slight modification of the approach taken by Newmark for a conventional composite beam[12], the theory can still by applied to a reinforced concrete beam provided a pseudo-interface is assumed. The application of the modified theory to the reinforced concrete beam enabled the computation of potential crack profiles which were inclined upward towards the load point. Furthermore, the estimated slip and strain variation along the tensile steel for incomplete interaction had characteristics which were qualitatively similar to those observed by

Evans and Robinson[14], and Manning[13]. The results indicated that reinforced concrete beams may well be considered as composite beams with incomplete interaction.

1.3 Objective and Extent of Investigation

The primary objectives of this investigation is to study analytically, the strain pattern and strain trajectories in the shear span of a reinforced concrete beam subjected to a two point load. Through preliminary investigation, the modified Newmark composite beam solution was used to estimate the bending strain and shear strain redistribution in an uncracked beam. The conventional combined strain equation was used to calculate the principal strains and their directions so that strain trajectories could be constructed, and their effects on the diagonal crack studied. After observation that the strain trajectories did not lead to further clarification of the problem, the investigation was extended to the study of visible crack profiles for an assumed cracking strain. The visible crack profile in a reinforced concrete beam subjected to various degrees of breakdown of interaction was studied. Furthermore, different degrees of interaction at the locations of two major cracks occurring in the shear span as well as its variation in between were assumed. The estimated steel strain and slip distributions were qualitatively compared with the measured values of other research workers.

An extension of the studies made by Wong[11] were carried out. The degree of interaction is dependent upon the load-slip characteristics of the connection, which in this case is considered to be the connection between the concrete and the steel reinforcement. An attempt was made to study the effect of various degrees of interaction determined from experimentally obtained load-slip characteristics. These characteristic curves were those obtained by Mathey and Watstein[15].

Finally, three series of test beams are reported. The primary objectives of these tests were to investigate the cracking profiles of reinforced concrete beams through the influences of varying bond quality in the reinforcement. Results are discussed and compared.

CHAPTER 2

Estimation of the Principal Strains in a Reinforced Concrete Beam

After reanalysis and further experiments by investigators, it is believed that the diagonal tension cracks lead to the ultimate diagonal tension failure. As these diagonal cracks cause the failure of members subjected to combined flexure and shear, it is reasonable to use the principal stress equation (1-1), to compute the principal tensile and compressive stresses. Many investigators have attempted to use this fundamental formula before. No successful results have been achieved owing to the complication of stress redistribution after cracking.

Robinson[1,9] in his investigation suggested that reinforced concrete beams may well be considered as composite beams with incomplete interaction.

Wong's[11] analytical work demonstrates the validity in this respect. During his investigation, the Newmark composite beam theory with slight modification was used to furnish an estimated crack profile for both complete and incomplete interaction. This provides a more reasonable approximation of both flexural and shear stresses after cracking.

On the basis of this speculation, it is of interest to investigate the shear stress redistribution after the reinforced concrete beam subjected to two point load starts to crack.

Figure (2-1) shows the loaded beam, the conventional shear diagram and the shearing stress distribution for a plain concrete beam. In the shear span, the vertical shear transmitted at any section should balance the externally applied load. Since there is no vertical shear inside the pure moment region, the resulting shearing stress distribution should be zero at any section.

The shear stress distribution for a cracked reinforced concrete beam subjected to pure bending has been determined by Broms[16] from equilibrium considerations of free body elements at a number of locations along the beam. These shearing stresses occurred because cracks cause different sections to have different depths. Figure (2-2) shows schematically the determination of shear stress and its distribution in the pure moment region. It indicates that the total net shear force at any section within the pure moment region is equal to zero.

The same approach is applied in analysing the shear stress distribution in the shear span. Owing to the influence of the bending cracks, it is assumed that the shear stresses are limited to the compression zone. The distribution of shear stress at different sections in the remaining compression zone is estimated as described and is shown in fiugre (2-3). By rough approximation, it is noted that the vertical shear stress resultant transmitted along the remaining uncracked sections varies. The magnitude of this shear stress resultant is much less than the externally applied shear and increases along sections away from the

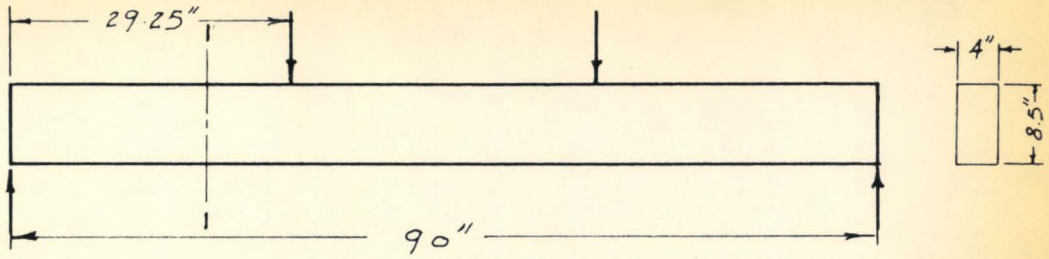

Loading Position

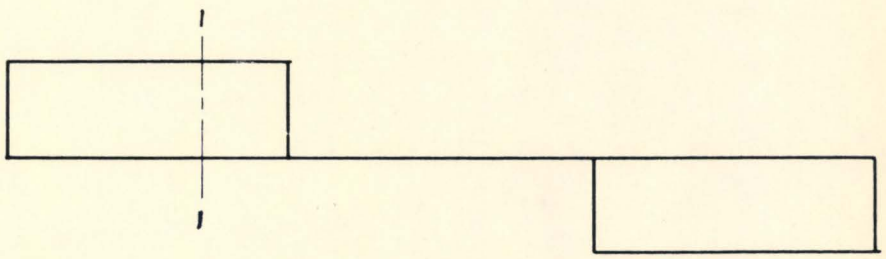

Shear Diagram

Shear Stress
at section I-I

Figure 2.1

Conventional Shear Diagram and Shear Stress Diagram

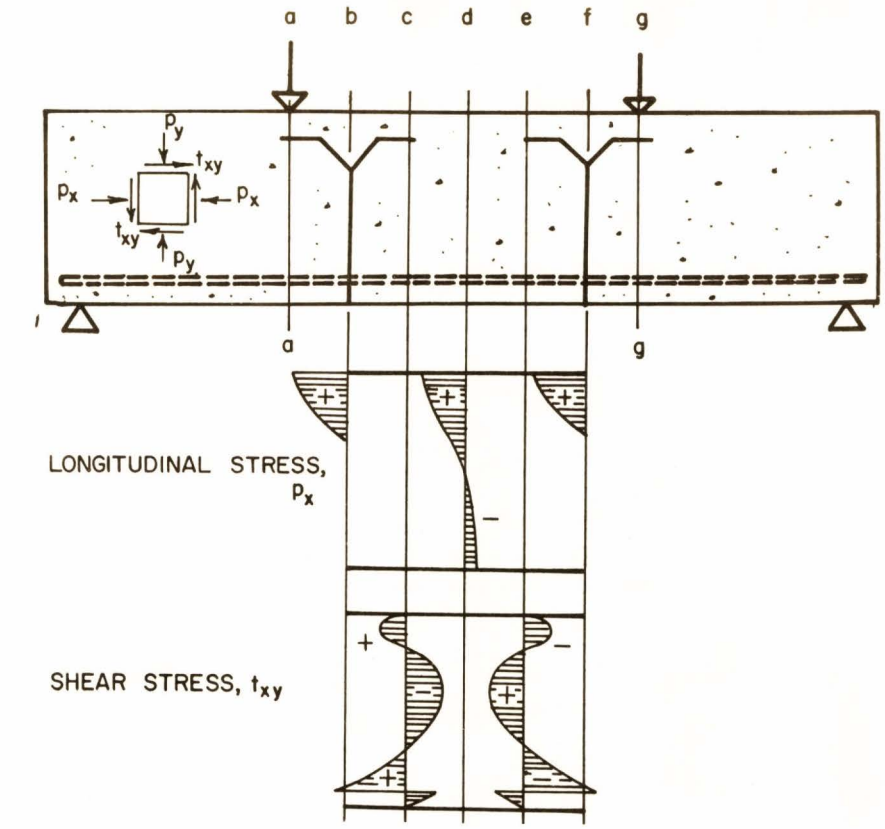

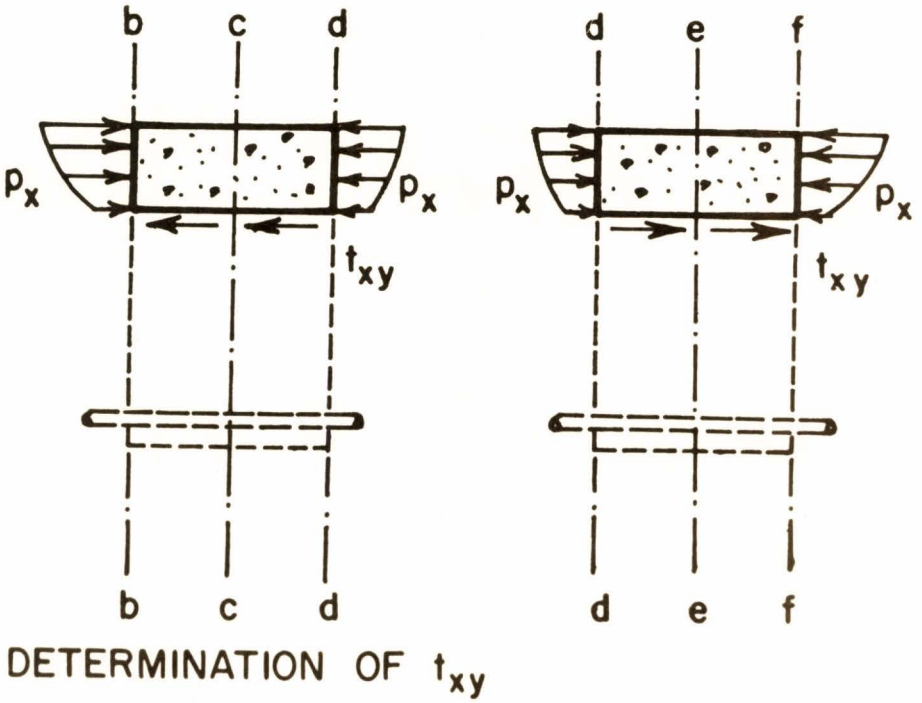

Figure 2.2

Stress Distribution Between Load Points (due to Broms)

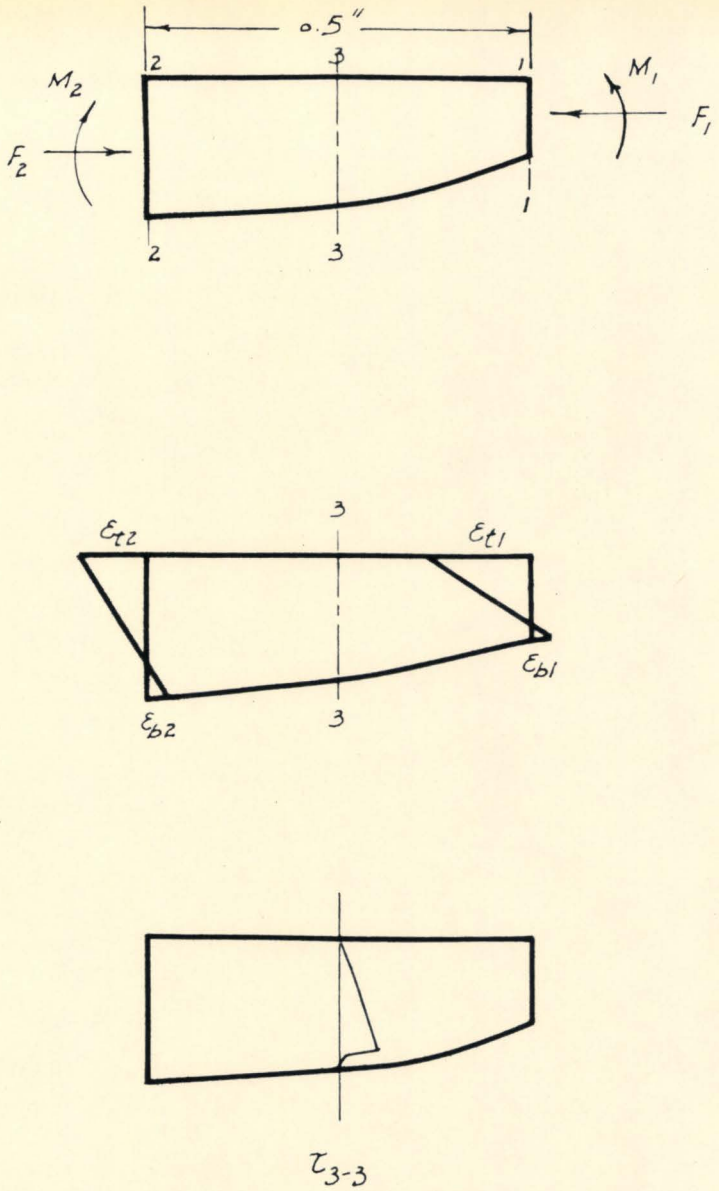

Figure 2.3

Strain Distribution at Two Sections and the Estimated Shearing Stress Distribution at the Section in Between

load points. In other words, for a section close to the load point where the largest crack height, crack width and slip are likely to occur, the vertical shear transmitted in the remaining uncracked section is about 15 percent of the total externally applied shear. And for a section away from the load point near to extremity of the cracked zone, the shear transmitted in the uncracked section is about 19 percent of the total shear. The only reasonable explanation to offset the remaining vertical shear force is the possible dowel effect as described by a number of investigators[10,17,18]. Moe[10] in his development of the vertical cantilever theory, suggested that shear forces are transferred by the interlocking of grains in the concrete across the flexural cracks and possibly includes some dowel effects. According to Moe, the shear force allotted to the cracked zone in the shear span may be as high as 70 percent of the total shear. He further predicted that the amount of shear transmission across the flexural cracks decreases gradually as the widths of the cracks increase, and said that the amount of shearing stresses in the uncracked section increases accordingly. The estimated shear forces attributed to the remaining uncracked sections were found to have a different distribution from those assumed by Moe. At design load, the uncracked section close to the load point carries about 15 percent of the total shear, while for a section away from the load point, the concrete carries about 19 percent of the total shear. If the remaining shear force is assumed to be carried by the steel, then for a high degree of breakdown of interaction (represented by $1/C = 2.0$ at a section close to the load point; where $1/C$ is the interaction coefficient which depends upon the load slip characteristic between the reinforcing bar and the surrounding concrete with given length of the beam and cross sectional area).

the estimated dowel force may be as high as 85 percent of the total shear.

The significance of the shear force on the tensile reinforcement (commonly termed as dowel force) has been demonstrated experimentally by Mathey and Watstein[17]. Their results appear to show that the dowel force becomes large after the diagonal crack is well formed, and then falls off to zero as the diagonal crack extends under the load pad during which time the beam is reaching a stage of complete collapse. The magnitude of the dowel force was computed from the strains measured at the lower fibre of the steel at the location of the crack in the shear span. The dowel force reached a maximum when the tip of the diagonal crack approached the edge of the loading plate. It was estimated that the dowel force on the steel may be as high as 75 percent of the total vertical shear. Under increasing load, the tensile strain in the steel increased rapidly while it was estimated that the dowel force decreased as the diagonal crack progressed to the inside of the loading pad. This is based on theoretical reasoning since there is no shear within the pure moment region.

In the comparison of the estimated shear force and the dowel force estimated from measurements by Mathey and Watstein, it is noted that they are in qualitative agreement.

Since the formation of the diagonal tension crack is believed to cause the ultimate diagonal tension failure in a reinforced concrete beam, it is suggested that the study of the principal strain trajectories

due to the influence of loss of interaction and the principal tensile strain magnitudes may lead to a more rational explanation of this problem[3,4,5,10,11].

The location and inclination of diagonal tension cracks tend to indicate that they could be caused by excessive principal tensile strains. A rational analysis of the principal tensile strength should logically be based on the conventional combined strain equation. During the course of this investigation, two sets of curves were constructed. They are the isoclinics and isostatics defined as follows:

> Isoclinics are curves connecting points at which the principal directions of strains are the same.
>
> The isostatics are lines parallel or perpendicular to the two principal strain directions at all points through which they pass, and as such they give a graphic representation of the directions of the principal strains, thus indicating the flow of strains. These are commonly called strain trajectories.

These two sets of curves are closely related owing to strain trajectories being constructed by a purely graphical process from the isoclinics. Figure (2-4) shows one of the methods for the construction of the strain trajectories.

I_1 , I_2 = Isoclinics

S = Strain Trajectory

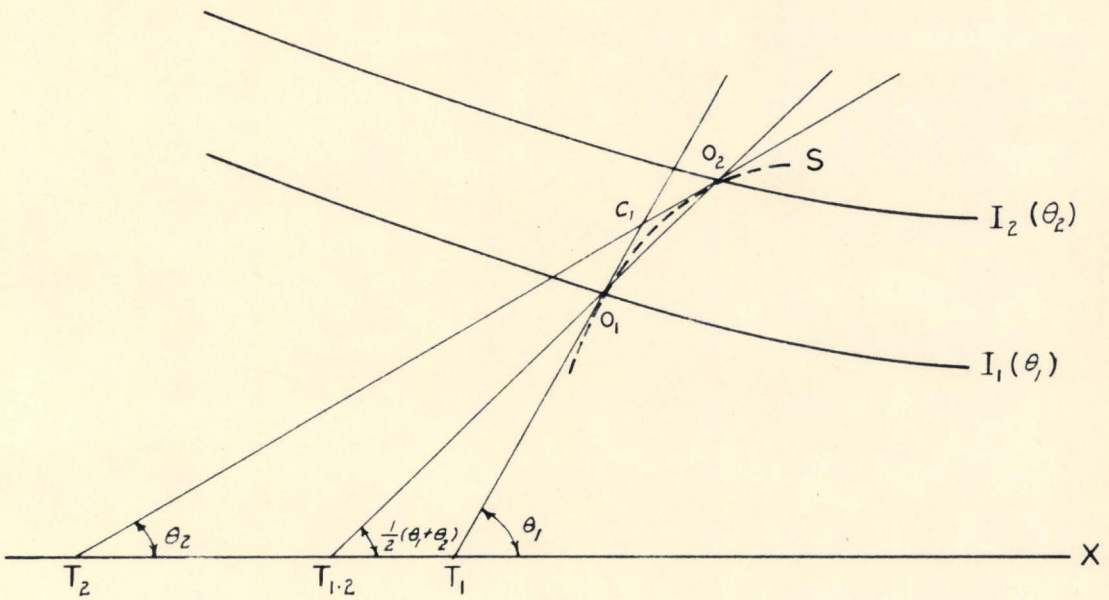

Figure 2.4

Schematic Representation of the Construction of Strain Trajectory

By using the combined strain theory, it is noted that at most points of the beam one of the principal strain is tension and the other is compression. Since these two systems of strain trajectories are orthogonal to each other, they are referred to as tensile and compressive strain trajectories.

For preliminary investigation, a plain concrete beam with cross section as shown in figure (2-1) is analysed by using the conventional combined strain theory. For a beam subjected to a two-point load, the shear span is divided into various sections and each section is subdivided into different levels. The bending strain, shear strain, principal tensile and compressive strains as well as their directions at various levels at different sections are calculated. For purposes of illustration, only the compressive strain trajectories above the neutral axis are constructed. Figure (2-5) shows the compressive strain trajectories above the neutral axis in the shear span for a plain concrete beam by conventional approach.

An uncracked reinforced concrete beam with the same cross section was then investigated. Owing to the effect of steel in the section, the neutral axis would be in a different position in the case of complete interaction. During this investigation the Newmark conventional composite beam solution is used to compute the concrete strain both at the top and the bottom fibre. The derivation is outlined in reference 11. The shearing strains at different levels in various

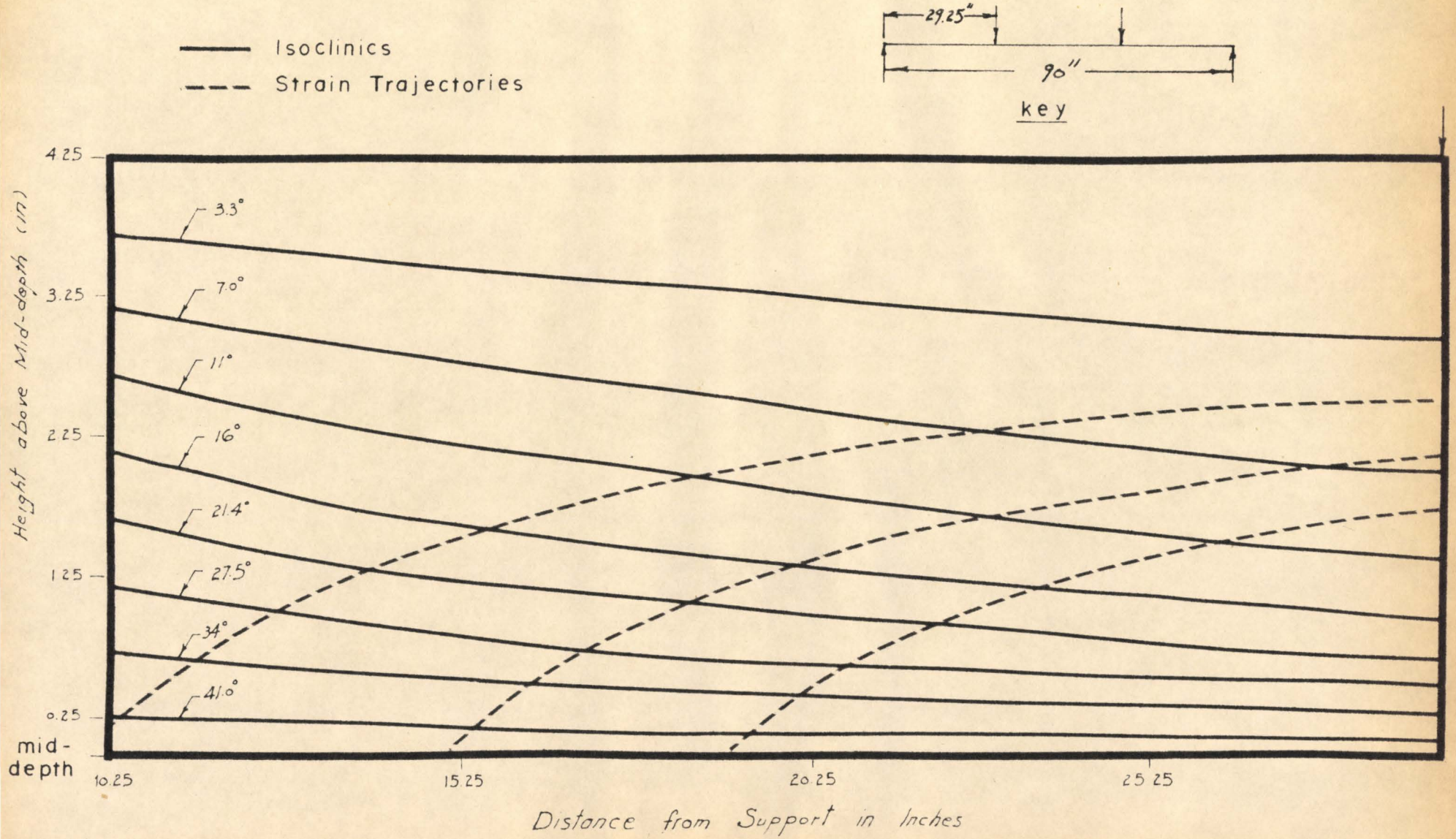

Compressive Strain Trajectories of a Plain Concrete Beam

Figure 2.5

sections were estimated as described by Broms[16]. The strain equation for concrete has the form[11]

$$\epsilon_c = [S_c - {}^{F}/_{F'} \frac{\overline{EA}\, Z}{\overline{EI}} (S_c Z + \frac{1}{E_c A_c})] M_t \quad (2\text{-}1)$$

The above strain equation shows that the strain depends on the applied moment, the properties of the reinforced concrete section and the degree of interaction ${}^{F}/_{F'}$ at the particular section at which strains are desired; ${}^{F}/_{F'}$ depends on the value of 1/c, the interaction coefficient.

In the light of his observations and speculations, Wong[11] arbitrarily assumed that for a cracked beam with varying sections, the value of 1/c would vary linearly from 200 at the supports to 0.4 at the load points where a crack is most likely to occur.

The same procedure as mentioned above is employed to compute the principal strains and their directions. Figures (2-6) and (2-7) show the compressive strain trajectories in an uncracked reinforced concrete beam by composite beam theory for both cases of complete ($1/c = \infty$), and incomplete ($1/c = 200$ to 0.4) interaction.

By comparing the strain trajectories of an uncracked beam for both complete ($1/c = \infty$) and incomplete ($1/c = 200$ to 0.4) interaction, no marked difference can be obtained. They merely show a path through which the principal tensile or compressive strains pass. The similar explanation holds true for the strain trajectories of a cracked beam. These strain trajectories provide inadequate information in the study of the so-called diagonal cracking phenomenon.

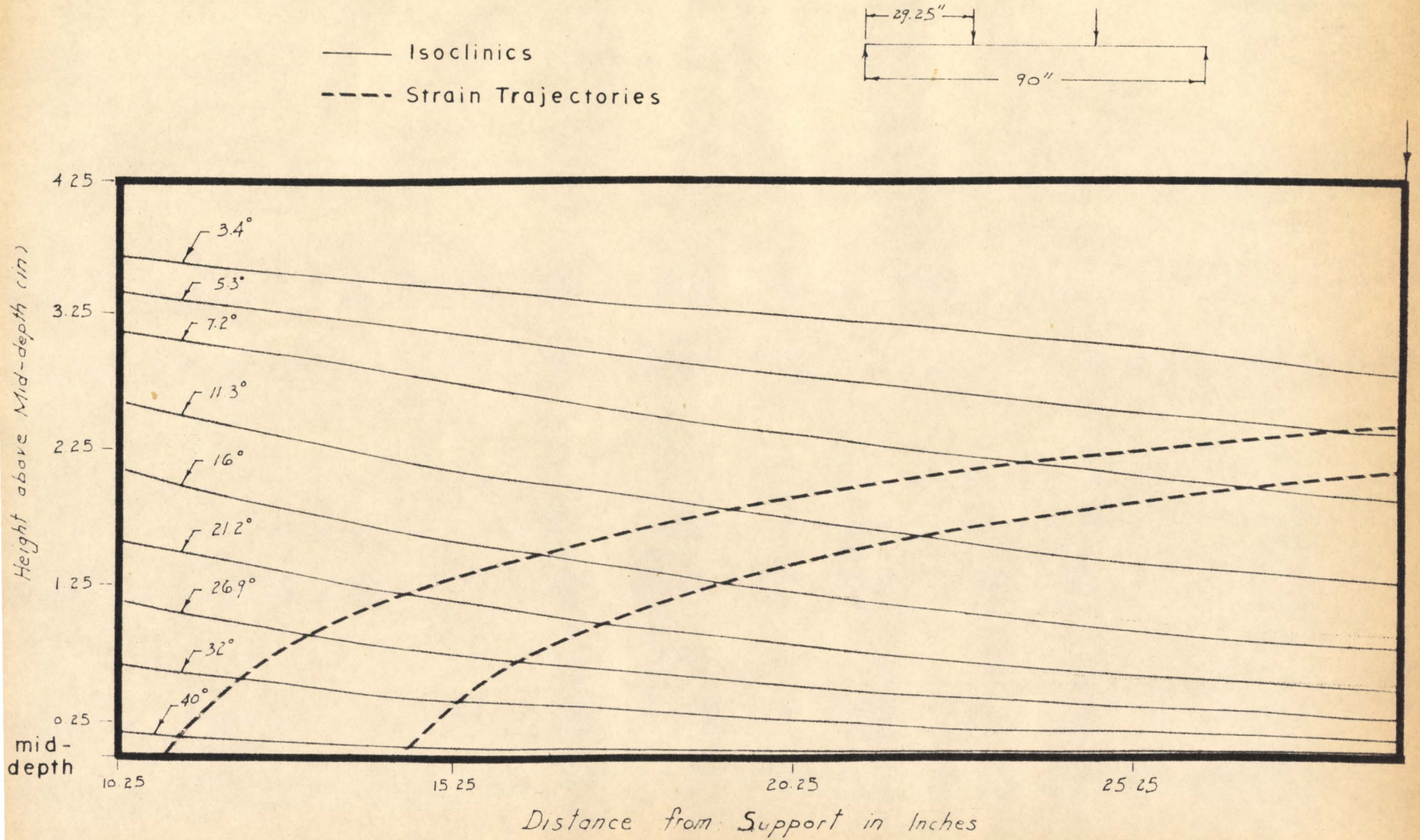

Compressive Strain Trajectories of an Uncracked Reinforced Concrete Beam (Complete Interaction)

Figure 2.6

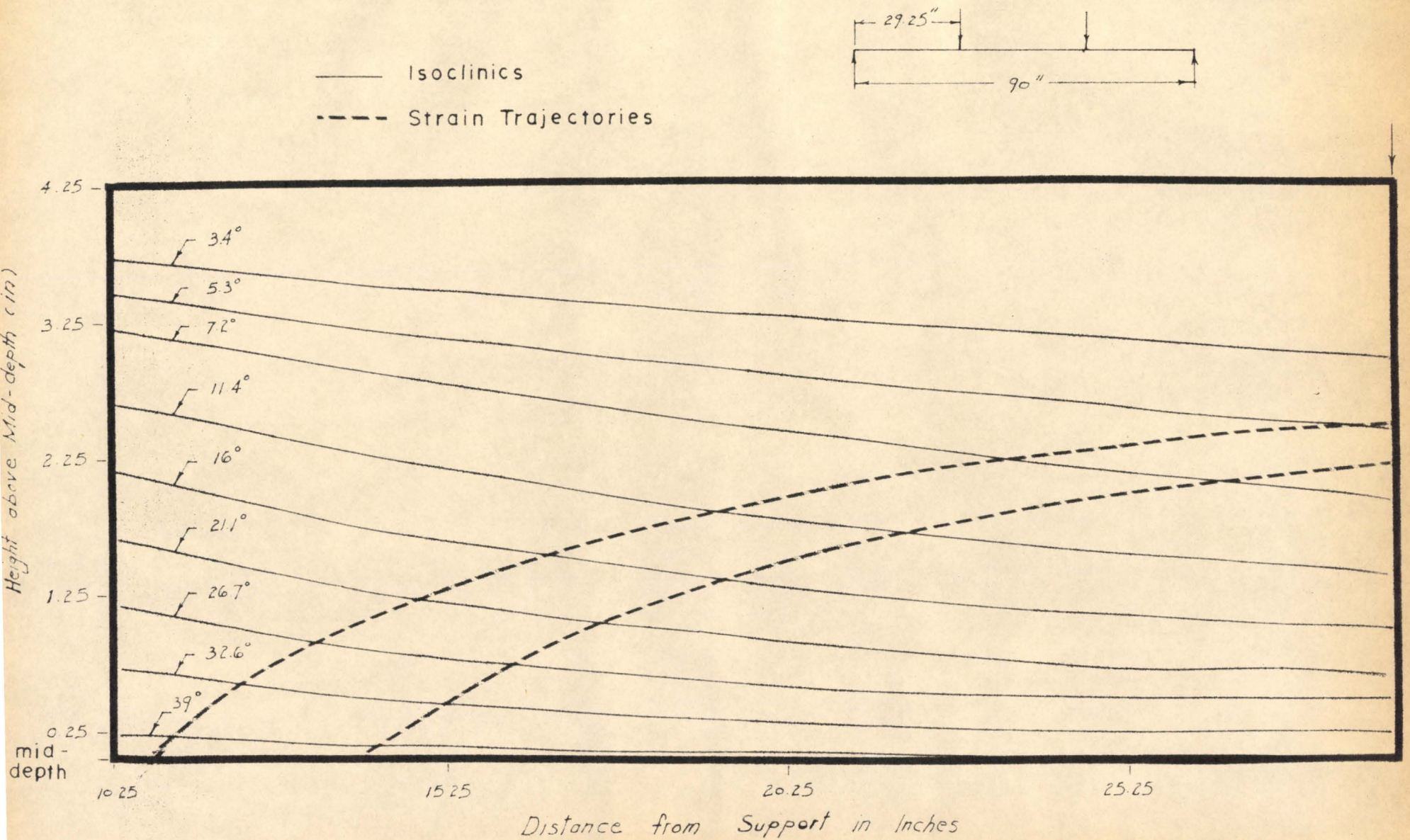

Compressive Strain Trajectories of an Uncracked Reinforced Concrete Beam (Incomplete Interaction)

Figure 2.7

Consideration of the strain trajectories did not appear to give much insight into the nature of the development of diagonal cracking, the investigation was then extended to further study of the principal tensile strains. Based on the speculation that the location and inclination of the diagonal tension crack is an indication of excessive principal tensile strain, it is assumed that the diagonal cracking would start to occur whenever the principal tensile strain exceeds 100 micro in/in. However, from the computed principal strains in the remaining uncracked section of the beam, resulting from various degrees of breakdown of interaction, is is noticed that no principal tensile strain magnitude exceeds 100 micro in/in. The principal tensile strain in the remaining uncracked section is governed by the concrete cracking strain (100 micro in/in) which in turn determines the extent of the flexural cracking. If the diagonal cracking ever occurs at 100 micro in/in, it would probably crack at the extremities of the potential cracking profile at an angle of 90 degrees. The assumed 100 micro in/in cracking strain only furnishes the potential cracking profile. Various potential crack profiles were estimated for different load increments.

It was observed in a number of test beams subjected to an increasing load, that there were no cracks visible to the naked eye at half times the design load. At design load, cracks begin to appear inside the pure moment region. At 1.5 or even 2.0 times the design load, the first crack began to appear in the shear span at about two

to three inches away from the load points. However, one should bear in mind that these are only the visible cracks at that load intensity. For the same loading, it is likely that the actual cracks extend some distance beyond the visible part. These micro-cracks are assumed to extend up to the limit of the potentially cracked zone. The potential crack profile is assumed to be that profile at which the tensile strain is equal to 100 micro in/in. It is then reasonable to assume that at the same load intensity, the tensile cracking strain for the visible crack profile would be higher than that for the potential crack profile.

For purposes of illustration, a cracking strain of 200 micro in/in was arbitrarily chosen for computing the visible crack profile, and the principal tensile strains based on the visible cracking strain were computed. It was hoped that by increasing the cracking strain, it would be possible to induce higher shearing strains within the remaining uncracked section. This in turn would affect the principal tensile strains as well as their directions, and a more rational explanation on the so-called diagonal tension crack could be obtained. It was found, however, that the increase in shearing strains is very small and insignificant.

Based on the assumed tensile cracking strains of both 100 micro in/in and 200 micro in/in, the potential crack profile and the visible crack profile were estimated at both 1.5 and 2.0 times the design load in the case of incomplete interaction; represented by

1/c = 3.125 constant and 1/c varying linearly from 200 at the supports to 0.4 at the load point. The principal tensile strains were computed based on the remaining uncracked sections above the visible crack zone. Figures (2-8), (2-9),(2-10) and (2-11) show the visible crack zone, potential crack zone and the principal cracking boundary (at which the principal strain is equal to 100 micro in/in) for both 1.5 and 2.0 times the design load in the case of incomplete interaction. It is noted that the locus of these principal tensile strains (or the so-called diagonal tensile strains represented by 100 micro in/in) is located within the two cracking extremities of both the potential crack profile and the visible crack profile. In most cases, the diagonal cracking boundary is very close to the potential crack extremities. The inclination of these principal strains vary from 85 degrees to 90 degrees. In other words, the diagonal cracks would begin to form almost at a right angle. Under increasing load, these assumed diagonal cracks would eventually extend upward and meet the existing potential crack boundary. This would give rise to another potential crack profile with which the problem had started. From the strain pattern in the remaining uncracked section, the above cracking behaviour is quite logical. The cracking strain of 100 micro in/in is being used as a basis to compute the potential crack profile, any cracking strain equal to or greater than 100 micro in/in should therefore occur below the potential cracking limit. In other words, there should not be any diagonal crack with a magnitude of 100 micro in/in occurring above the potential crack zone. The increased shear

strain in the remaining uncracked section estimated from the assumed visible cracking strain affects the principal tensile strain only to a limited extent. This would cause a tensile crack to form at about 2 to 5 degrees difference from a vertical crack. This difference is insignificant as far as the diagonal tensile crack is concerned. In order to explain the behaviour of the diagonal cracks which occur in reinforced concrete beams, a different approach other than the principal strains has to be established.

After the study of the internal strain redistribution in a reinforced concrete beam where cracks are present, it is believed that the principal tensile strains alone could not provide a rational explanation of the diagonal cracking behaviour. In the comparison of the theoretical potential crack profile with the actual crack profile which could visibly be observed in test beams, it is noticed that the assumed potential cracking strain (ϵp = 100 micro in/in) is comparatively lower than the cracking strain visually indicated by visible cracks in an actual test beam. For example, with ϵp = 100 micro in/in at design load, the beam starts to crack at about the mid-shear span. (see figure 2-12). At 1.5 and 2.0 times the design load, the cracks would occur further out towards the supports. However, results of the tested beams showed that in most cases, cracks were limited to within the pure moment region at design load or below. The first crack appeared in the shear span at about 1.5 to 2.0 times the design load somewhere about one to three inches away from the load point. Since these are visible cracks in a test beam, their cracking strain should

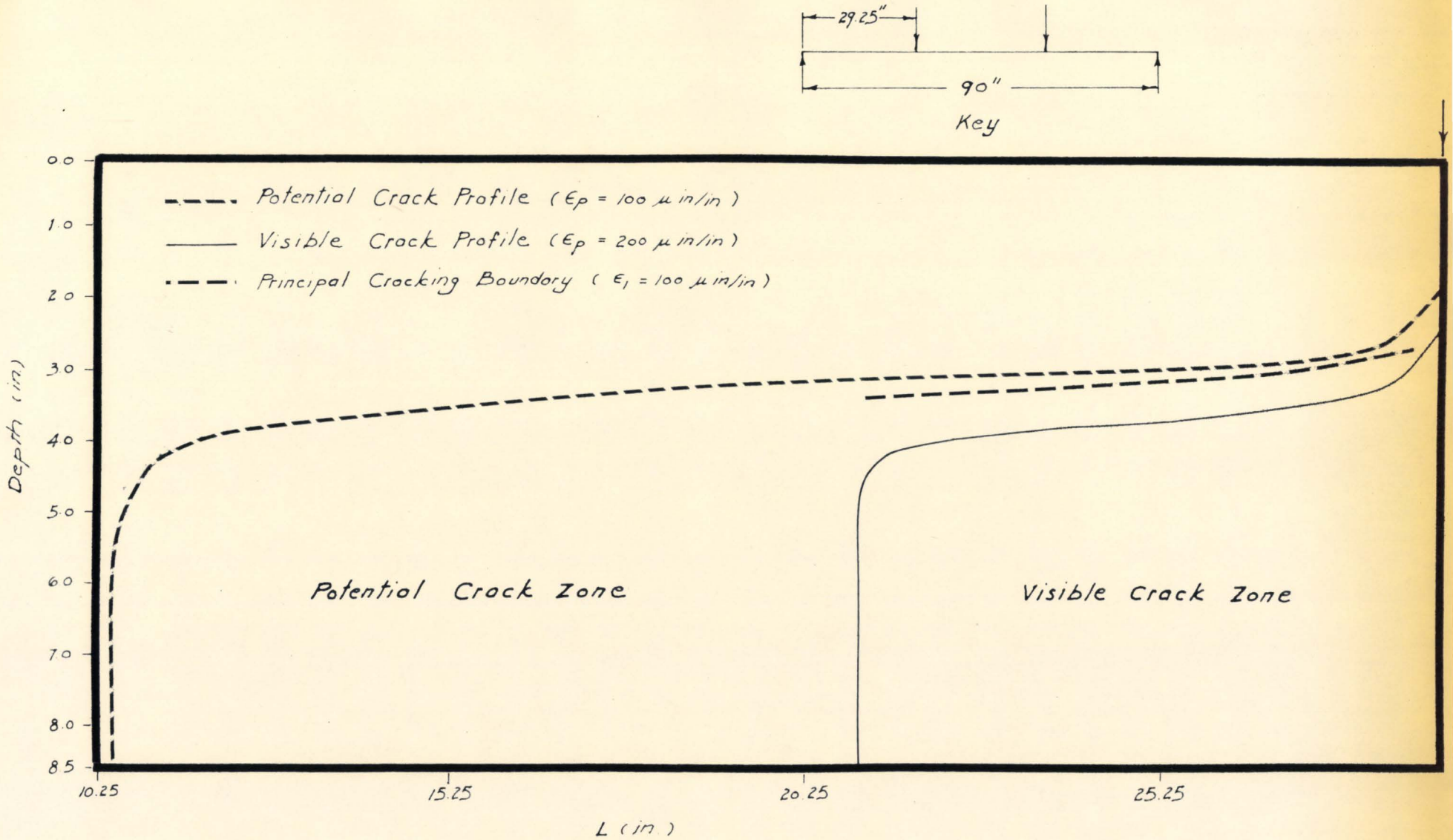

Figure 2.8

Estimated Potential, and Visible Crack Zones, and the Principal Cracking Boundary of a Reinforced Concrete Beam in the Case of Incomplete Interaction (1/c varying along the beam) at 1.5 x Design Load

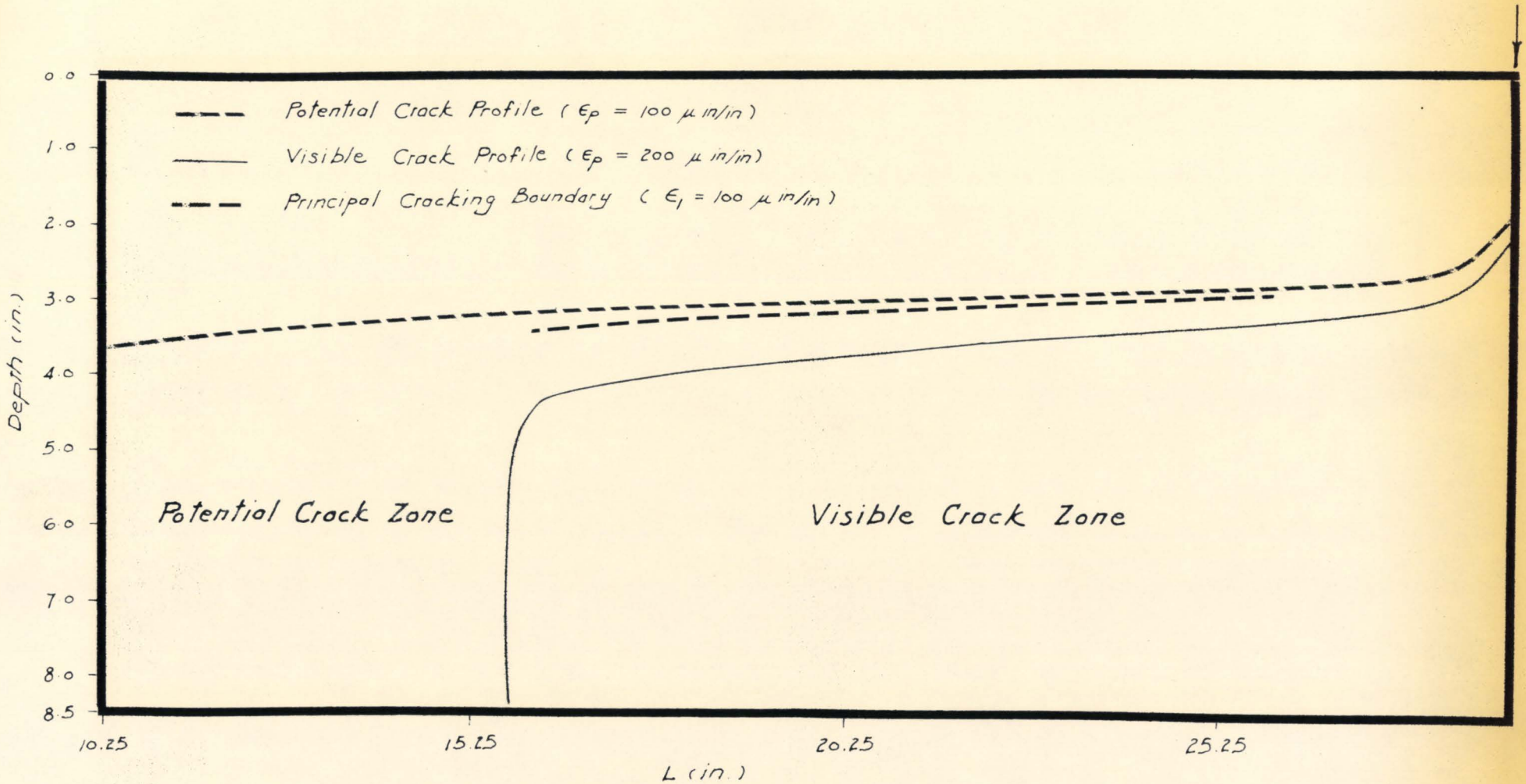

Figure 2.9

Estimated Potential, Visible Crack Zones and the Principal Cracking Boundary of a Reinforced Concrete Beam in the Case of Incomplete Interaction (1/c varying along the beam) at 2.0 x Design Load

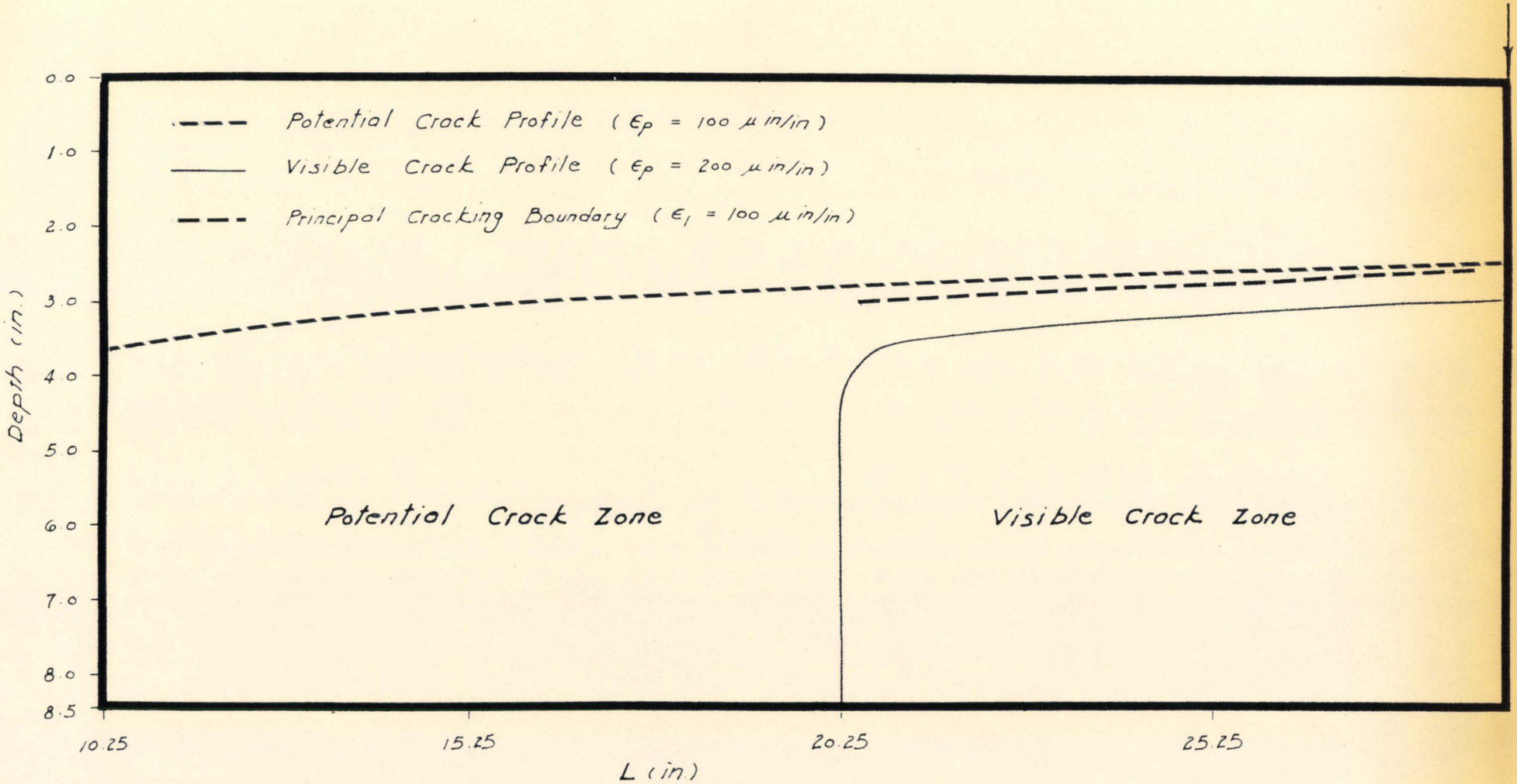

Figure 2.10

Estimated Potential, Visible Crack Zones and the Principal Cracking Boundary of a Reinforced Concrete Beam in the Case of Incomplete Interaction (1/c = 3.125 constant) at 1.5 x Design Load.

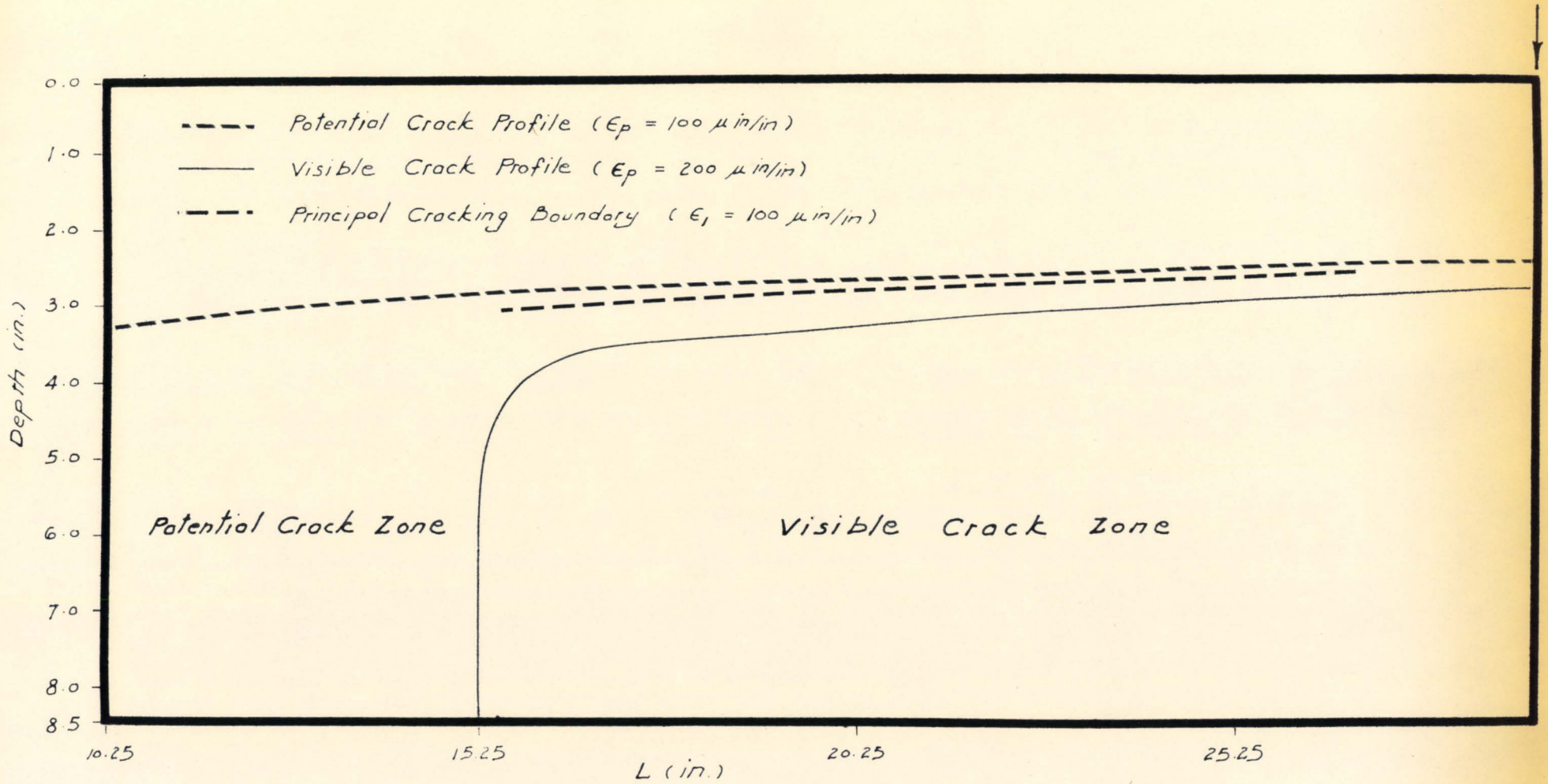

Figure 2.11

Estimated Potential, Visible Crack Zones and the Principal Cracking Boundary of a Reinforced Concrete Beam in the Case of Incomplete Interaction (1/c - 3.125 constant) at 2.0 x Design Load

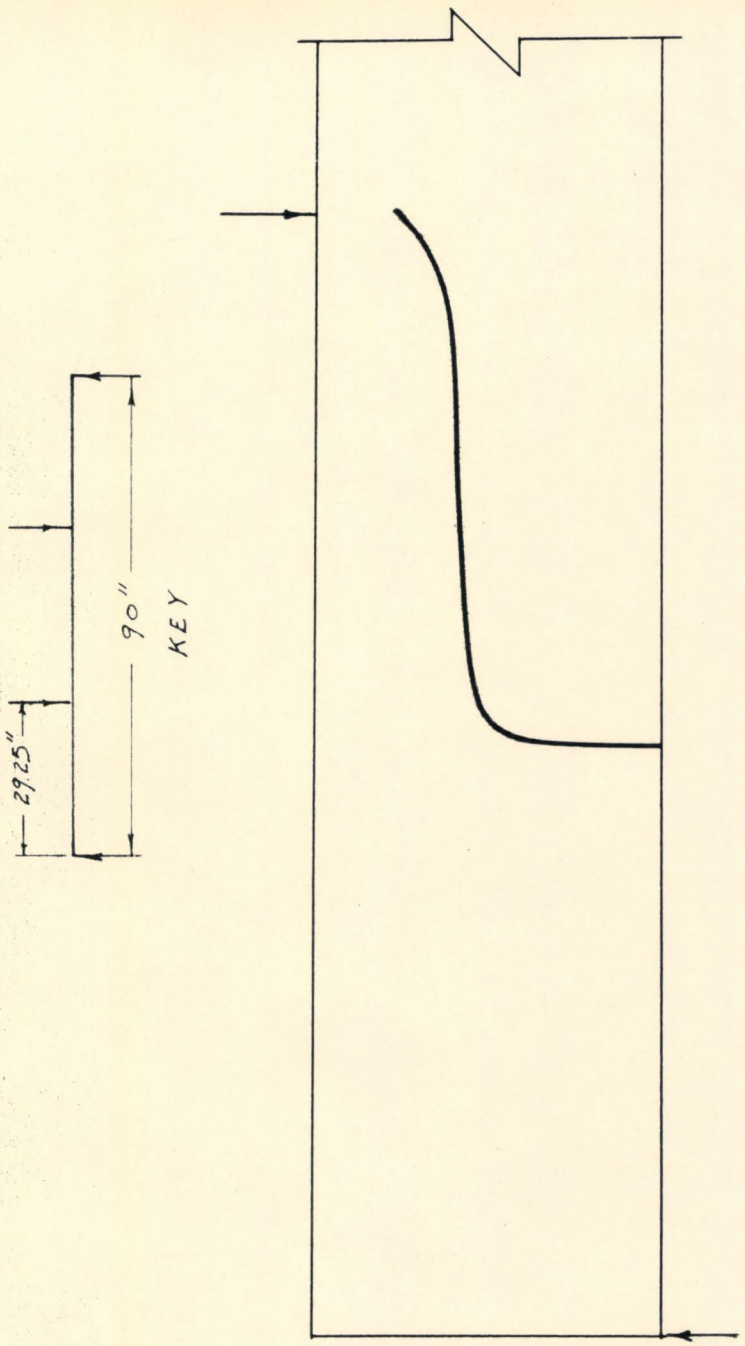

Figure 2.12

Estimated Extremities of Potential Cracks of a Reinforced Concrete Beam at Design Load (Incomplete interaction, 1/c varying along the beam)

be higher than the potential cracking strain. For purposes of illustration, various cracking strain values are arbitrarily chosen to compute the corresponding visible crack profiles at design load, 1.5, 2.0 and up to 3.5 times the design load for cases of complete interaction ($1/c = \infty$) and incomplete interaction ($1/c = 0.4$ constant). Figures (2-13),(2-14) and (2-15) show the crack profiles for cracking strain 250, 300 and 350 micro in/in respectively.

In the case of $\epsilon p = 250$ micro in/in, it is estimated that the visible crack appears at 1.5 times the design load at about 3 inches away from the load point in the shear span. At 3.5 times the design load, (approximately the failure load of the test beams) it is estimated that the crack profiles extended outwards towards the supports to about 18 inches away from the load point. In the case of $\epsilon p = 350$ micro in/in, cracks initiated in the shear span at 2.0 times the design load at about 1 inch away from the load point. At 3.5 times the design load, the final visible crack profile occurs at about 13 inches away from the load point. Figure (2-16) shows tested beams which have the similar a/d ratio as the analysed beam. The cracking strain of the beam is not known. However, it could be seen that at the final failure stage, the outermost crack is located at about the mid-shear span. Therefore, the assumed visible cracking strain may be considered to lie within the range of 300 to 350 micro in/in. The cracking strain as well as the crack profile changes quite markedly among test beams owing to the fact that there is a large number of parameters

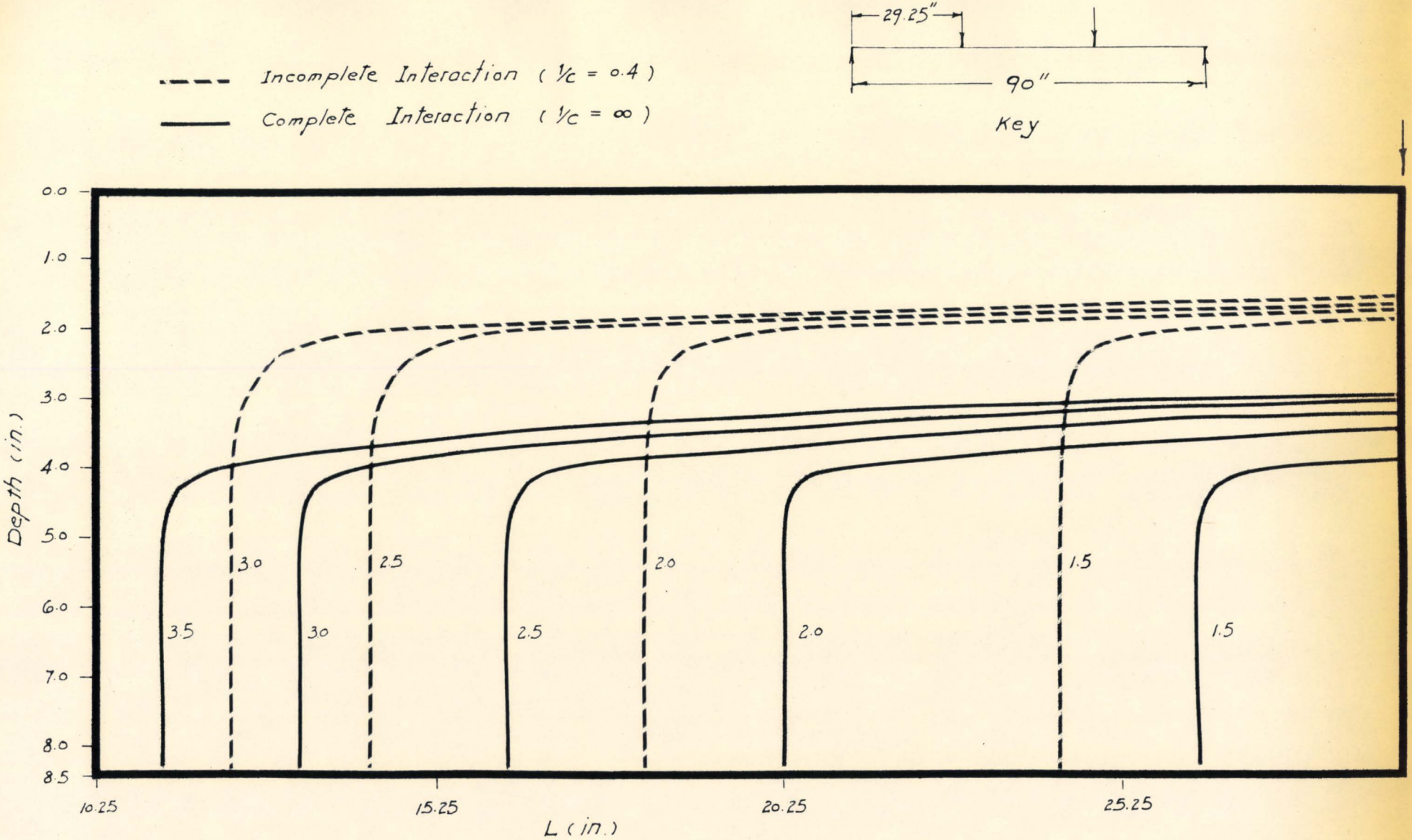

Figure 2.13

Estimated Visible Crack Profiles (ε_p = 250 micro in/in) For Both Complete and Incomplete Interaction at Various Loadings.

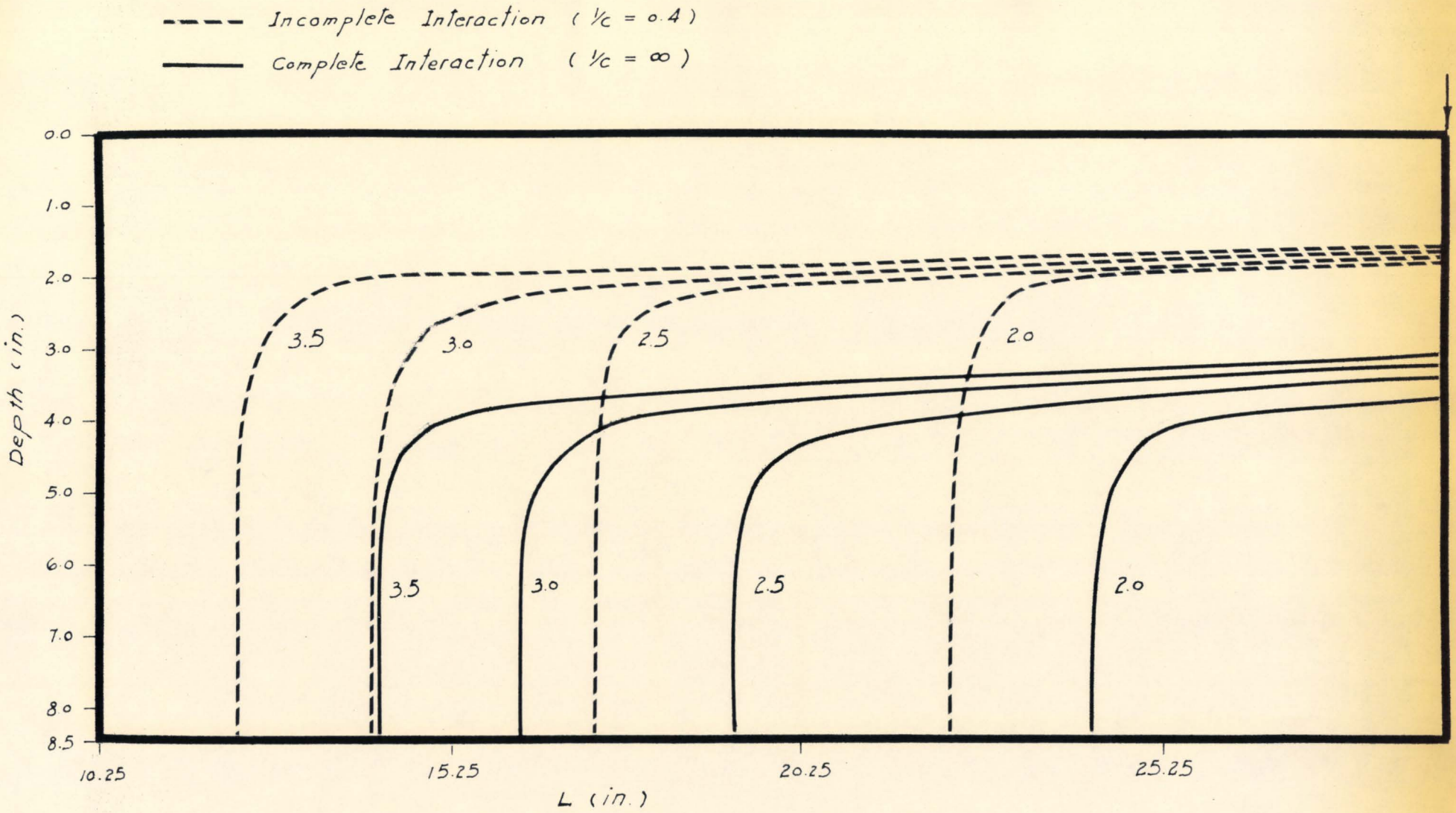

Figure 2.14

Estimated Visible Crack Profiles (ε_p = 300 micro in/in) For Both Complete and Incomplete Interaction at Various Loadings.

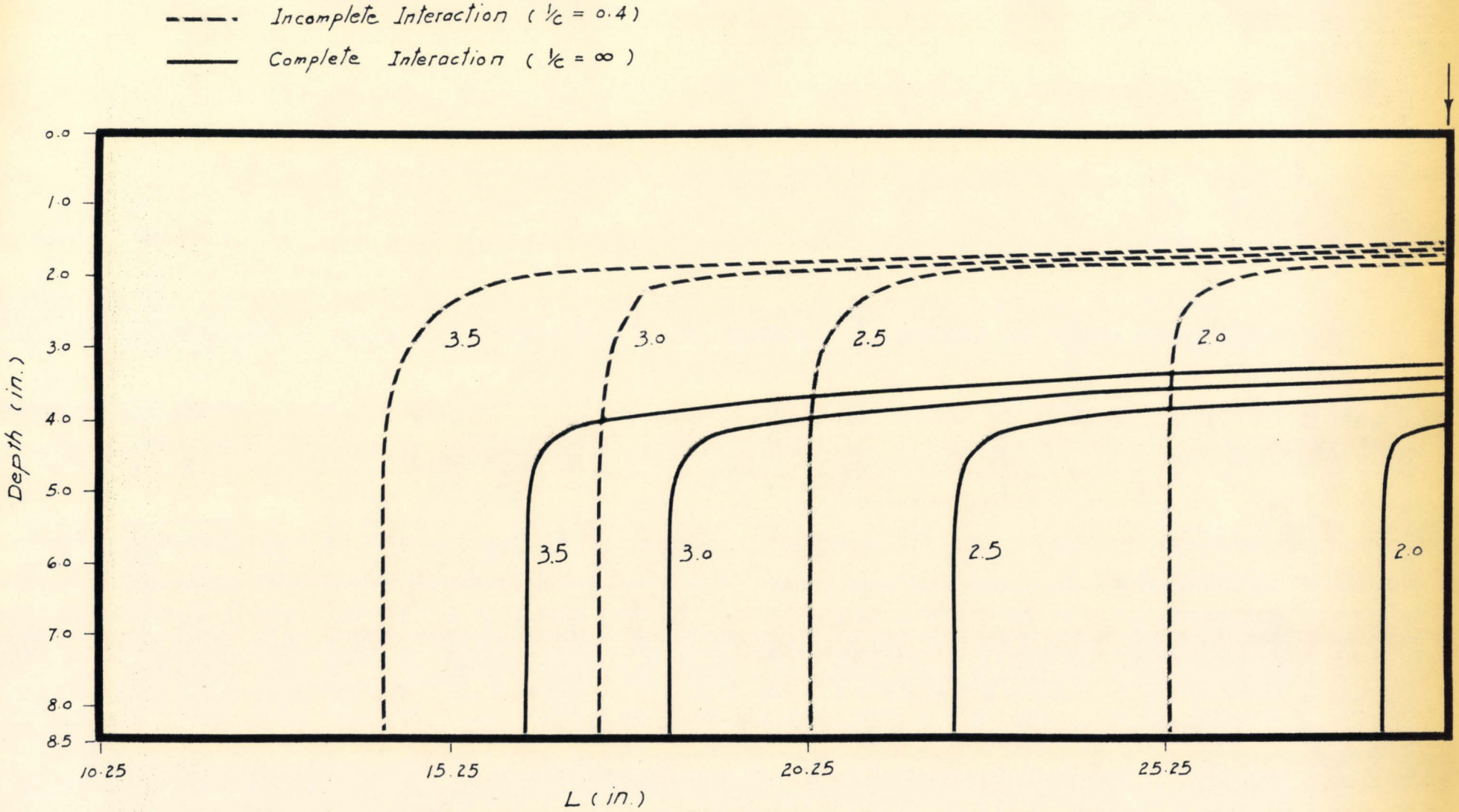

Figure 2.15

Estimated Visible Crack Profiles (ε_p = 350 micro in/in) For Both Complete and Incomplete Interaction at Various Loadings.

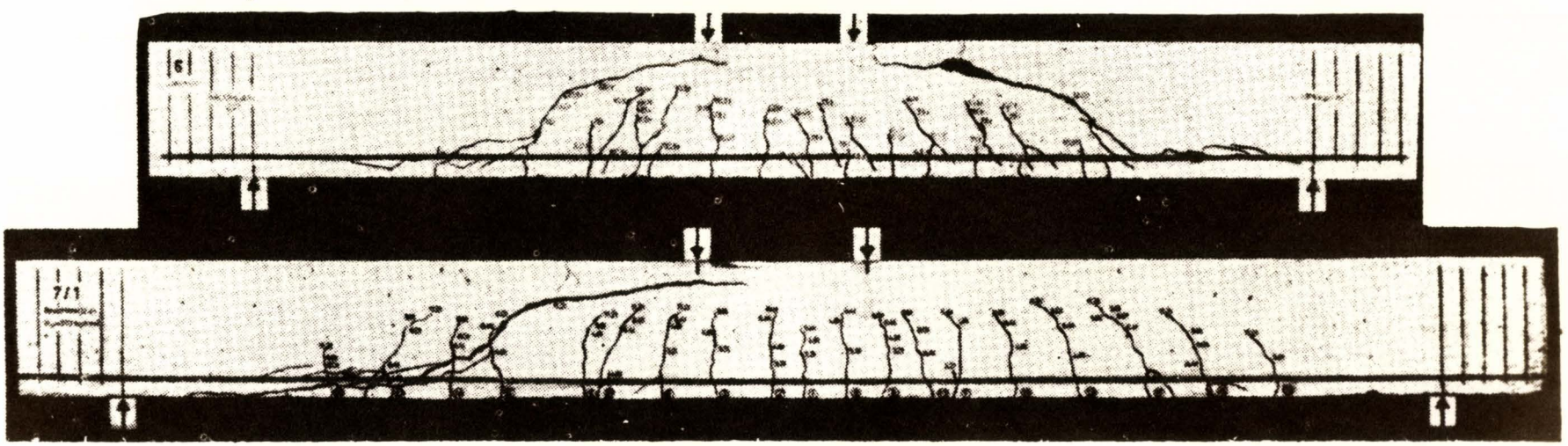

Figure 2.16

Visible Crack Profiles Observed in Test Beam with Different a/d ratio (due to Leonhardt and Walther)

involved; such as the concrete strength, reinforcement ratio, shear span ratio, size of aggregate, etc. These could not be determined by any simple mathematical formula.

By estimating the probable range in the cracking strain, the investigation was extended to study the effect due to breakdown of interaction for a reinforced concrete beam subjected to various loadings. As observed in all the test beams, the diagonal crack tends to start somewhere near the mid-depth, in between two existing vertical cracks. This has been reported by other investigators[4,10]. In recent years, many research workers have attempted to analyse the diagonal failure mechanism by introducing the spacing and the length of cracks as governing parameters[7,10]. Moe's "cantilever beam" theory and Kani's "tooth" theory are the classical examples. These effects are more pronouncedly observed in test beams. It has been noted[8] that the cracks are wider and longer under or close to the load point. Away from the load point in the shear span, cracks become shorter and narrower.

When the composite beam concept is applied, it indicates that when the length of the crack is longer, the breakdown of interaction is greater. Based on this speculation, crack profiles are estimated for both complete interaction ($1/c = \infty$) and incomplete interaction ($1/c = 0.4$ constant). For purposes of comparison, concrete tensile strain of 350 micro in/in is chosen to compute the crack profiles as shown in fig. (2-15). This particular strain magnitude is chosen mainly

because at 3.5 times the design load, it would produce an appropriate crack profile which is believed to be the ultimate crack profile, as observed in a tested beam. Inside the shear span, it is assumed that there are a number of flexural cracks. These cracks are further assumed to have a constant crack spacing between them, and the outermost crack occurs somewhere near the mid-shear span (at about 3.5 times the design load). It is reasonable to speculate that the degree of breakdown of interaction would be highest at the section of a crack under or close to the applied load. It would decrease gradually at the section of cracks away from the load point.

For purposes of illustration, two hypothetical cracks with a certain crack spacing in the shear span are arbitrarily chosen. At the same load intensity, these two cracks have different width and length. In other words, the crack closer to the applied load is subjected to a higher degree of breakdown of interaction (represented by a smaller 1/c), and resulted in a wider and longer crack. For the other one, which is further away from the applied load, a comparatively higher degree of interaction and a shorter and narrower crack are assumed. In between these two cracks, the variation of degree of interaction is not known. Experimental results[13,14] indicate that the magnitudes of the steel strain and the slip are higher at sections where major cracks are present. In between these two cracks, there is a section where the steel strain and the slip are the lowest. Slip can be defined as the relative movement of the steel with respect to the concrete. By using the composite beam theory, the slip is inversely

proportional to the value of 1/c; the interaction coefficient. In other words, the measured slip at any section can be considered as an indication of the degree of interaction at that particular section. For the two hypothetical cracks, the degree of breakdown of interaction is arbitrarily assumed to be 0.2 for the one which is closer to the load point and 0.8 for the other. The crack spacing is assumed to be 4 inches. For purposes of computation, it is further assumed that the degree of interaction is very high between the cracks. The degree of interaction is assumed to vary linearly from 0.8 at one crack to 100 at the mid section, and then from 100 to 0.2 at the other crack. The steel strain and slip distributions based on both the cracked and uncracked sections were computed by composite beam solutions as outlined in reference 11. Fig. (2-17) shows the two hypothetical cracks, the 1/c distribution, the steel strain distributions for both cracked and uncracked section and the computed slip distribution in between these two cracks at 2.5 times the design load. These theoretical results are compared qualitatively with the experimental observations and measurements performed by other investigators[13,14].

Figure (2-18) and figure (2-19) show the steel strain distribution and the slip (or crack width) measurements at the level of reinforcement performed by Evans and Robinson[14], and Manning[13]. It may be seen that the steel strain was the highest where the cracks occurred under or close to the applied load. It decreased curvilinearly until the lowest strain was reached at a particular section in between

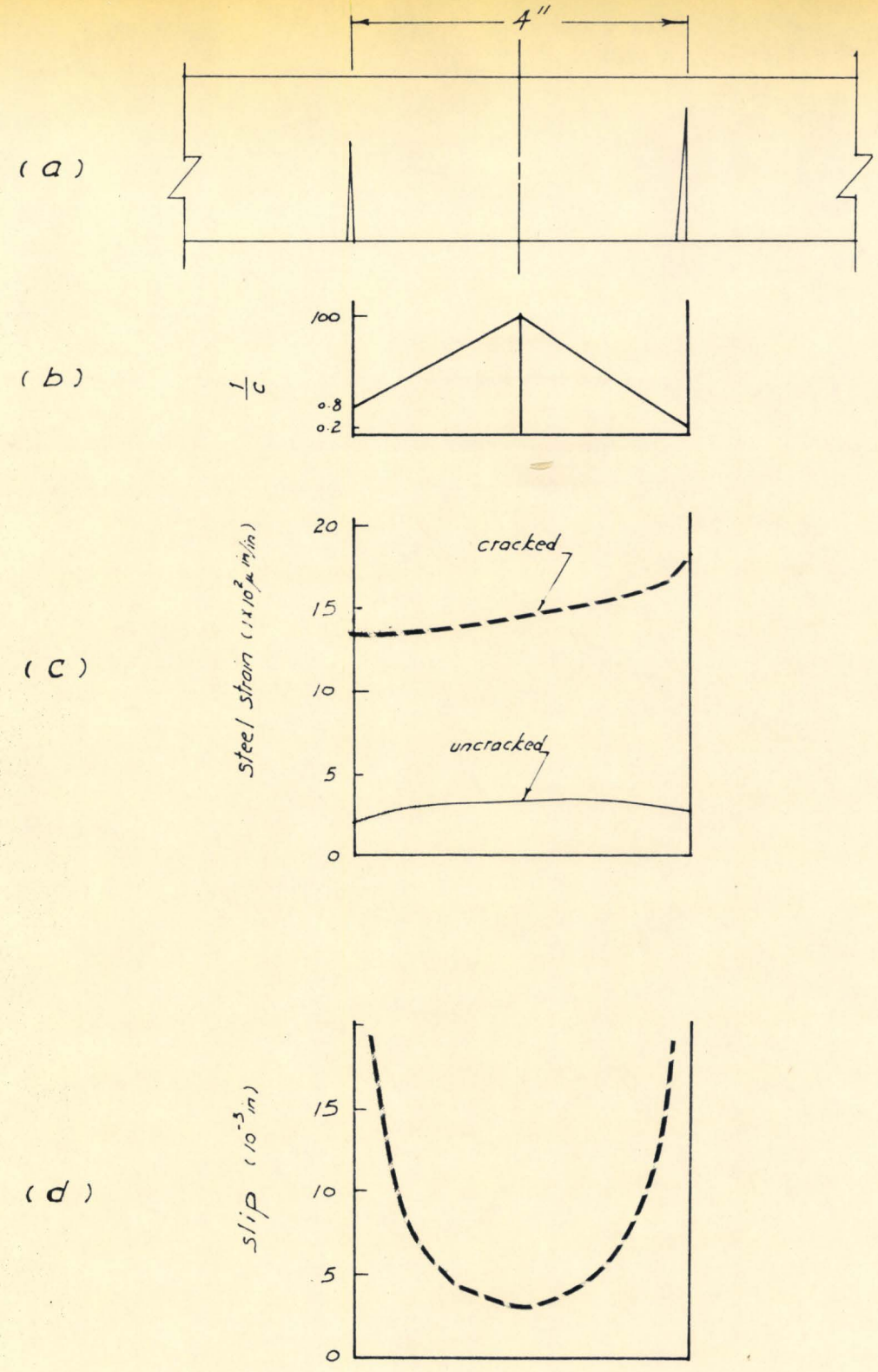

Figure 2.17

Estimated Steel Strain Distributions for Both Cracked and Uncracked Sections, and Slip Distribution in Between Two Cracks.

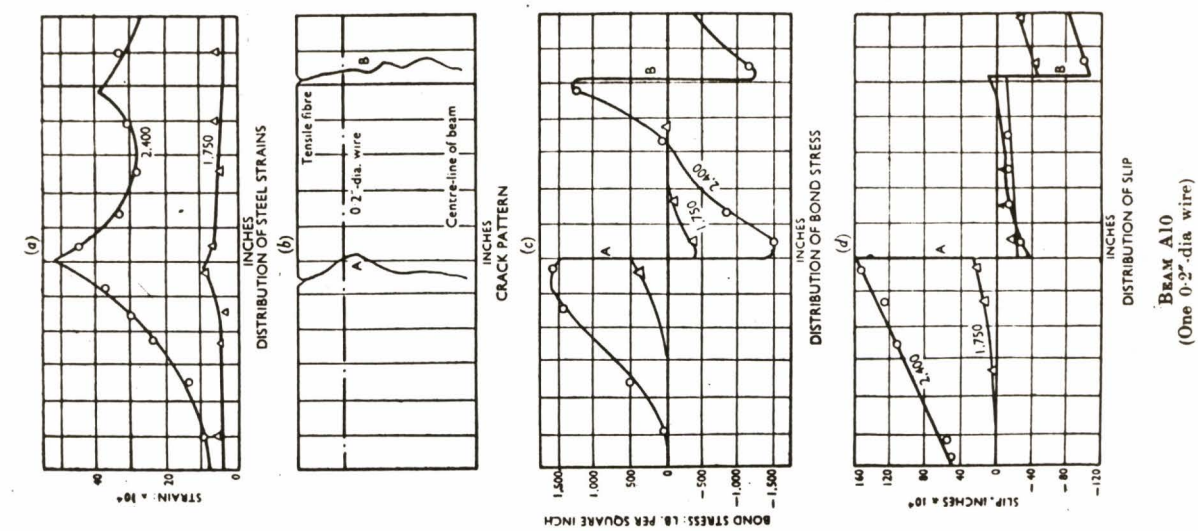

BEAM A10
(One 0·2"-dia wire)

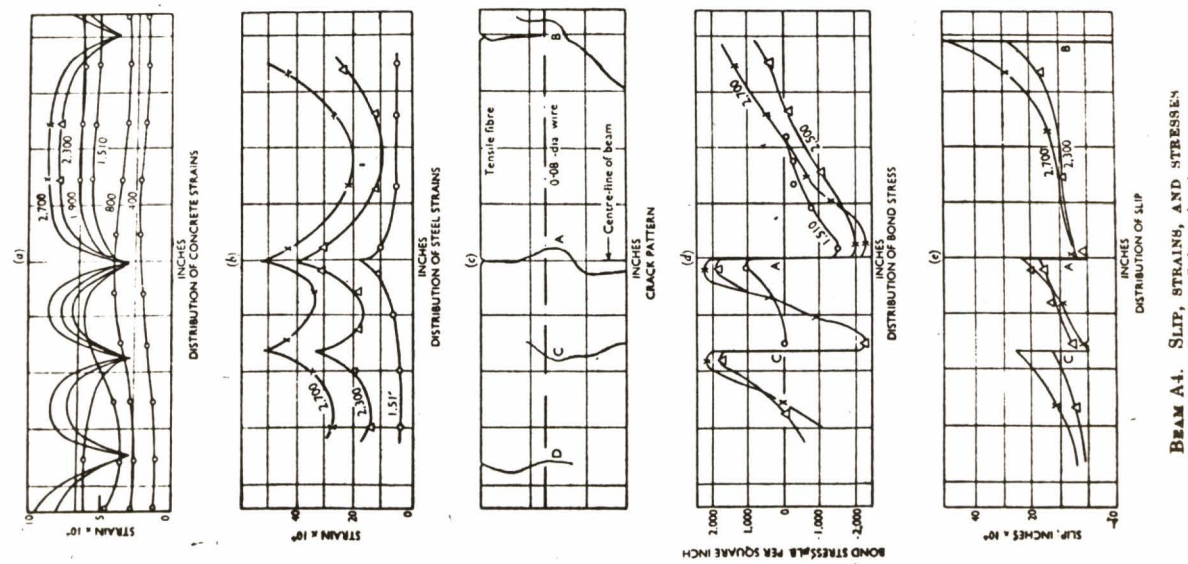

BEAM A4. SLIP, STRAINS, AND STRESSES
(Six 0·08"-dia wires)

Figure 2.18

Slip Distribution, due to Evans and Robinson

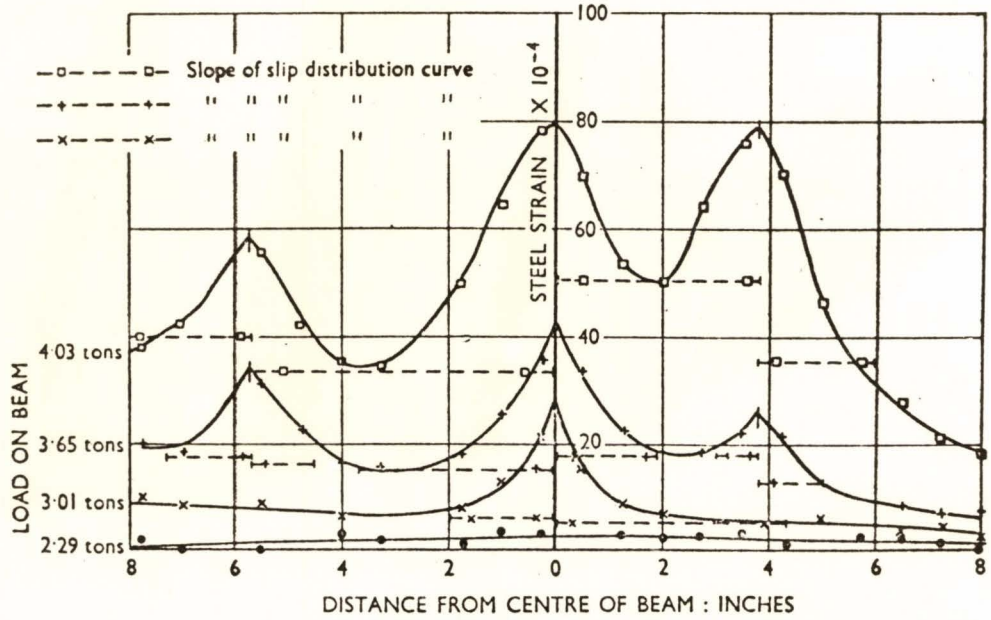

STEEL STRAIN DISTRIBUTION FOR BEAM X2

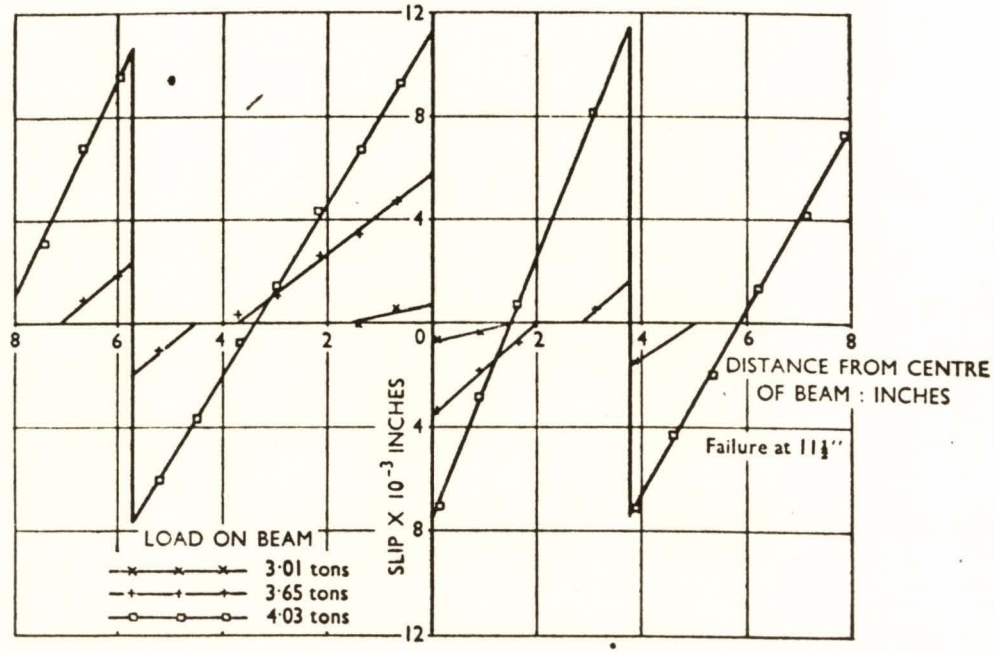

CRACK WIDTHS AT LEVEL OF REINFORCEMENT

				0·0010				
0·0050	6·3"	0·0022	5·7"	0·0088	3·8"	0·0028	7·7"	0·012
0·0220		0·0172		0·0208		0·0134		0·0465

: SLIP DISTRIBUTION FOR BEAM X2

Figure 2.19

Slip Distribution, Due to Manning

two cracks. Then it started to increase again in a similar manner until another higher strain value was reached at another crack, the one which was away from the applied load. The distribution of slip had a similar behaviour. The magnitude of slip was largest where the crack occurred (would reach a maximum under the load point), and diminished with distance away from the crack.

Theoretically, by the assumption of two different 1/c distribution in between two cracks, two characteristic steel strain curves could be obtained. The lower steel fibre strains were much higher when computed by "cracked section" theory than by "uncracked section" theory. These two curves (as shown in figure (2-17)) differ quite markedly from those measured experimentally as in figures (2-18) and (2-19). The computation based on the "uncracked section" theory could not be justified owing to the strains in steel and concrete increasing uniformly until the tensile strain of the concrete is reached. After the section has been cracked, the steel strain is increased because the tensile reinforcement carries the additional load which was previously taken by the concrete. The steel strains between the two cracks can be computed on the basis of the uncracked section. However, the portion in between the two existing cracks might have cracked.

The possible occurrance of micro cracks in between two major cracks could be reasoned by considering a reinforced concrete beam as a composite beam with incomplete interaction. Figure (2-20a) shows a portion of the beam with both uncracked (1-1) and cracked (3-3)

sections. If section (1-1) is uncracked, the section is in complete interaction. The strain distribution of the composite member has the form as shown in figure (2-20b). At an infinitesimal distance away from section (1-1), a major crack occurs at section (3-3). In this section, the strain distribution would have a form as shown in figure (2-20d), resulting from a high degree of breakdown of interaction. By observing the steel strain distributions at both the crack and uncracked sections, it is noticed that the steel strain at section (3-3) is very high, and the steel strain at section (1-1) is very low. However, in between these two sections, it is improbable for the steel strain to drop abruptly from a very high magnitude at the cracked section to a very low magnitude at the uncracked section. Possibly there will be a gradual transition taking place in between these two sections. Based on this speculation, it is reasonable to assume that in between the uncracked (1-1) and the cracked (3-3) sections, there would be a section (2-2) where the value of steel strain is comparatively lower than that at a cracked section, and comparatively higher than that at an uncracked section. The strain distribution at this particular section would have a form as shown in figure (2-20c). From the composite beam concept, the strain distribution at section(2-2) indicates that there is a loss of interaction at that section, resulting in a possible crack formation. For the remaining sections in between two major cracks, more cracks could be formed in a similar manner. Those may be micro cracks which

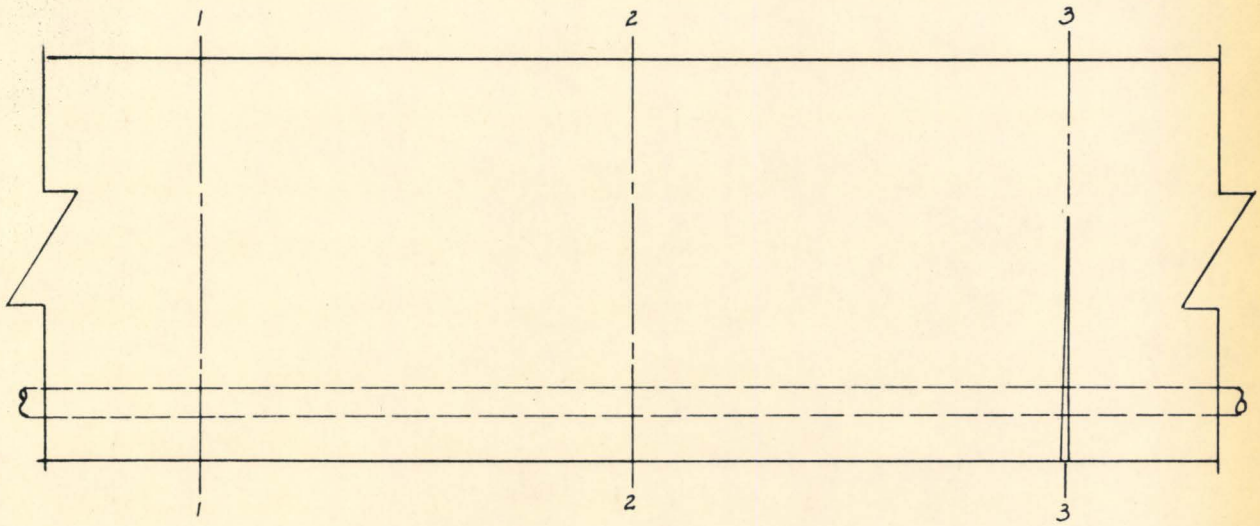

(a)

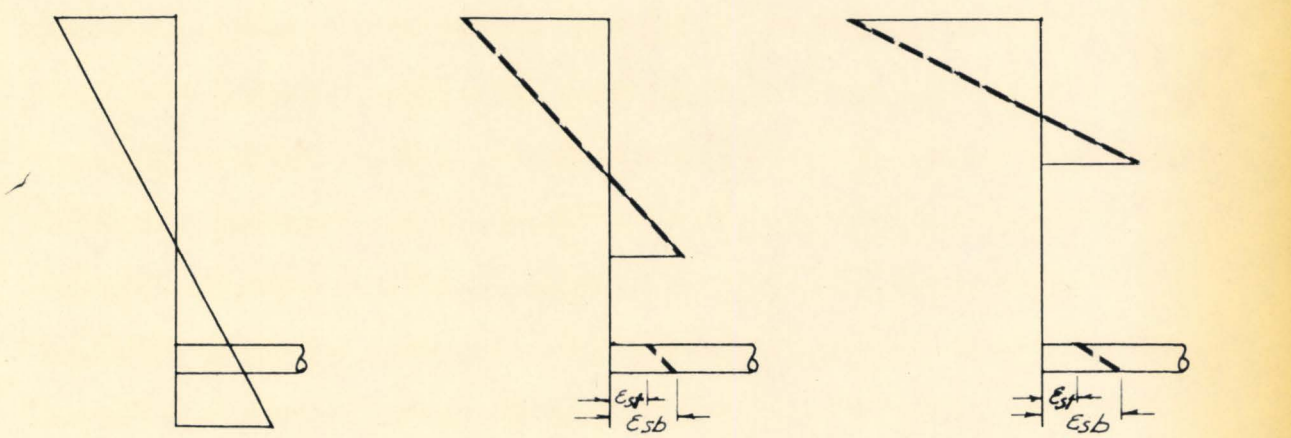

(b) Uncracked Section 1-1 (complete interaction)

(c) Cracked Section 2-2 (incomplete interaction)

(d) Cracked Section 3-3 (incomplete interaction)

Figure 2.20

Strain Distribution in Uncracked and Cracked Sections

cannot be detected by the naked eye. The main difference in the steel strain distribution between the theoretical computation based on the "cracked section" theory and the experimental measurements is probably governed by these micro-cracks; which in turn is linked to the degree of breakdown of interaction. The value of 1/c at the crack, as well as its linear variation is an arbitrary assumption. A more likely variation of 1/c along the length of a reinforced concrete beam subjected to an increasing load is not clearly known; neither is the variation between two existing cracks. From the assumed 1/c variation and the computed steel strain distribution, it is noted that the strain is greatly affected by the corresponding 1/c; the degree of breakdown of interaction. At the section of a crack where the degree of breakdown of interaction is larger (represented by smaller 1/c), the higher steel strain is obtained. The steel strain computation is affected to some extent by the external moment variation. In between two major cracks, there may be a section with high degree of interaction (represented by a large 1/c). With this speculation, it could be reasonable to assume that for two hypothetical cracks, the 1/c would be very high somewhere between the cracks. It would degenerate rather rapidly in some curvilinear manner until it reaches a very low value at the crack close to the load point; and to a slightly higher 1/c value at the other crack. (The one which is away from the first). This would result in a comparatively lower steel strain in between the two hypothetical cracks. The degree of breakdown of interaction occurring in a reinforced concrete beam affects the slip distribution in a similar

manner. The magnitude of slip computed by the composite beam solution is related to the steel strain at a particular section. The suggested steel strain distribution and the probable slip distribution based on the modified 1/c variations (curvilinear) in between two hypothetical cracks are shown in figure (2-21). This will have a shape more like that of the steel strain and slip measured by Evans and Robinson (compare figures 2-18 and 2-21). It is likely that the magnitude of the estimated slip and the measured slip may be different. The different approaches employed to measure the slip at any section of a beam account for the difference. The slip distribution measured radio-graphically by Evans Robinson was the relative movement of the steel with respect to the adjacent concrete. This slip would be the actual slip at any section provided the beam is not cracked. Whenever the beam starts to crack, there will be a series of cracks along the length of the beam, or a beam with concrete "teeth" has been formed as described by Kani[6,7]. Under increasing load, these concrete teeth or strips are subjected to relative movement, or possible rotation with respect to the remaining uncracked zone of the beam. If, the slip measurement at any particular section is desired, the relative movement of the steel with respect to the concrete in the remaining uncracked section of the main body of the member should be measured. This would be the relative movement of the steel with respect to the so-called pseudo interface, when a reinforced concrete beam is considered to be a composite beam with

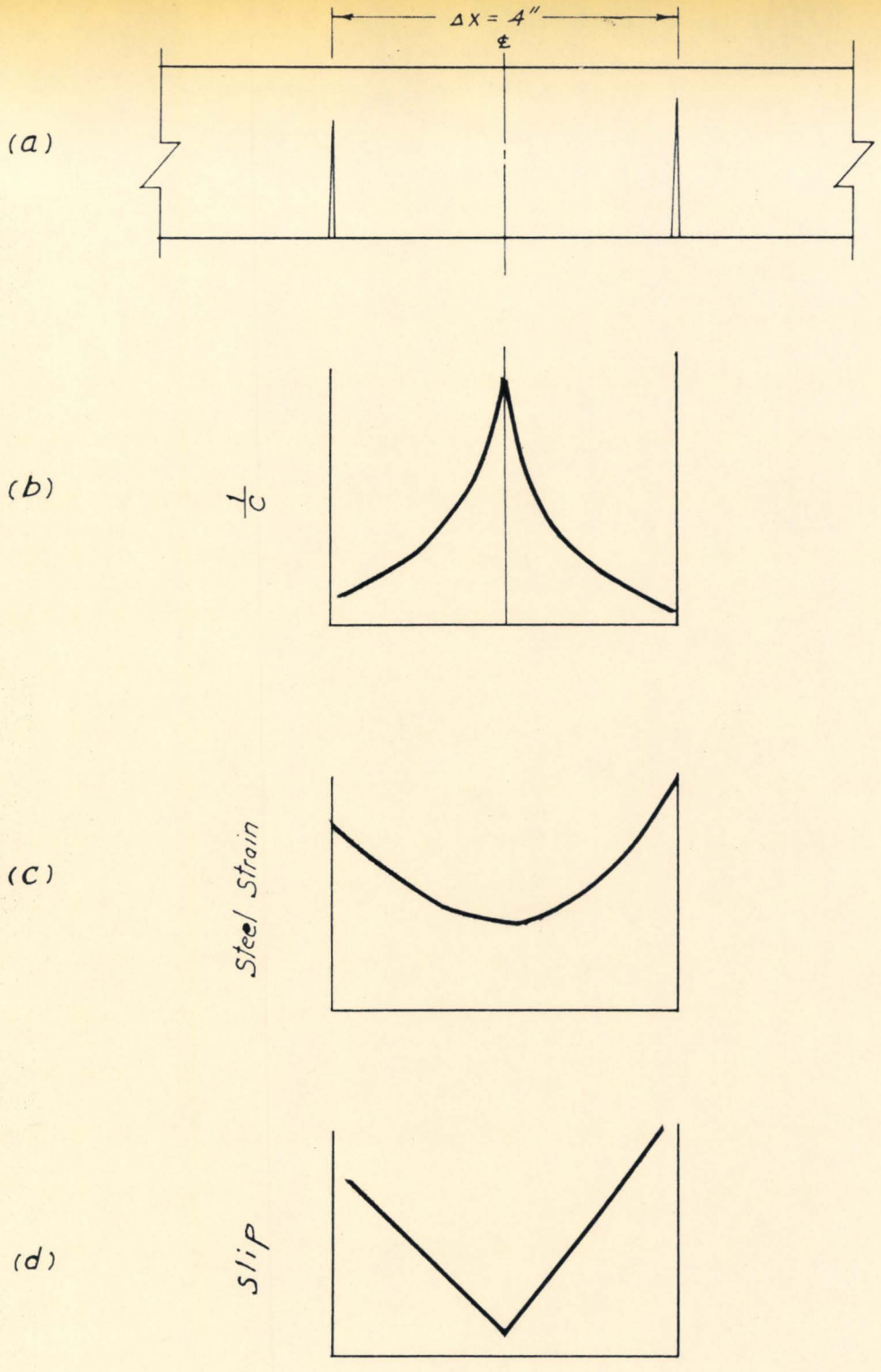

Figure 2.21

Suggested 1/c, Steel Strain and Slip Distribution in Between Two Cracks (not computed).

incomplete interaction. Figure (2-22) shows schematically the two different possible approaches in measuring the slip at a particular section.

Experimental results are always reliable provided suitable techniques and devices are available. By interpreting the experimental results performed by other investigators, it is hoped that the importance of the degree of interaction in a reinforced concrete beam through the composite action would be demonstrated.

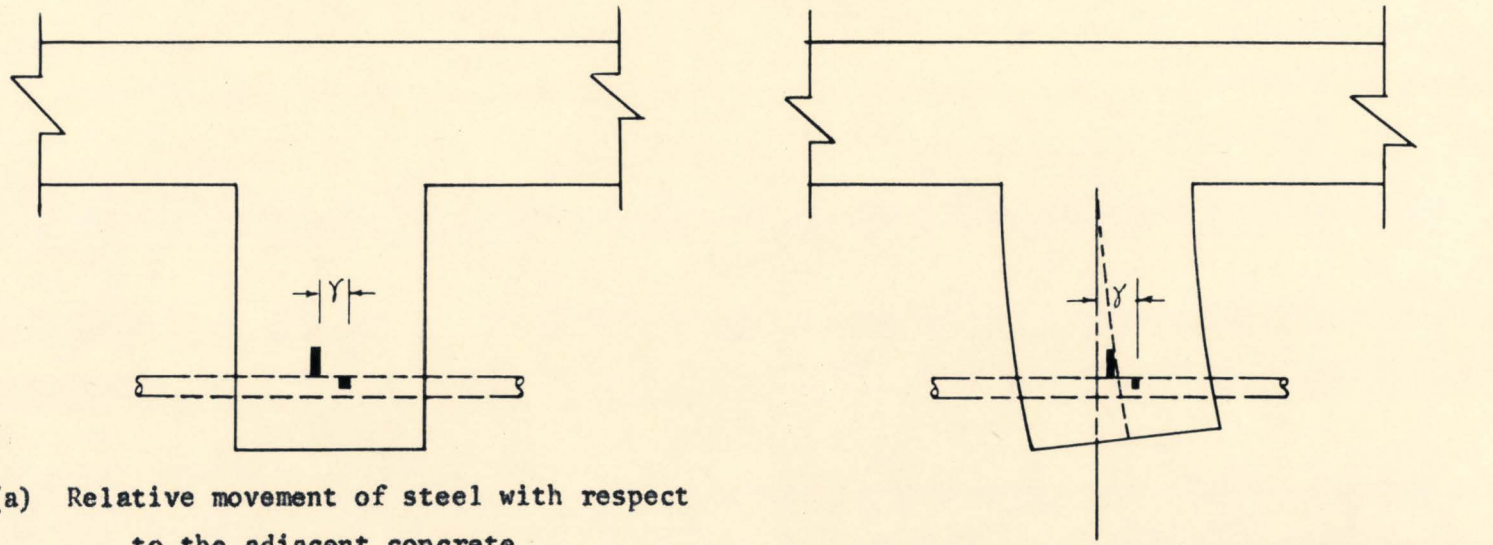

(a) Relative movement of steel with respect to the adjacent concrete

(b) Relative movement of steel with respect to the main concrete member

Slip Measurements of Steel With Respect to Concrete

Figure 2.22

CHAPTER 3

The Investigation of Degree of Interaction Based on Experimental Load-Slip Characteristics

It has been found that the arbitrarily assumed linear variation of 1/c from supports to the load points is not applicable, the variation of degree of interaction needs to be readjusted. Figure (3-1) shows the variation of upper, mid-height and lower strains along the tensile reinforcement of a cracked beam at both the design load and 1.7 times the design load. The degree of interaction was assumed to vary from 200 at the supports to 0.4 at the load points. It had been suggested[2,8] that for a reinforced concrete beam subjected to to increasing load, the strain distribution along the reinforcement does not necessarily follow the bending moment curve.

Figure (3-1) shows an envelope for steel strain that could provide limits of strain along the reinforcement similar to those measured by Plowman[2]. The computed mid-height steel strain along the reinforcement is comparatively lower in magnitude, while the bottom fibre steel strain is higher than that predicted by the straight line theory, especially in the region of the load points where the degree of breakdown of interaction is thought to be greatest. From Figure (3-1), it is noticed that at about 1.7 times the design load, the resulting steel strain under the load point approaches the yield value. Owing

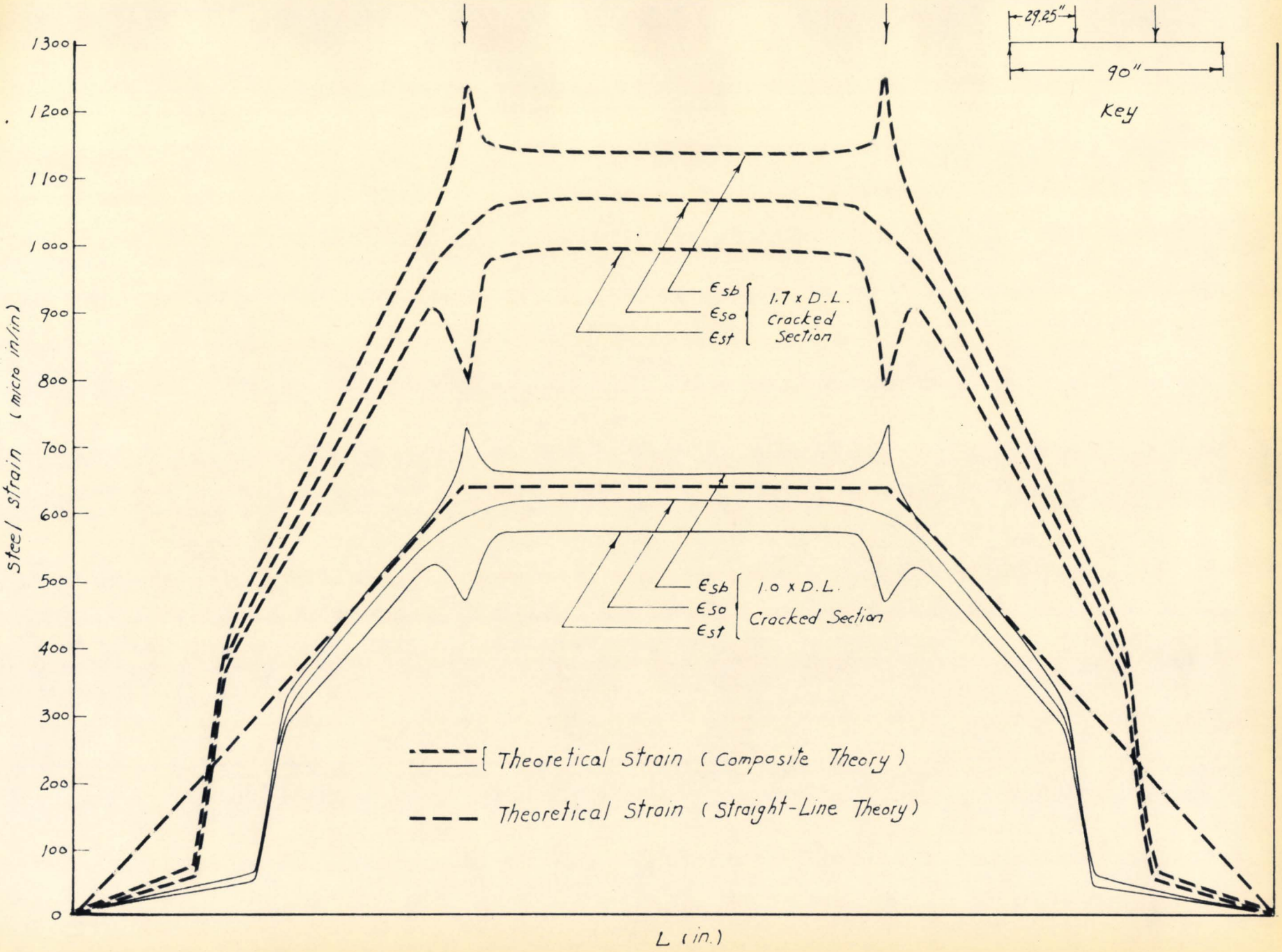

Figure 3.1 Variation of Top, Mid-Height and Bottom Steel Strain Along the Reinforcement

to the high degree of breakdown of interaction under the load point, the cracking path tends to upshoot rapidly towards the applied load (see figure 3-2).

On the basis of this speculation, the assumed linear 1/c is under investigation. From Newmark's composite beam solution[11], the amount of slip permitted by the shear connection (or bond) is directly proportional to the load transmitted by the steel, ($\gamma = Q/k$). However, the load transmitted through the steel depends on the ratio of the horizontal force for incomplete interaction (F) to the horizontal force for complete interaction (F') or F/F'. This ratio in turn depends on the degree of interaction (1/c) at any particular section and the applied moment. For purposes of comparison, the load transmitted through the steel at design load was computed for an assumed linear variation of 1/c. From the geometry of the remaining uncracked section, the modulus k was obtained. The slip distribution and the corresponding force in the bar was computed. Figures (3-3) and (3-4) show the 1/c vs. Q_s and Q_s vs. slip curves respectively. It is of interest to note that the computed load-slip curve has a similar form to those measured by other experimenters[15]. In order to obtain a better distribution of 1/c which would occur in an actual test beam, a load-slip characteristic curve, from a beam test, measured by Mathey and Watstein[15] has been chosen.

The load and slip from the chosen curve were obtained from test results of a beam specimen reinforced with #4 high-yield strength

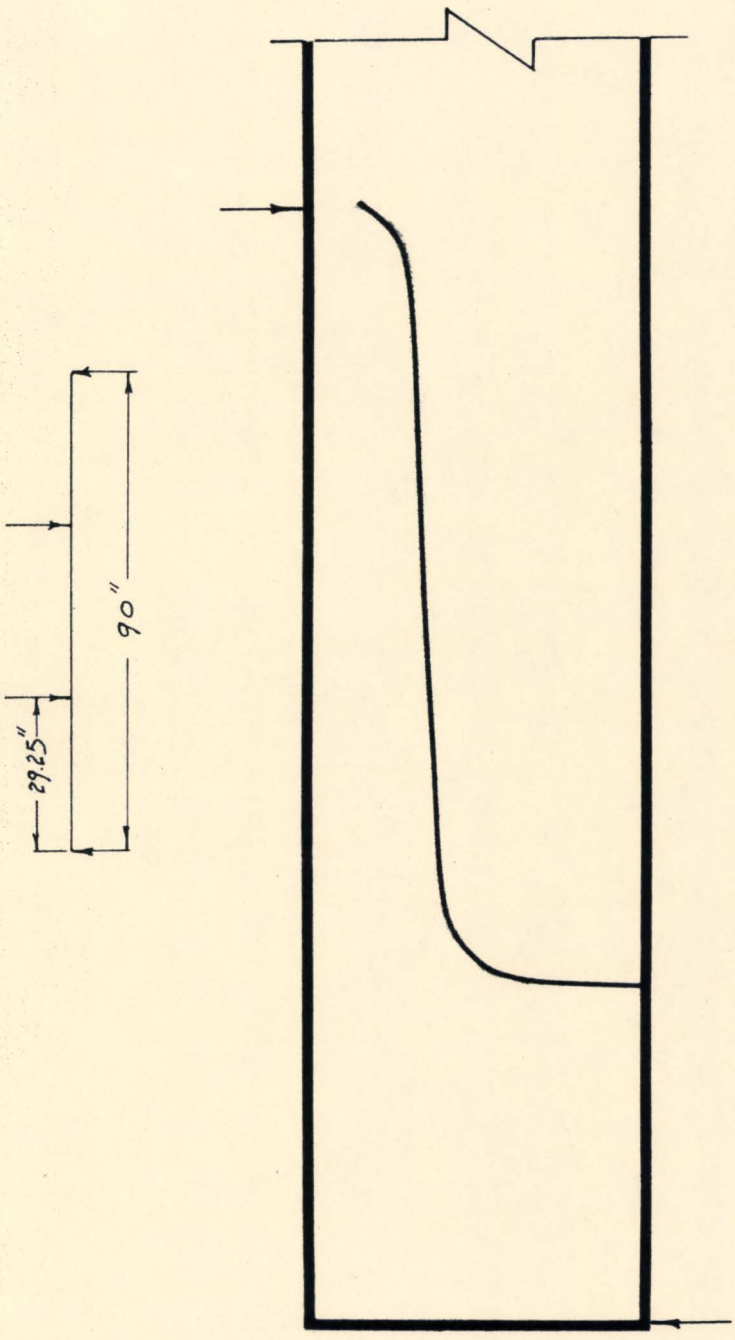

Figure 3.2

Estimated Extremities of Potential Cracks of a Reinforced Concrete Beam at 1.7 times Design Load (1/c varying along the beam)

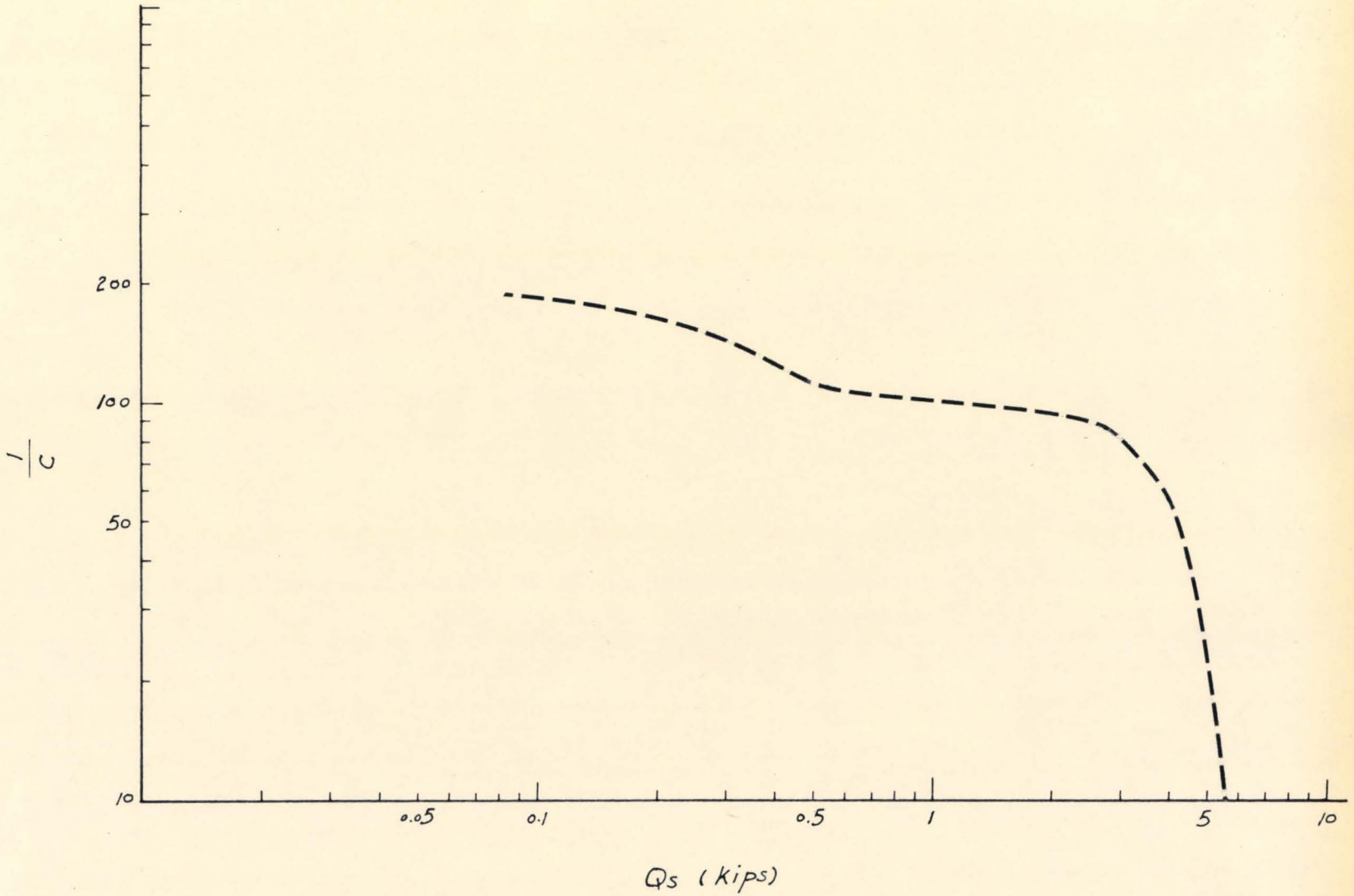

Figure 3.3

1/c vs. Q_s Curve

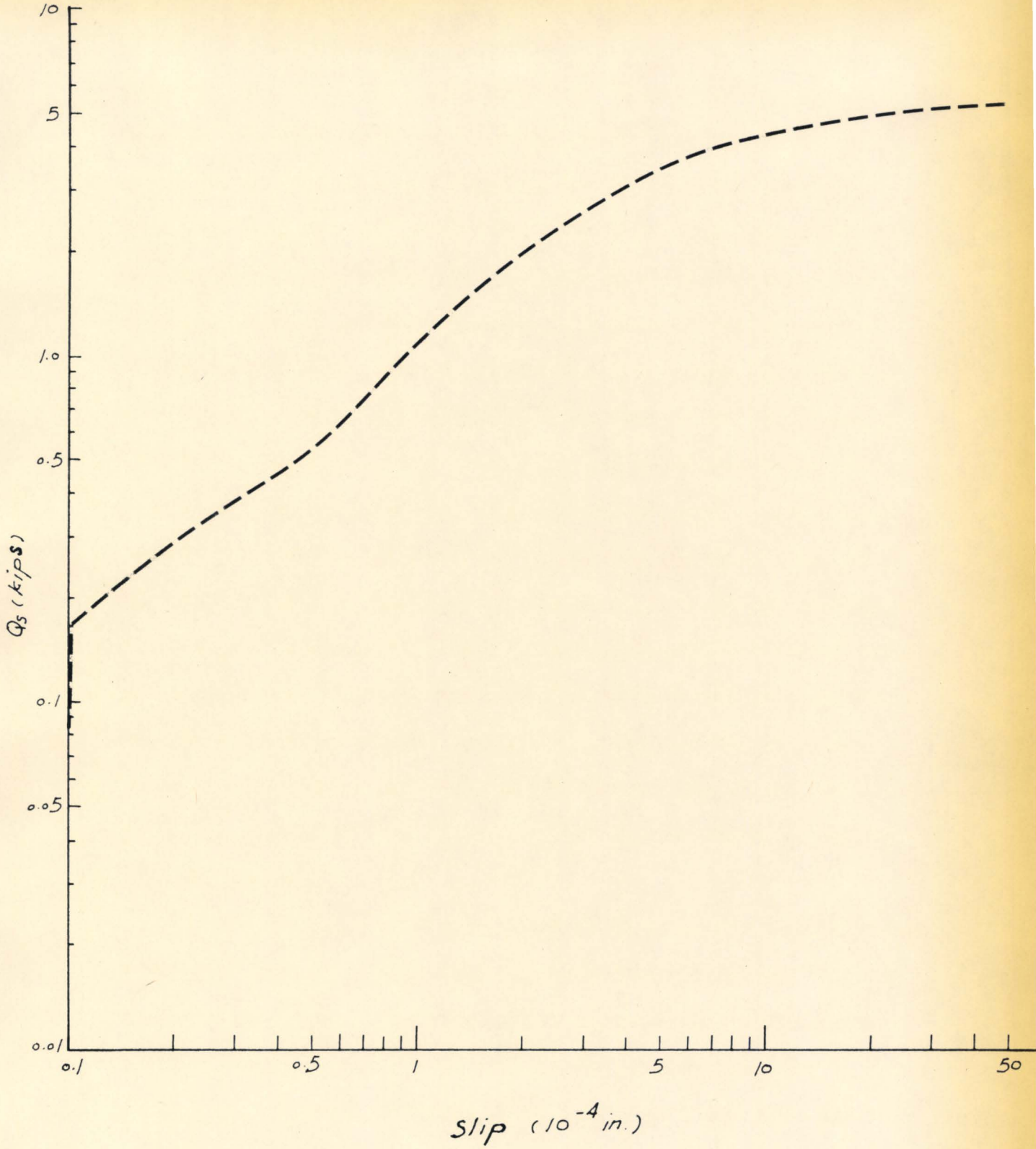

Figure 3.4 Q_s **vs. Slip Curve**

deformed bars. Details of beam specimens, testing arrangements and location of strain gages due to Mathey and Watstein are shown in figure (3-5). The beam specimens were tested as simply supported beams subjected to a two point load. The load points were directly over the outer edges of the 3-in. notches which exposed the bar at the loaded ends of the reinforcement. A yoke was clamped into the drilled contact points in the exposed bar. Dial gages were attached to the yoke, permitting measurement of the slip of the bar directly under the concentrated loads. The gages were mounted on steel angle clips which were attached with screws to the concrete. Strain in the tensile reinforcement at about 7/8 inches from the inner edges of the 3-in. notches was measured with bonded wire electrical resistance strain gages. The computed force in the reinforcing bar versus loaded-end slip curve is shown in figure (3-6). For purposes of computation, this characteristic curve is slightly modified as shown in figure (3-7). The curve is so modified, so that for a small force exerted in the steel, a value of slip can be obtained and the iteration process could be started.

The process of computation is based on the Newmark composite solution[11] and the chosen load-slip characteristic curve. A hypothetical beam subjected to a two point load is under investigation. On the consideration of a beam with complete interaction, the F' and q' diagrams are as shown in figures (3-8) and (3-9). The F' is the

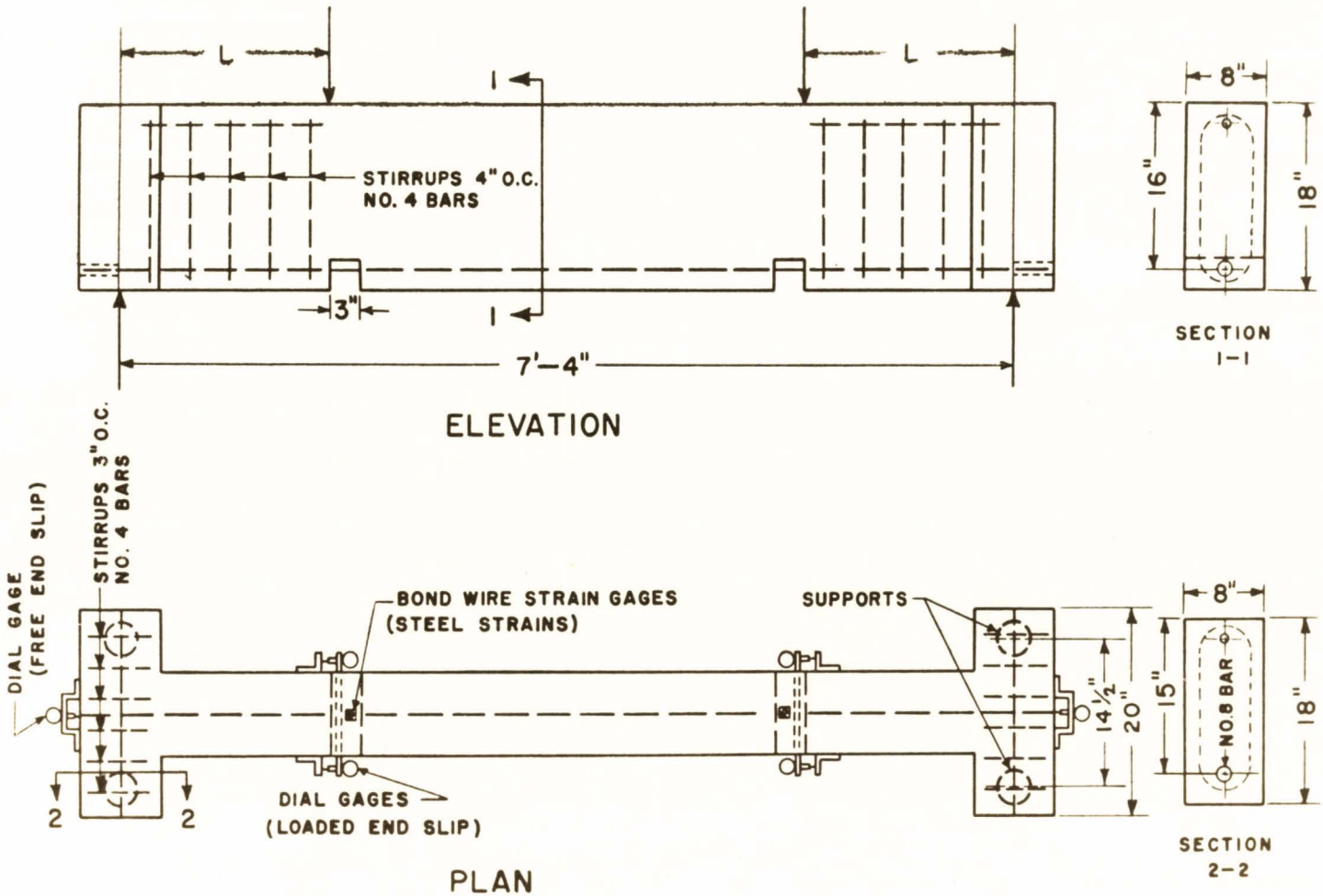

-Details of beam specimens, testing arrangement, and location of strain gages

Figure 3.5 Details of Beam Specimen, Due to Mathey and Watstein

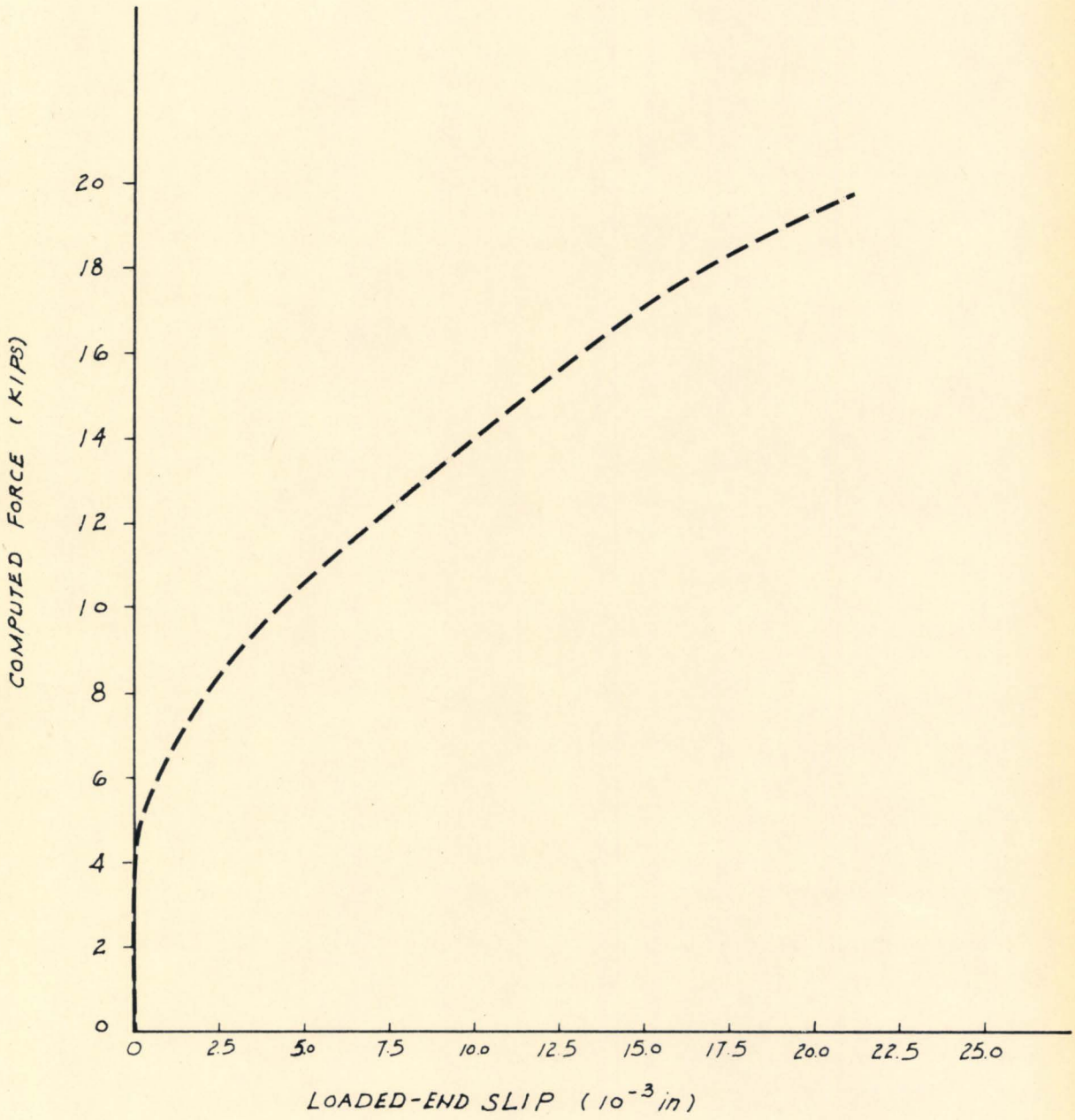

Figure 3.6

Load-Slip Characteristic Curve (beam specimen), Due to Mathey and Watstein

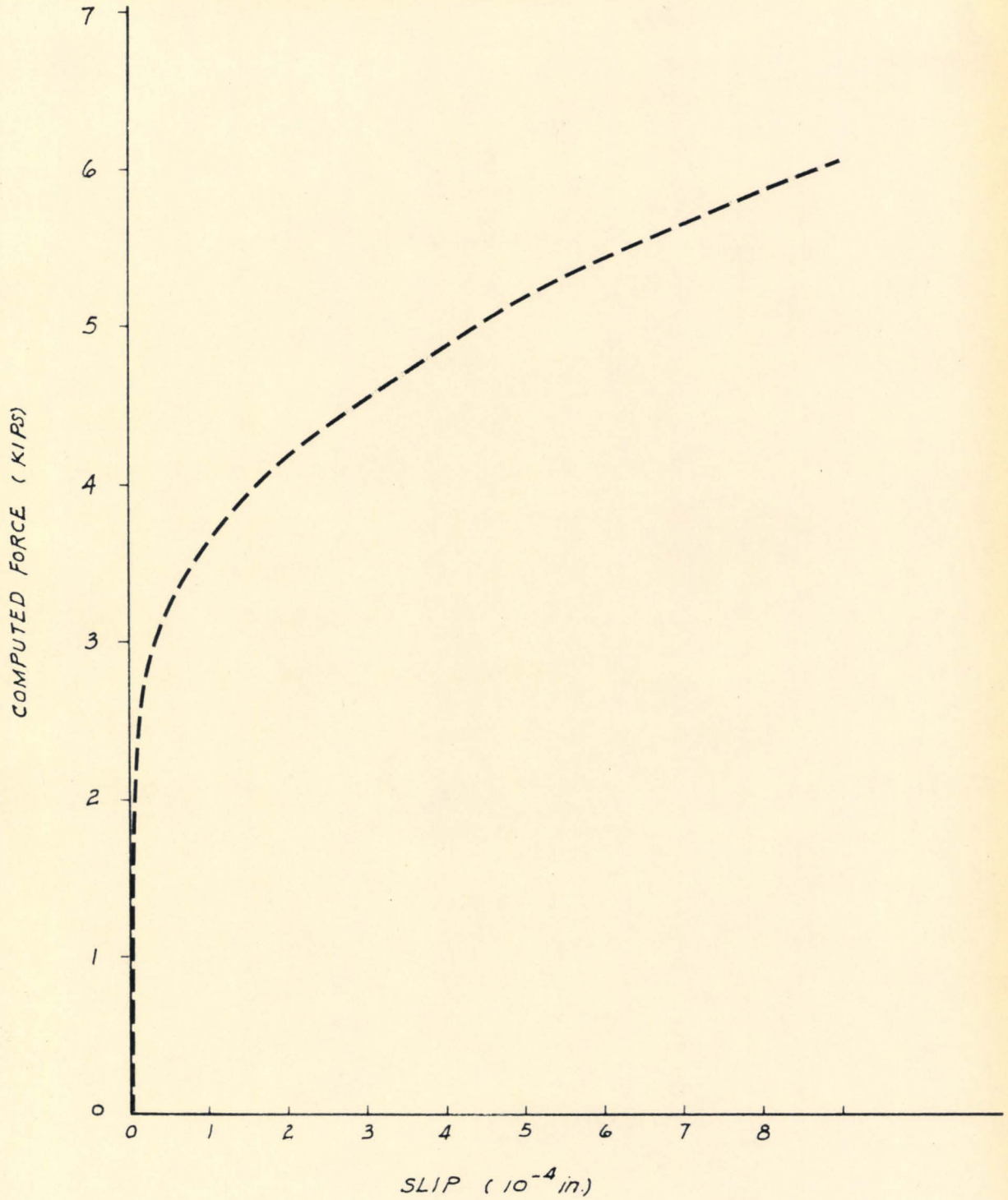

Figure 3.7

Modified Load-Slip Characteristic Curve

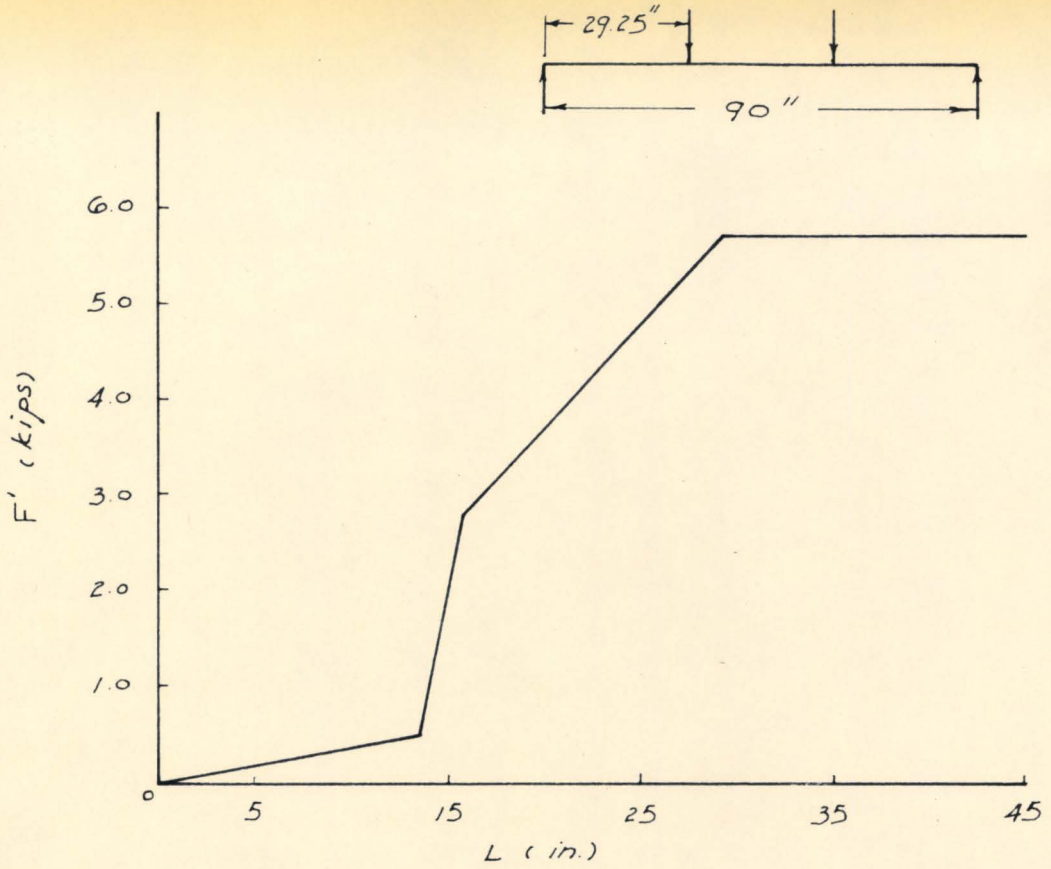

Figure 3.8 F' vs. Length of the Beam Curve

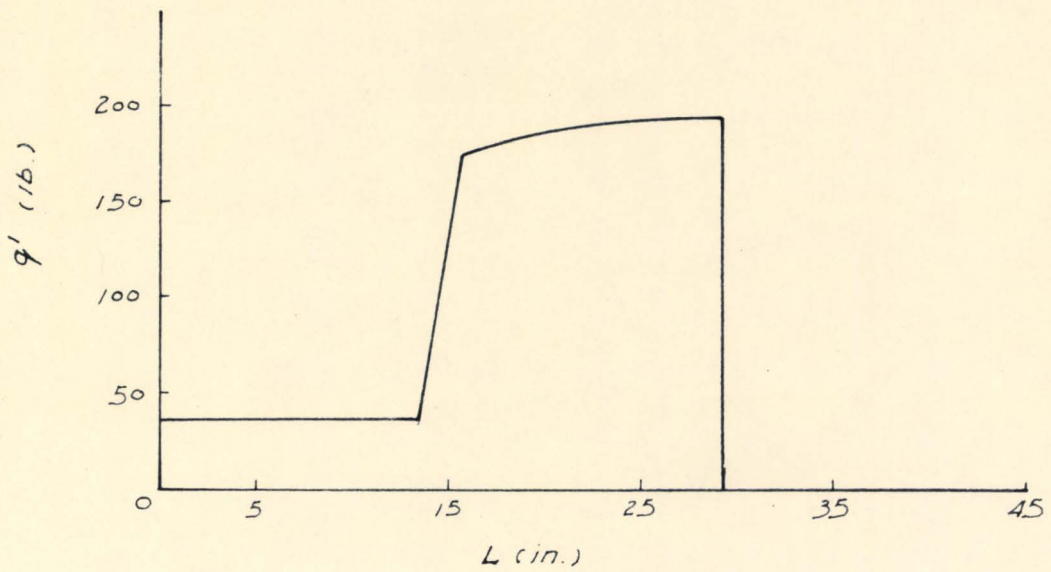

Figure 3.9 q' vs. Length of the Beam Curve

horizontal direct force acting at the centroid of the cross-sectional area of the steel and q' is the horizontal unit shear. It is noticed that F' is a function of the applied moment and the section geometry as it varies along the length of the beam ($F' = \frac{\overline{EA}}{\overline{EI}} Z M$), while q' is a function of the vertical shear and the section geometry ($q' = \frac{\overline{EA}}{\overline{EI}} Z V$). After the beam has been cracked, the remaining uncracked sections above the extremities of flexural cracks varied; causing variation in the section geometry. At this stage the beam is considered to be subjected to breakdown of interaction. Through the influence of varying degrees of interaction, the F' and q' have changed to F and q; where both F and q are the horizontal force and shear in the case of incomplete interaction.

The beam was first treated as a cracked beam with complete interaction. The F' at various sections along the length of the beam were computed by the composite beam solution. With the known forces F', the corresponding slips were obtained from the load-slip characteristic curve. Then values of q' were computed. Since there is no vertical shear between the load points, the values of q' within these sections should be zero. For purposes of computation, a constant value of q' was assumed along these sections inside the pure moment region in the first iteration. With the known value of q' and slip at each section, the modulus k could be obtained ($k = \frac{q's}{\gamma}$). Once the values of k and the section geometry were known at different sections, then C or 1/c; the interaction coefficient could readily be computed. The beam was

then considered to suffer a loss of interaction. With the known values of 1/c at the appropriate sections, F and q were computed. With the computed values of F, corresponding slips were obtained from the curve. Modulus k was estimated from the known values of q and slip at different sections, and 1/c was again computed. The process was repeated for several iterations until a convergence of F had been reached.

The computed 1/c values at 1.0, 1.5 and 2.0 times the design load are presented in figure (3-10) and show that 1/c varies in some curvilinear manner along the beam. At design load, the value of 1/c is very high at the support, and decreases to about 25 at the load point. From the composite beam notation, for 1/c = 25 the interaction is practically perfect. At 1.5 times the design load, the 1/c values diminished in a similar manner to a value of 8 at the load point. Under further loading, the value of 1/c at the load point has been lowered to 5 at 2 times the design load.

The computation of 1/c by using the process described above gives reasonable results only in the shear spans. For a short distance close to the supports and sections within the pure moment region, the 1/c values could not be justified. For sections close to the supports, values of F and q were very small and the corresponding slips were practically negligible. From the first iteration of the above described process, the initial values of q' within the pure moment region were assumed. After six iterations, it was found that no convergence was obtained for the region between the load points.

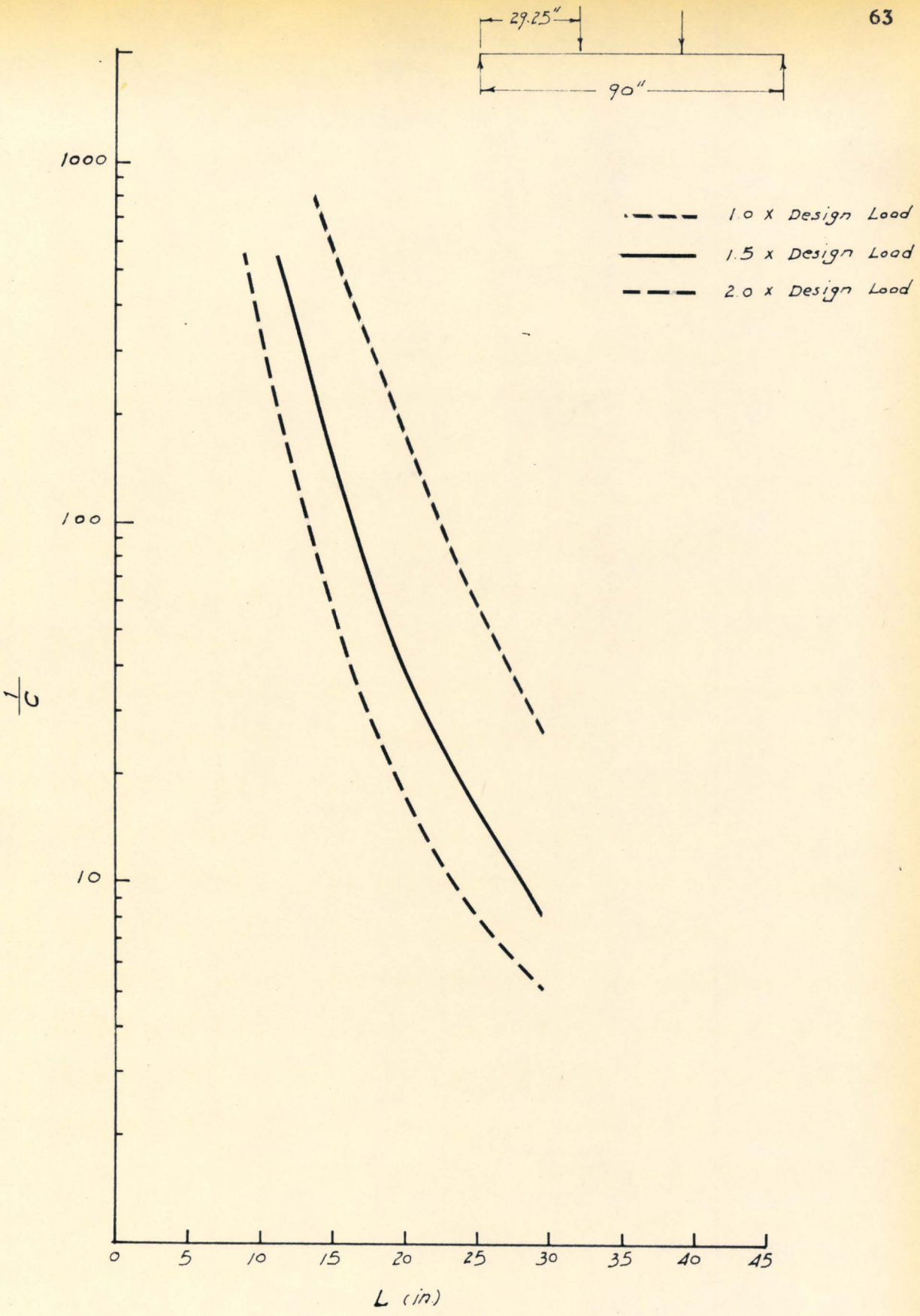

Figure 3.10 Values of 1/c Obtained From the Beam Load-Slip Characteristics at Various Loadings.

These computations indicate that values of 1/c do not degenerate too much; especially in the case of the 1/c value under the load point. At 2.0 times the design load, a value of 1/c = 5 is still considered to be a high degree of interaction. The value of 1/c is proportional to the modulus k; which in turn is inversely proportional to the slip:

$$c = \frac{s}{k} \quad \frac{\pi^2 \overline{EA} \; \Sigma \; EI}{L^2 \; \overline{EI}} \qquad k = qs/\gamma$$

A high value of 1/c indicates that the modulus k is high and the corresponding slip is small. In other words from the beam specimens load-slip characteristic curve, the slip under the load point at 2.0 times the design load is not high enough to generate what is considered to be an appropriately small value of 1/c; small enough to push the cracked zone upwards.

It has been suspected that the instrumentation used by the authors[15] would account for the relatively low slip measurements . The loaded-end slip was measured by the movement of the exposed bar directly under the load point. Since there is no adhesion in the exposed bar, the measured slip would not be the true slip as would be the case when the steel bar is totally surrounded by concrete. Furthermore, the measured slip was the relative movement of the steel with respect to the adjacent concrete. The "concrete teeth" or "concrete strip" between two cracks may be subjected to a small rotation

or relative displacement with respect to the remaining uncracked zone (or the main body of the member). Then the slip measured from the relative movement of the steel with respect to the adjacent concrete would be smaller than the relative movement of the steel with respect to the main member, or the so-called pseudo-interface.

A comparatively higher slip would result from a pull-out test than for the beam specimen test. For purposes of comparison, a pull-out specimen load-slip characteristic curve measured by the same authors[15] was chosen. It was hoped that by such a load-slip curve, a greater degree of breakdown of interaction would be obtained, and the importance of bond slip characteristic could be further demonstrated.

The measured values were obtained from the tested pull-out specimens. These specimens were reinforced with the same size-strength bars. The specimen, loaded as shown in figure (3-11), was seated on a leather cushion on two segments of a 2 in. base plate attached to spherical bearing blocks. Slip of the bar was measured with micrometer dial gages. At the loaded end of the specimen, two dial gages were attached to the steel bar mounted on the face of the concrete. The average of the two gage readings indicated the amount of movement of the point on the reinforcing bar with reference to the face of the concrete.

Figure (3-12) shows the pull-out specimens load-slip characteristic curve measured by Mathey and Watstein[15]. In computing the degree of breakdown on interaction (values of 1/c), the same

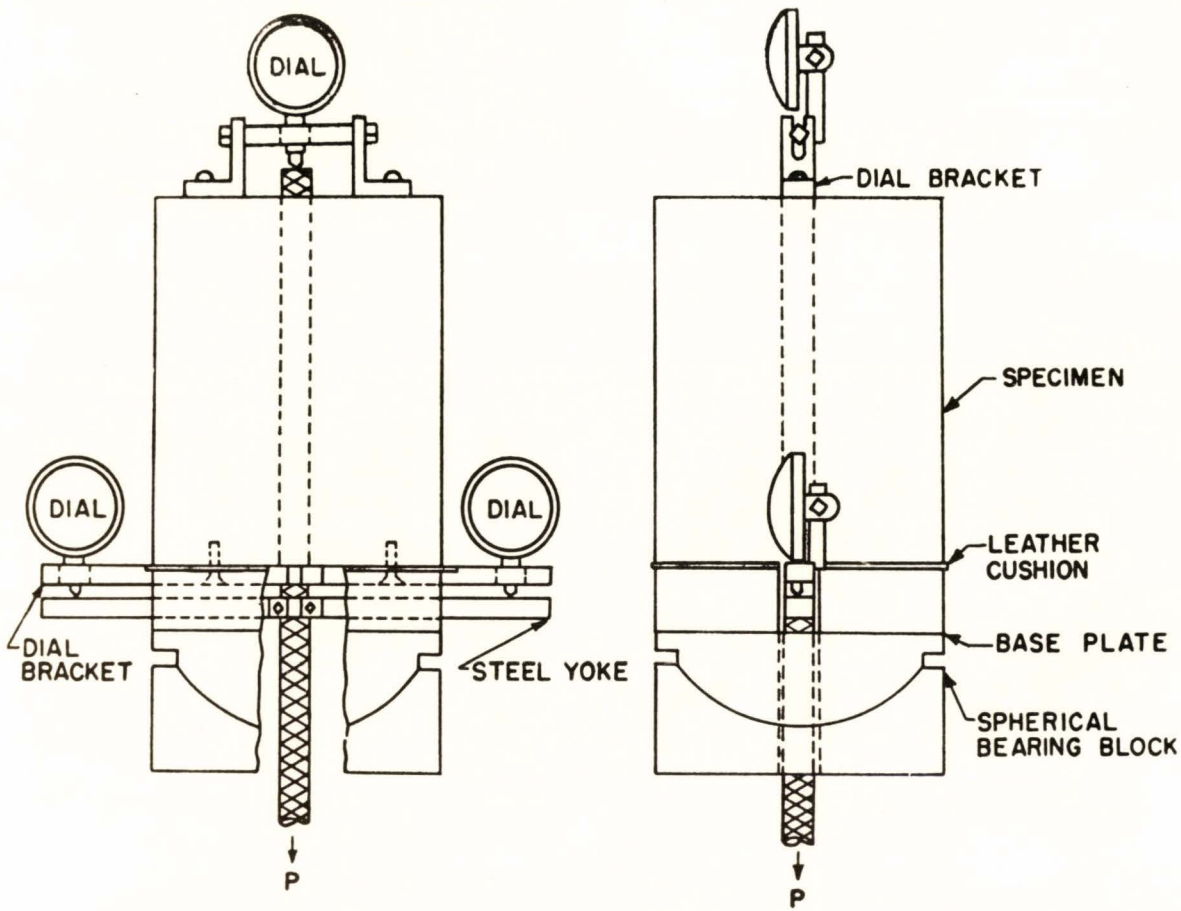

—Details of
specimens, testing
ment, and location
gages

Figure 3.11

Due to Mathey and Watstein

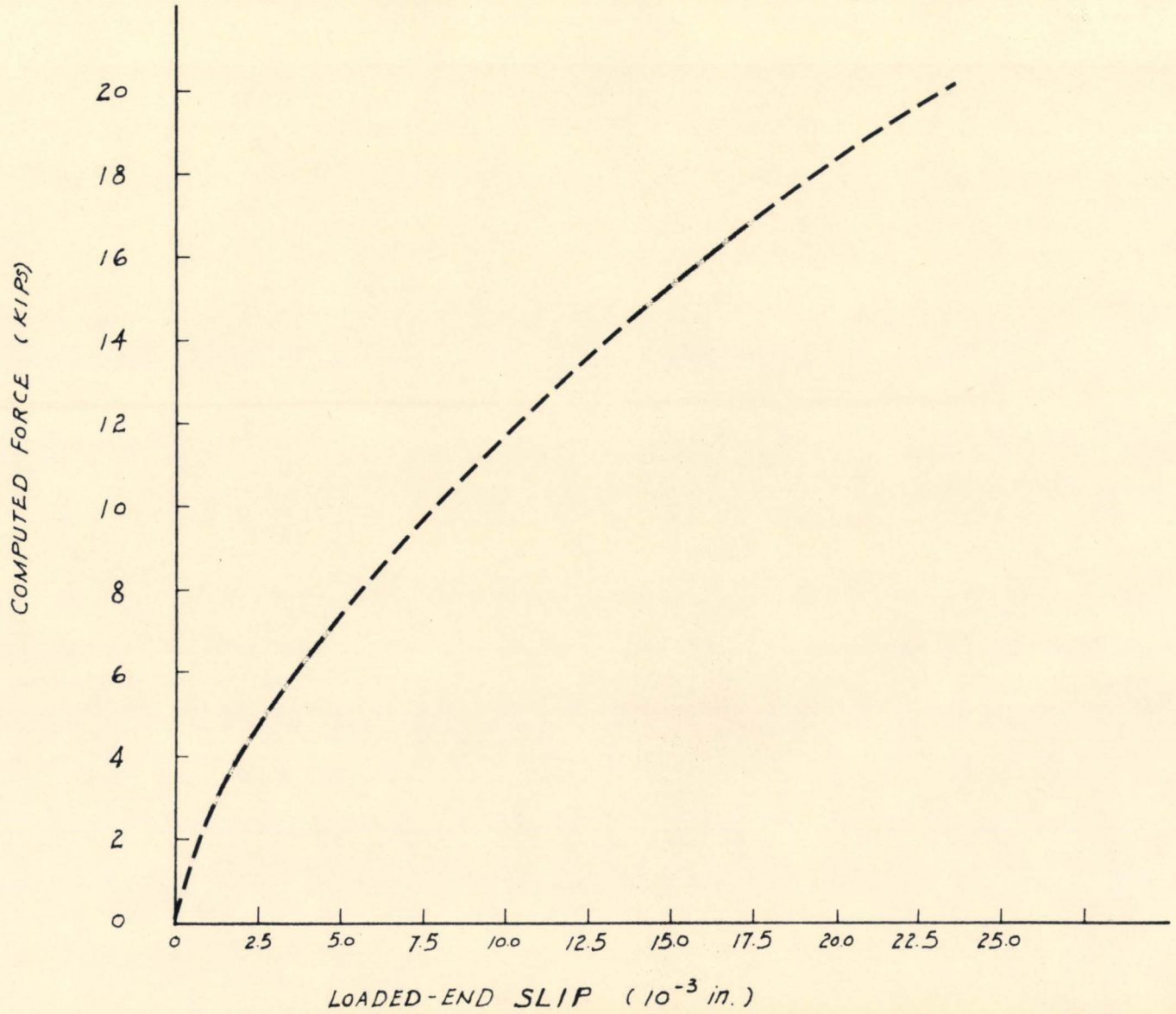

Figure 3.12

Load-Slip Characteristic Curve (Pull-Out Specimen) Due to Mathey and Watstein

procedure for the computations of the beam specimen as described above was employed.

The computed 1/c values at 1.0, 1.5 and 2.0 times the design load are presented in figure (3-13). These computated 1/c distributions were generally similar to those from the beam-specimen test. At design load, the degree of interaction (represented by 1/c) is about 4.5. At 1.5 times the design load, the degree of interaction decreases to 3.0. At 2.0 times the design load, it decreases further to about 2.5.

In the comparison of the two sets of 1/c values computed from both the beam specimens and pull-out specimens load-slip characteristic curves, it has been noted that with a higher magnitude of slip, a higher degree of breakdown of interaction would result. The slip values measured from the pull-out specimens are higher than those from beam specimens. The greater disparity between them is due to the different testing conditions and the effects of flexural cracks. Since the beam-specimens are usually tested by a point-load system, both the steel reinforcement and the surrounding concrete would be in tension when the beam is subjected to the applied load. In the pull-out tests, the steel rod is subjected to a pulling force at the loaded end. The steel rod would be in tension while the surrounding concrete would be in compression. Furthermore in the beam specimens, flexural cracks develop within the shear span. The effects of flexural cracking would tend to distribute the elongation of the steel in several places where cracks are present, resulting in a smaller load-end slip. It has been pointed out[19] that pull-out and beam

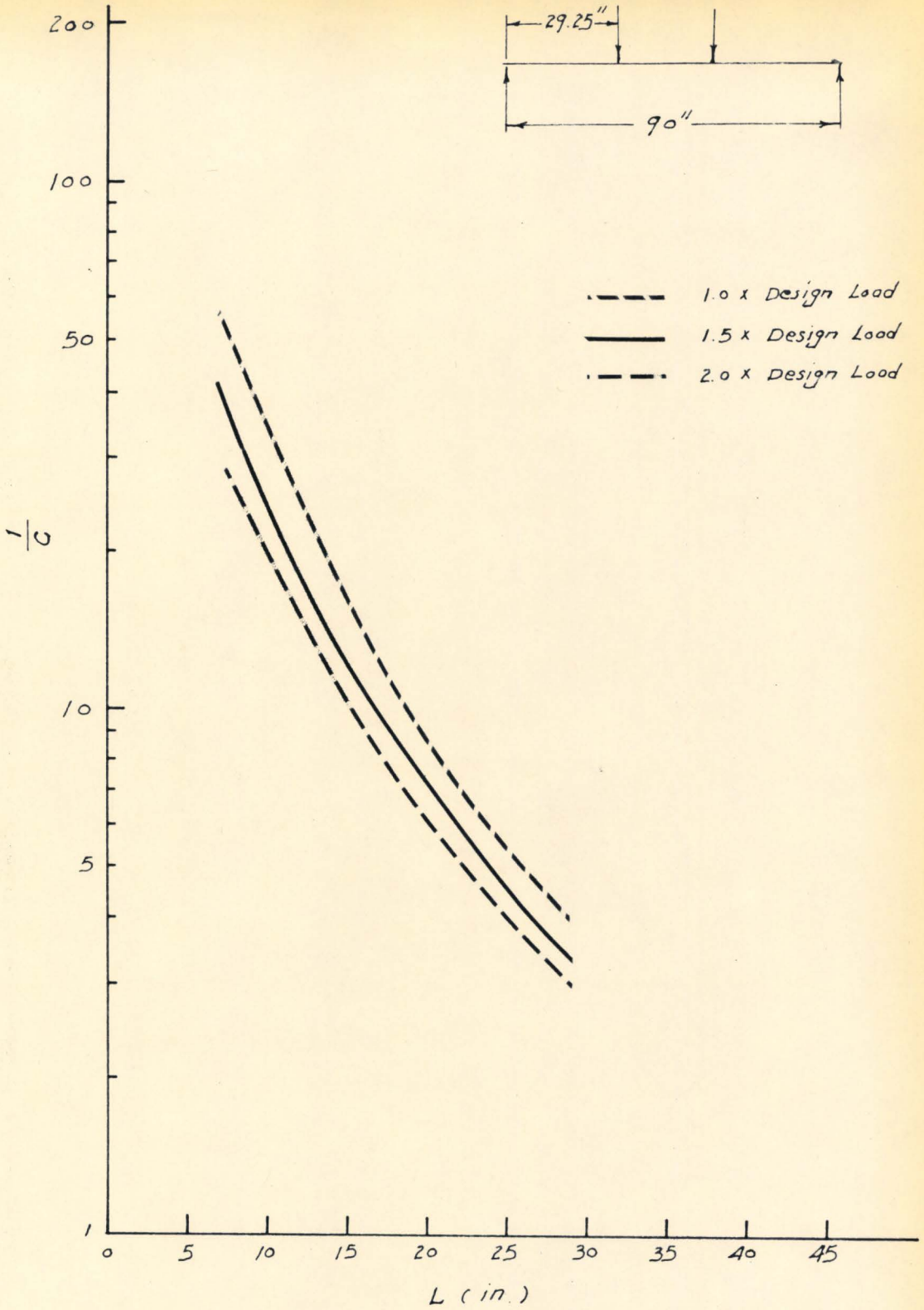

Figure 3.13 Values of 1/c Obtained From the Pull-Out Load-Slip Characteristics at Various Loadings

specimens yield comparable results only when the length of the pull-out specimen is comparable to the distance from the free end of the bar in a beam to the nearest crack within the shear span. On this basis, the flexural cracks at a given steel strain might well be narrower than the slip at the loaded end of a pull-out specimen. It would be reasonable to observe that a more reliable loaded-end slip could be obtained from the beam specimen, provided that the instrumentation is capable of measuring the actual total slip at that particular section.

Based on the 1/c values computed from both the beam and the pull-out curves, potential crack profiles were estimated at 2.0 times the design load as presented in figure (3-14). It is noted that in both cases, the values of 1/c at the load point are not small enough to push to crack significantly upwards into the compression zone. From both the beam and the pull-out load slip curves, it is further noticed that at the lower load stage, slip increase with load is small. At the higher load stage (approximately above 2.0 times the design load), the slip increases more rapidly. At 3.5 times the design load, it is found that no slip values could be obtained from the curves. However, it is speculated that for a load about 3 to 3.4 times the design load, a smaller value of 1/c could be obtained. The small 1/c indicates a very high degree of breakdown of interaction, resulting in the extension of the crack into the compression zone and bringing about the final failure of the member.

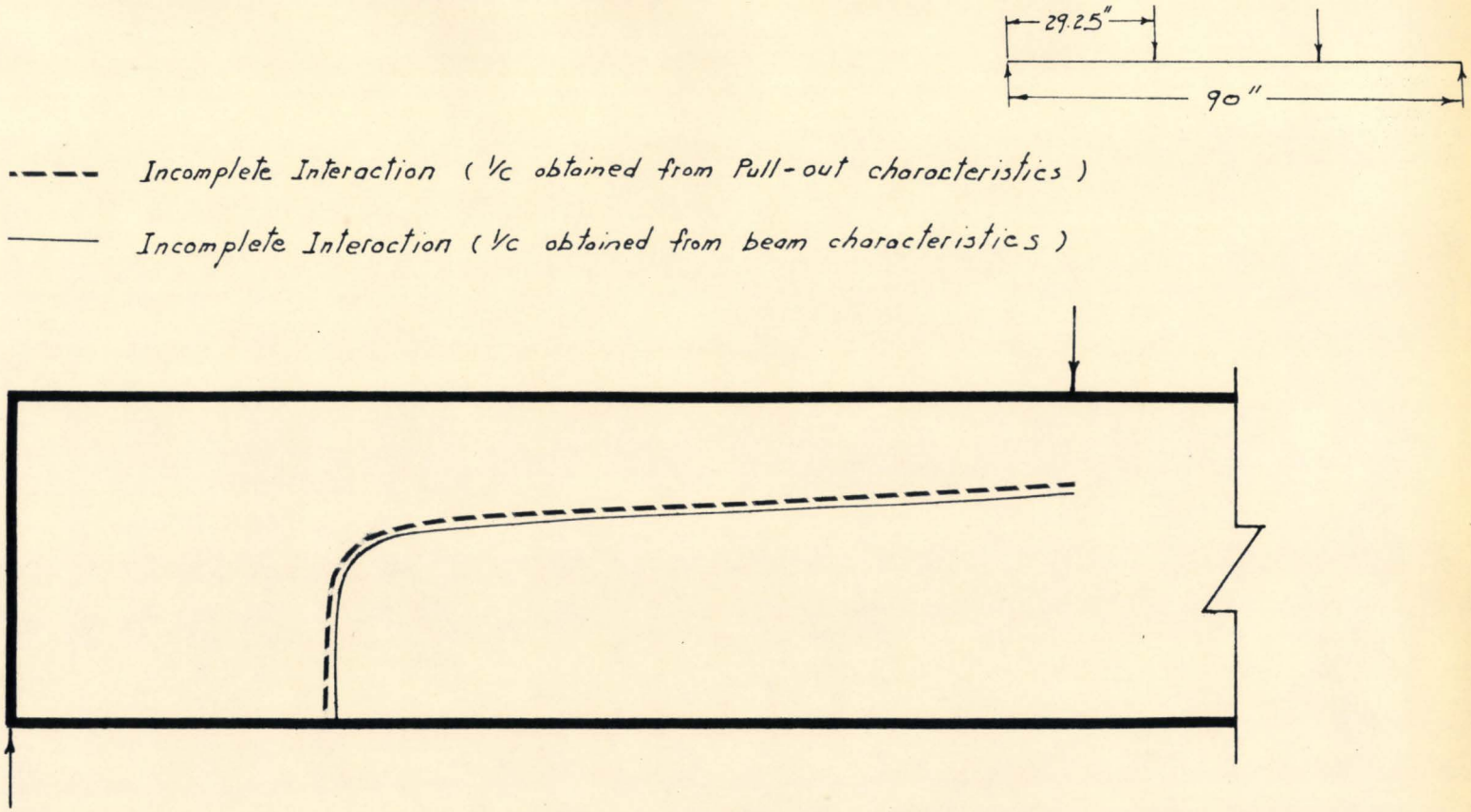

Figure 3.14

Estimated Extremities of Potential Cracks of a Reinforced Concrete Beam at 2.0 x Design Load

It is believed that the variation of 1/c along the length of the beam from supports to load points plays an important role in determining the failure modes of reinforced concrete beams. The degree of breakdown of interaction at any section depends upon the load slip characteristic of the reinforcing bar. For the beam reinforced with steel of poor bond, the major crack is expected to occur in the vicinity of the load point. Under increasing load, owing to the inadequate bond resistance, the slip and the length of the crack under the load point increases rapidly. The degree of breakdown of interaction would be very high (represented by a very small 1/c), and causes the flexural crack to propagate rapidly into the compression zone. Eventually the stress in the compression zone reaches the compressive strength of the concrete, resulting in the flexural failure of the beam before the premature diagonal crack can be developed. For the beam reinforced with steel of better bond, cracks are still expected to occur close to the load points. However, with better resistance the slip and the extension of these cracks could be reduced. The trigger mechanism of the so-called "diagonal cracking" phenomenon of reinforced concrete beams has not been known. By interpreting the test results obtained by other investigators, the measured steel strain and slip distributions show qualitative agreement with the estimated values when the composite beam concept is applied. It is further reasoned that micro-cracks would occur in the shear span,

resulting from the localized breakdown of interaction effect. The extremities of these flexural cracks, depending upon the degrees of interaction, govern the shape and possibly the formation of the matured diagonal crack.

CHAPTER 4

Load Tests on Reinforced Concrete Beams

4.1 Objectives of Investigation

The primary purposes of these tests were to study experimentally the cracking profiles of reinforced concrete beams subjected to a two point loading system, through the influences of loading condition and the varying quality of the bond in the tensile reinforcement.

From Newmark's conventional composite beam results, it has been found that the reduction in the interaction is a localized effect. Robinson[1,9] and Wong[11] further suggested that the major loss of interaction occurred at the section under the applied load, resulting in an estimated crack profile with an upshooting portion close to the applied load. In this series of tests, two beams were reinforced with plain bars and welded washers as shown in figure (4-1). The main purpose of the welded washers was to ensure better bond performance along the steel. Furthermore, by welding washers directly under the load point, it was hoped that the localized slip could be reduced. This in turn would increase the degree of interaction and decreased the height of the crack under the load point

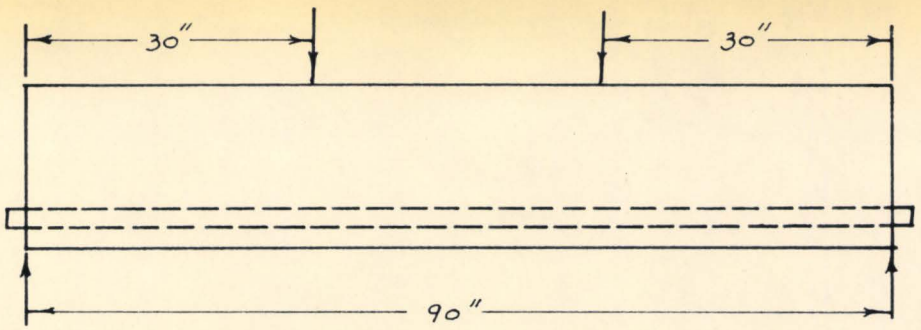

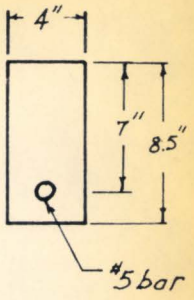

B1 & B5

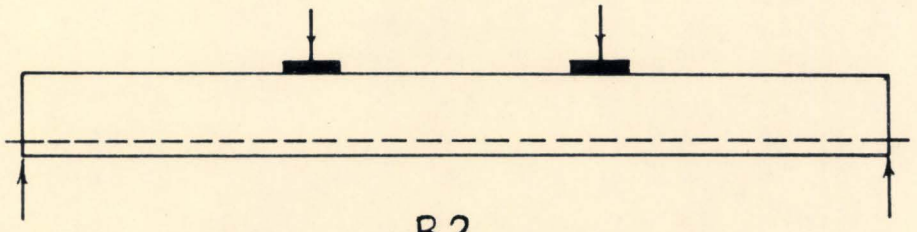

B2

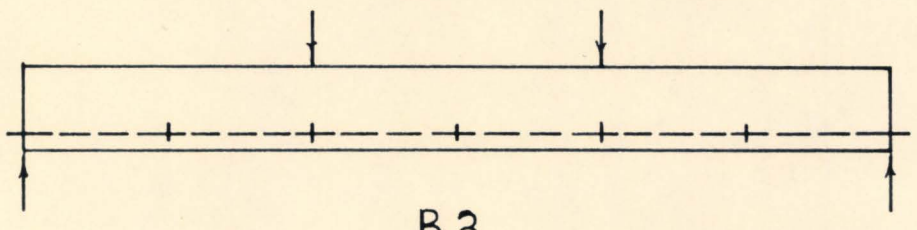

B3

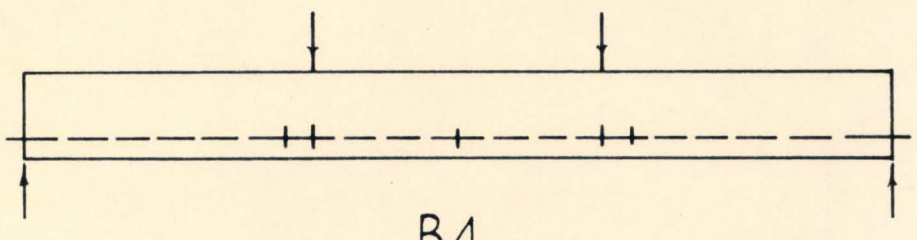

B4

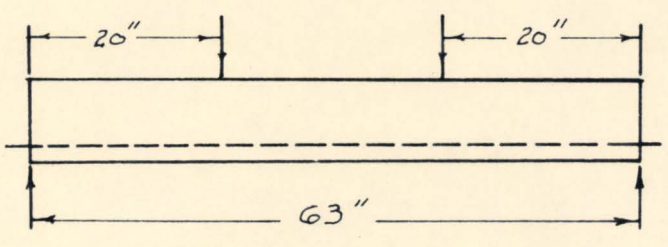

B6

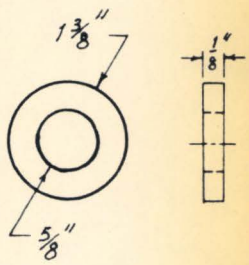

washer's dimensions

Figure 4.1 Details of Beam Specimens

4.2 Reinforcement

Six beam plywood forms were constructed. Three different types of reinforcement were used. Beams B1, B2, B3 and B4 were singly reinforced with 5/8 inch diameter plain bars. In beams B3 and B4, five steel washers were welded along the reinforcement. They were so distributed that in B3, washers were equally spaced along the reinforcement, while in B4 the two washers in the two shear spans were placed 3 inches away from the two load points. Beams B5 and B6 were singly reinforced with the same size galvanized steel bar. All beams were of the same cross-section and reinforcing ratio. Figure (4-1) shows the details of beams, loading positions and the location of washers along the reinforcement.

4.3 Concrete

The concrete used was a nominal 3500 psi commercial ready-mix concrete, containing a maximum aggregate size of 3/4 inch. Before pouring the concrete, water was added to the mix so that the concrete had a one-inch slump. Twelve standard 6" x 12" cylinders were made. The concrete was then poured into the forms uniformly in layers, and was vibrated internally with a commercial vibrator. After all beams and cylinders were made, they were covered with wet burlap. The burlap was kept wet for seven days and then removed.

These beam specimens were cured in the laboratory until time of testing.

The cylinders were tested either on the 28th day, when the first beam was tested, or at the time when the last beam was tested. The average compressive concrete strength and the modulus of elasticity were obtained.

4.4 Loading Arrangements and Test Procedure

All six beam specimens were tested with a two-point load. Beams B1 to B5 had the same "shear arm ratio" while B6 had a smaller a/d ratio , (see figure 4-1). The beams were simply supported by two roller type supports which were mounted on a steel I-beam. The beams were loaded by the testing machine through two knife edge assemblies. In beam B2, two load distribution steel plates (nominal dimension = 4" x 6" x 3/4") were placed directly under the load points in order to study their effect on the cracking profile.

During this testing programme, the Universal Testing Machine with a capacity of 120,000 lb. was used. In preparing the beams for testing, they were white washed so that any minute cracks could be traced by the naked eye. In addition, dial gages with magnetic bases were mounted at various locations under the testing beams to measure the deflections. The beams were then ready for testing. Figure (4-2) shows the general test arrangement.

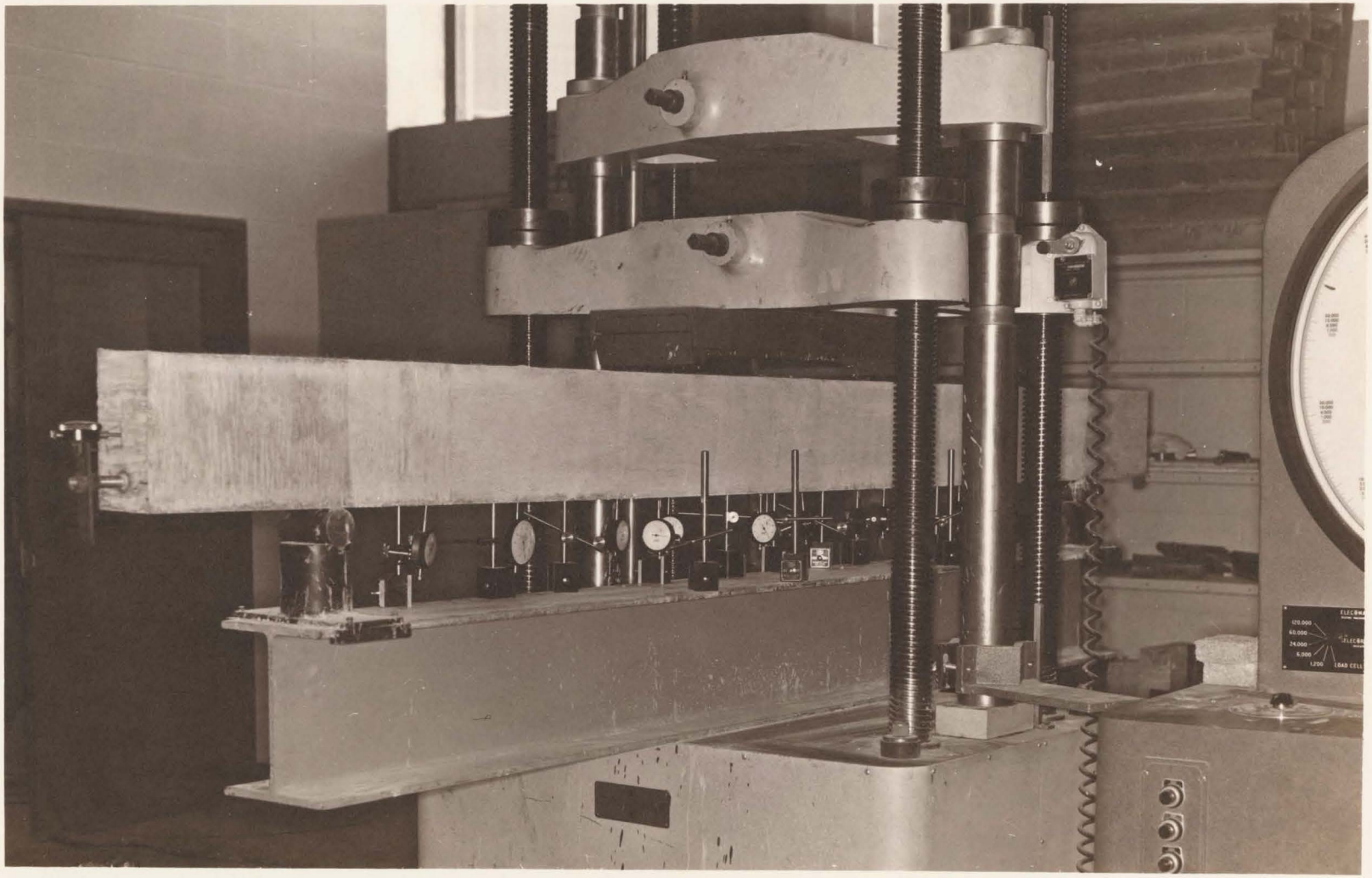

Figure 4.2 General Test Arrangement

The testing beam was loaded at a constant rate (0.1 inch per min) in 250 pound increments. At each load increment, dial readings were recorded and the surface of the beam was examined so that the development of the minute cracks could be carefully traced and marked.

4.5 Test Observations

Figure (4-3) shows the crack profile of beam B1. The first flexural crack was observed at the tension surface of the beam at about design load. As load increments were added, more and more flexural cracks occurred in the pure moment region. They all progressed vertically upward, passing the tensile reinforcement and extending towards the neutral surface of the beam. With further increase in load, flexural cracks in the pure moment region propagated upward towards the compression zone. The final characteristic Y-shape cracks[16] were formed.

Cracks in the shear span developed rather differently from those in between the load points. As observed from the test, cracks in the shear spans started to appear at about 1.5 times the design load. Under increasing load, the crack close to the applied load propagated rapidly into the compression zone. The crushing of the contact concrete under the applied load brought about the flexural failure of the beam.

The crack profiles of beam B2 are shown in figure (4-4). Cracks in the pure moment region and in the shear span developed in a similar manner to those observed in beam B1. The only noticeable difference observed between B1 and B2 was the spacing of cracks in the shear span.

The crack profiles of beam B3 with washers equally spaced along the reinforcement are shown in figure (4-5). The flexural cracks within the pure moment region had a pattern similar to those observed in beams B1 and B2. At about 1.3 times the design load, cracks began to show in the shear span. As the load increased, these flexural cracks extended upward. At about 2.2 times the design load, a characteristic inclined crack (or the so-called diagonal crack) began to form. It appeared at the existing flexural crack about 6 inches away from the applied load in the shear span. With further increase in load, this diagonal crack propagated, inclining upward towards the applied load. Close to the ultimate test load (about 9000 pounds), the inclined crack extended into the compression zone and backward towards the reinforcement, resulting in the final failure of the member.

Figure (4-6) shows the crack profiles of beam B4. It had been observed that the developments of the flexural cracks and the characteristic diagonal crack had a similar pattern to those observed in beam B3. The same type of final failure was noticed.

The crack profiles of beam B5 reinforced with galvanized steel are shown in figure (4-7). Flexural cracks began to appear inside the pure moment region at about one-half times the design load. The later developments of these flexural cracks were similar to those observed in the other beams. The first crack in the shear span appeared at about 1.4 times the design load. At about 2.5 times the design load, the crack started to incline from an existing flexural crack at about 8 inches away from the applied load. Under increasing load, this inclined crack propagated into the compression zone towards the applied load. At the same time, the inclined crack extended backwards towards the tension zone. At about 3.6 times the design load, the crushing of the intact concrete above the diagonal crack and the splitting of the concrete at the level of the reinforcement led to the ultimate failure of the member.

Figure (4-8) shows the crack profiles of beam B6 which was loaded with a smaller "shear arm ratio" as shown in figure (4-1). It was observed that a diagonal crack also formed from the existing flexural crack in the shear span (at about 1.9 times the design load). When load was increased, the existing diagonal crack propagated upward towards the compression zone, flattened under the load point and extending into the pure moment region. At the same time, a backward extension of this diagonal crack into the tension zone brought about the diagonal failure of the beam.

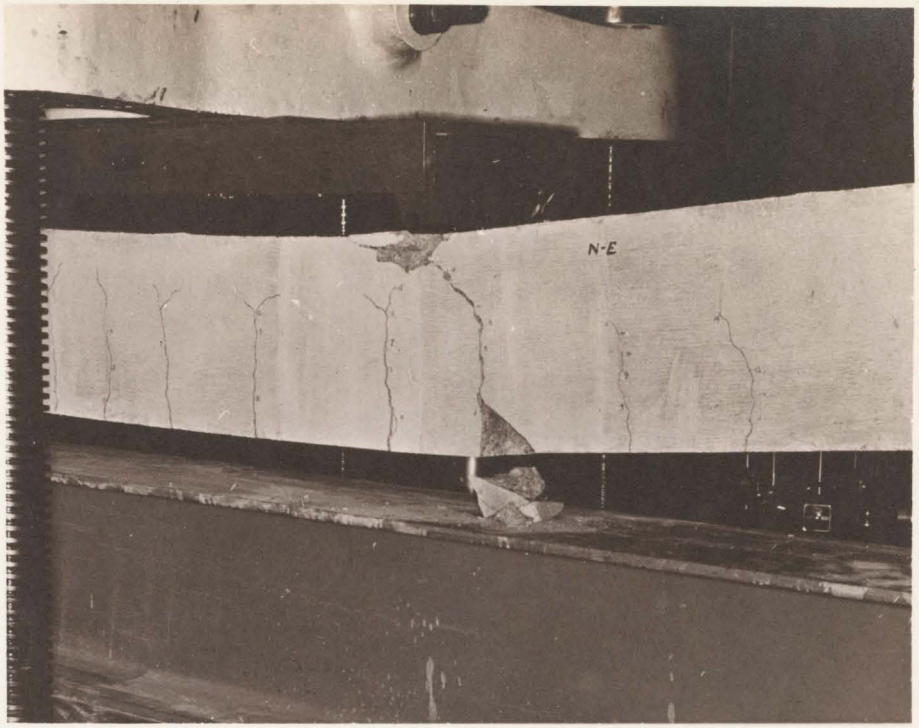

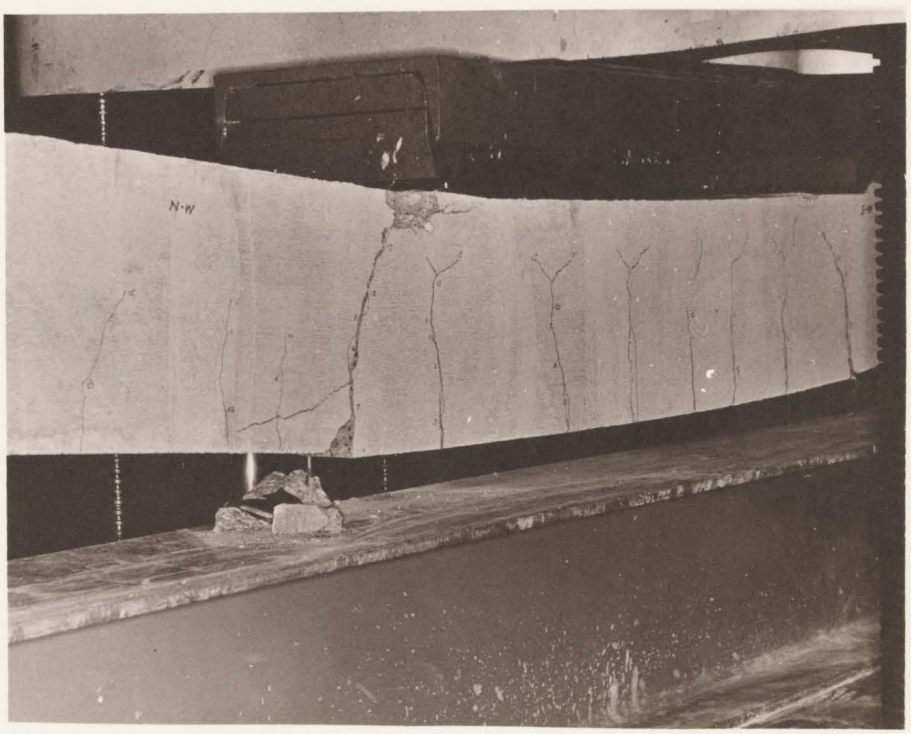

Figure 4.3 Crack Profiles of Beam B1

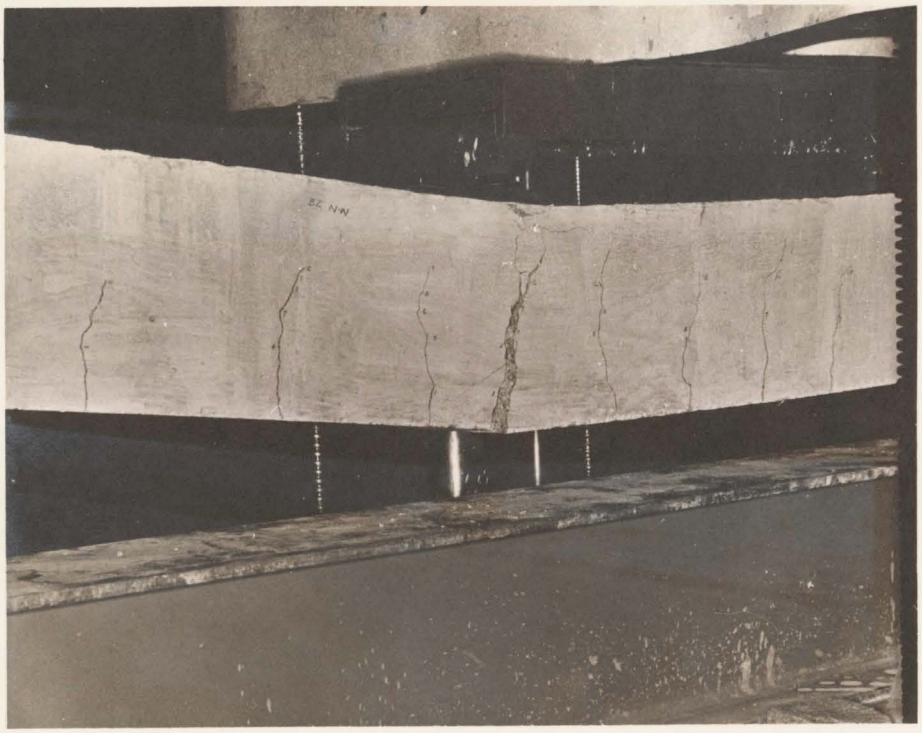

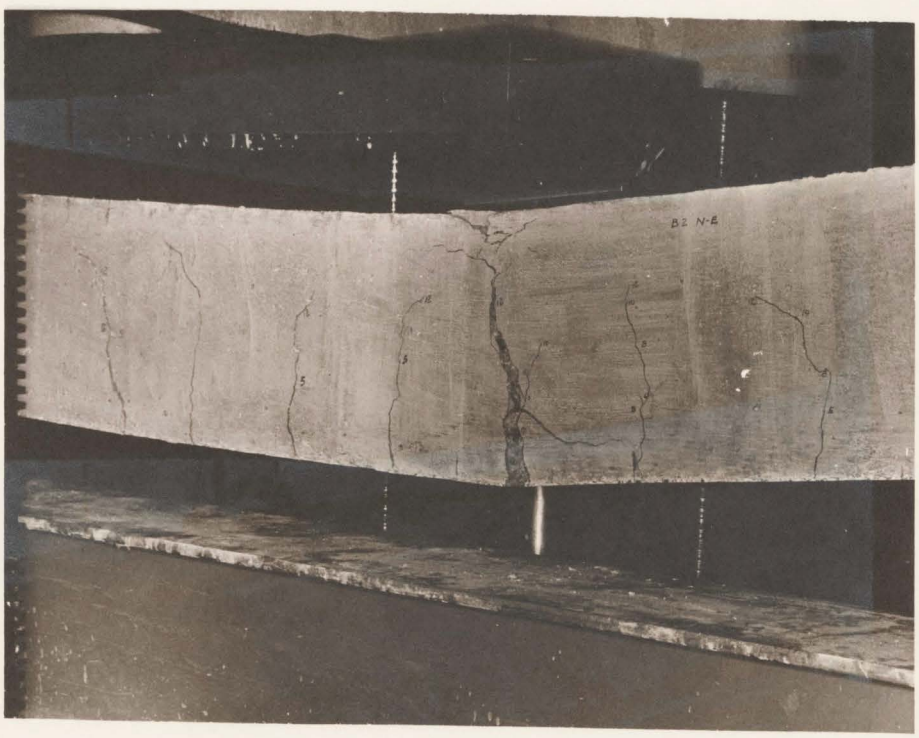

Figure 4.4 Crack Profiles of Beam B2

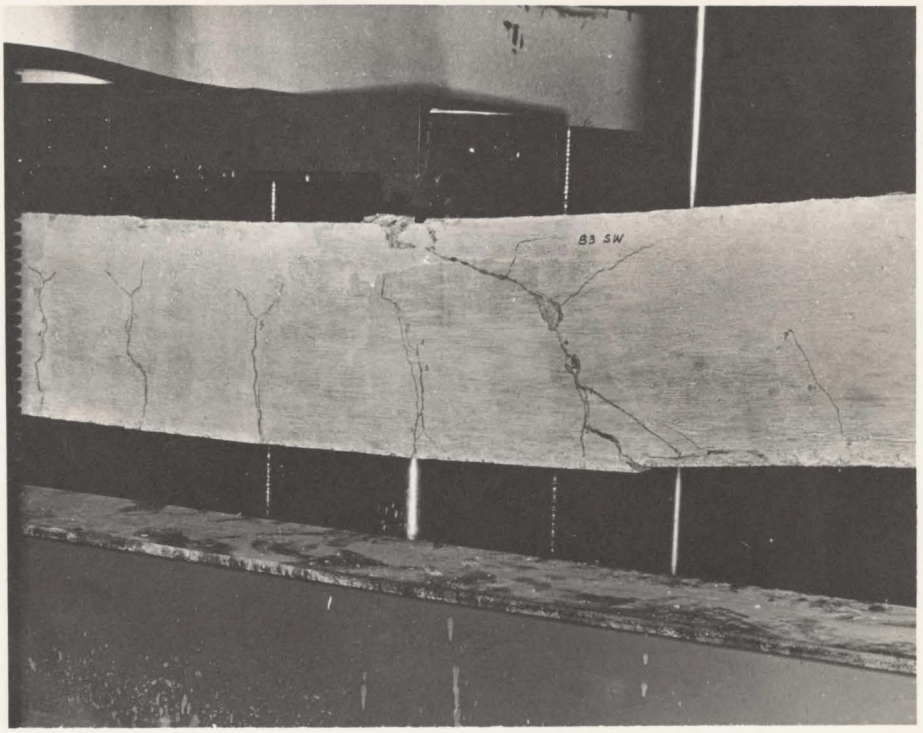

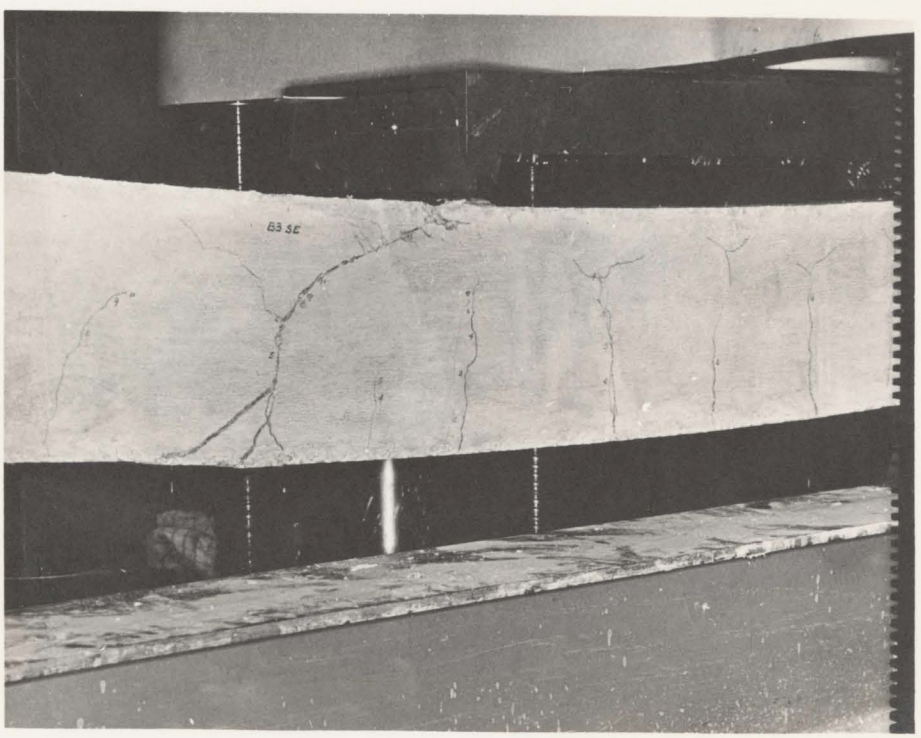

Figure 4.5 Crack Profiles of Beam B3

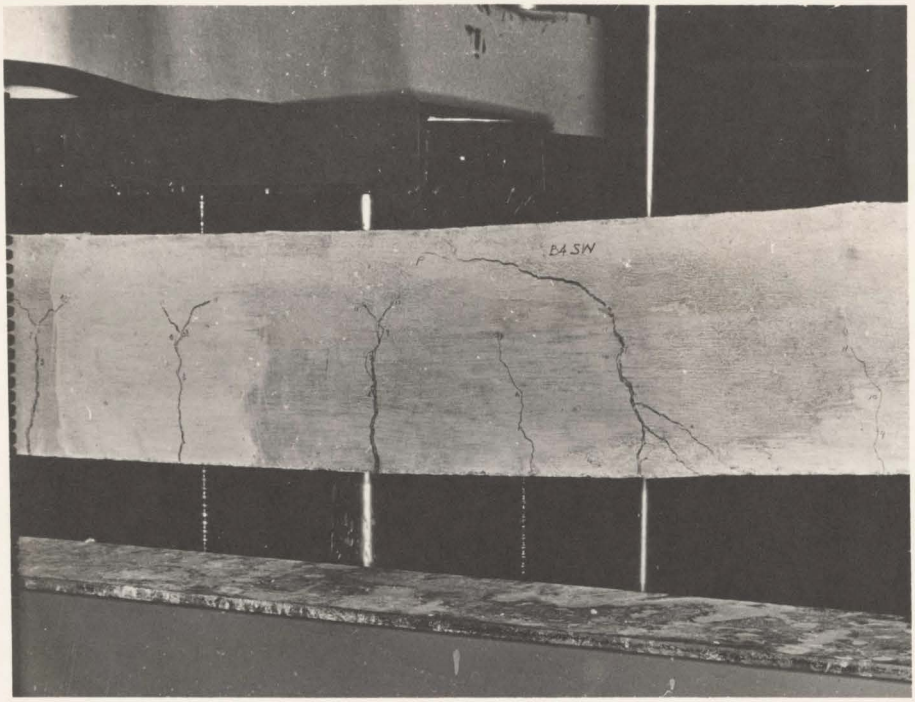

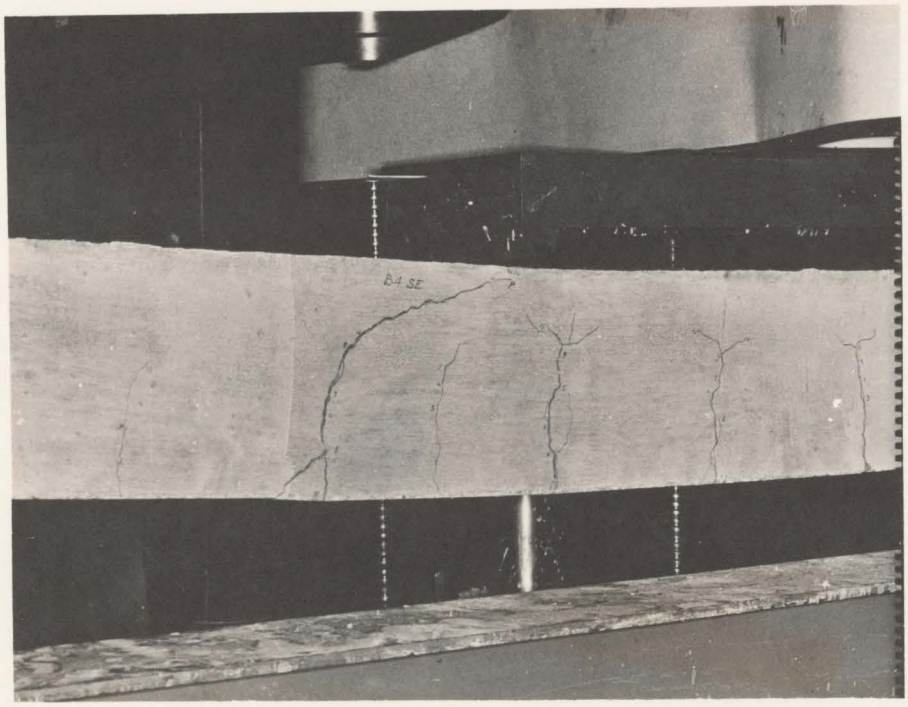

Figure 4.6 Crack Profiles of Beam B4

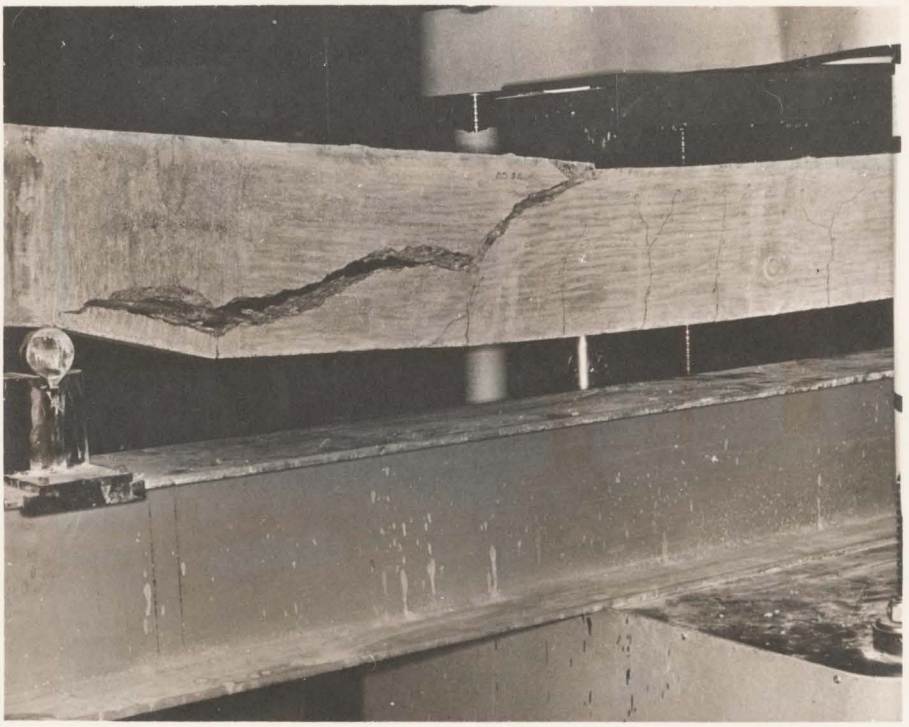

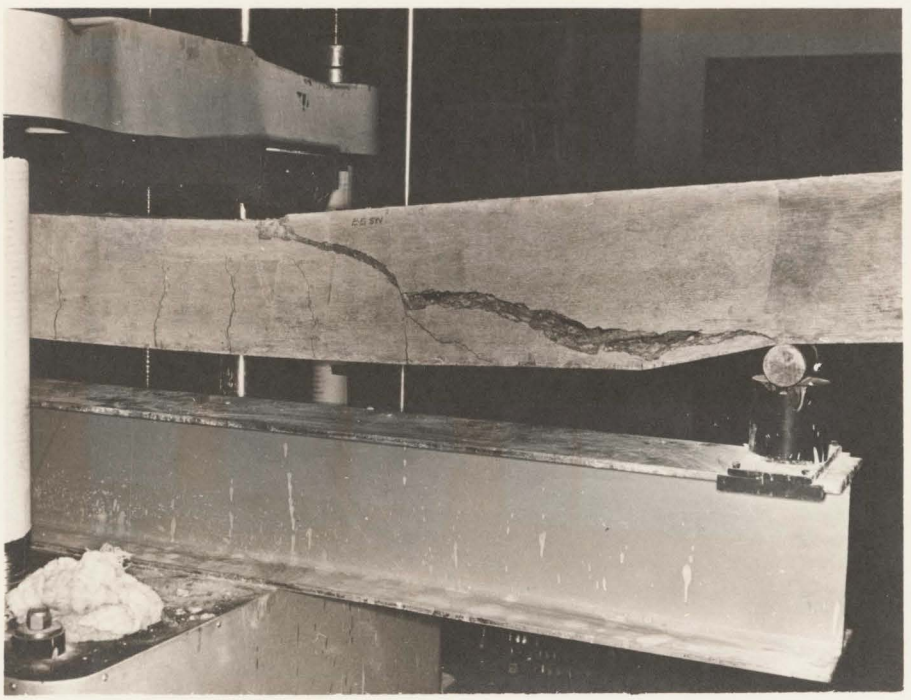

Figure 4.7 Crack Profiles of Beam B5

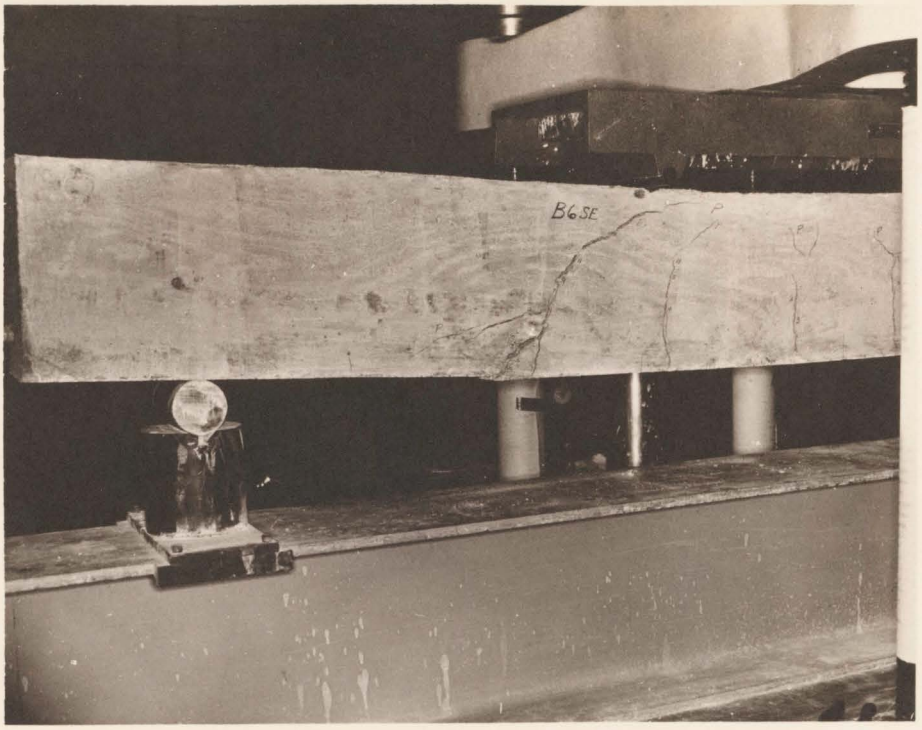

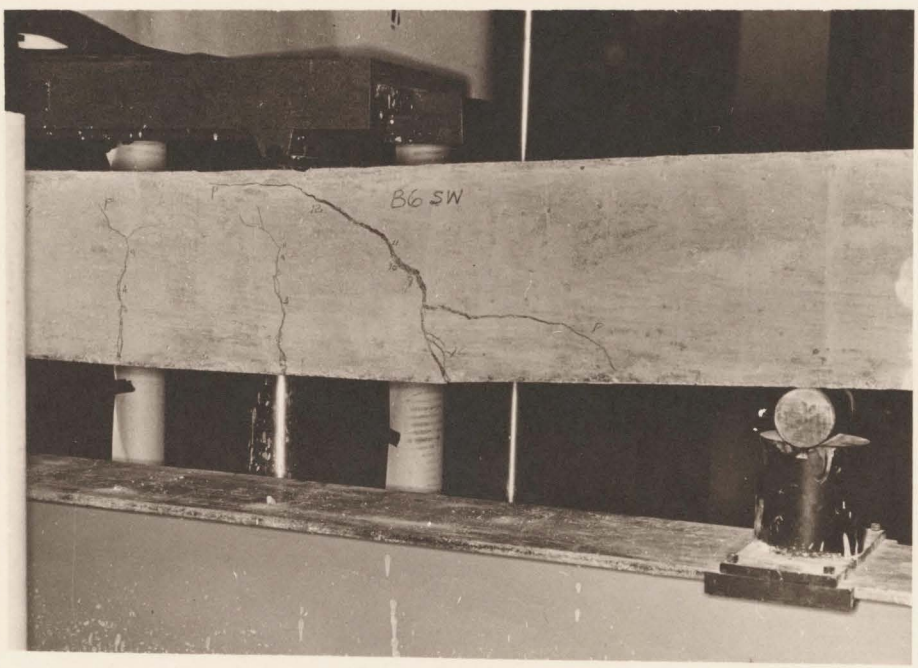

Figure 4.8 Crack Profiles of Beam B6

The steps in the development of the flexural cracks and diagonal cracks which led to the final failure of the beams are shown schematically in figure (4-9).

Summary of test results are given in Table (4-1).

4.6 Discussion

Both beams B1 and B2, reinforced with plain bars failed in bending. As observed in figures (4-3) and (4-4), it is noticed that a very small inclined crack occurred at the existing flexural crack. It has been suggested[4,8] that such a diagonal crack rarely becomes critical until further load is applied, causing it to propagate back towards the steel. A true moment failure may occur without the premature diagonal crack starting to form. In other words, owing to the local effect of a load applied on top of a beam, it is likely that the propagation of the crack under the load point reduced the remaining compression area. This effect may be further illustrated by considering the reinforced concrete beam as a composite beam with incomplete interaction. When a beam reinforced with a plain bar is subjected to a high loading, the largest crack length and crack width occurs close to or under the load point, resulting from the reduced bond brought on by breakdown of interaction. This crack propagates rapidly upwards into the compression zone. The stress in the remaining uncracked zone eventually reaches the compressive strength of concrete and brings about the flexural failure of the beam.

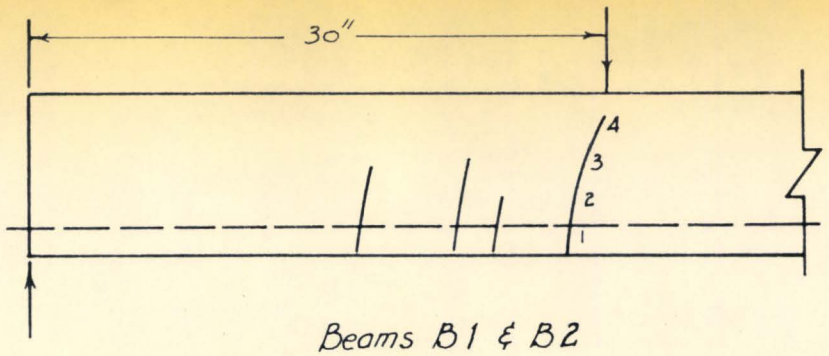

Beams B1 & B2

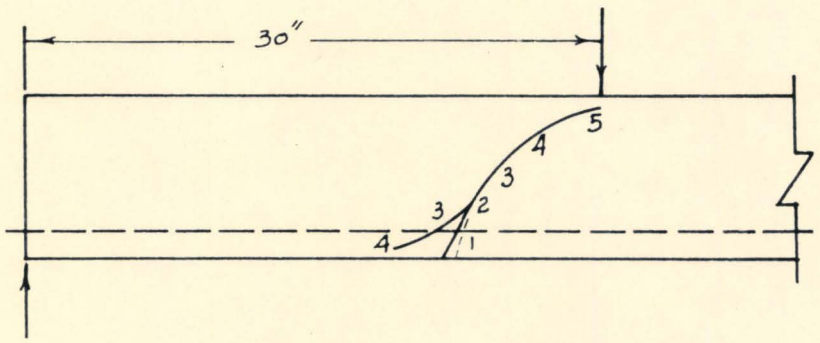

Beams B3 & B4

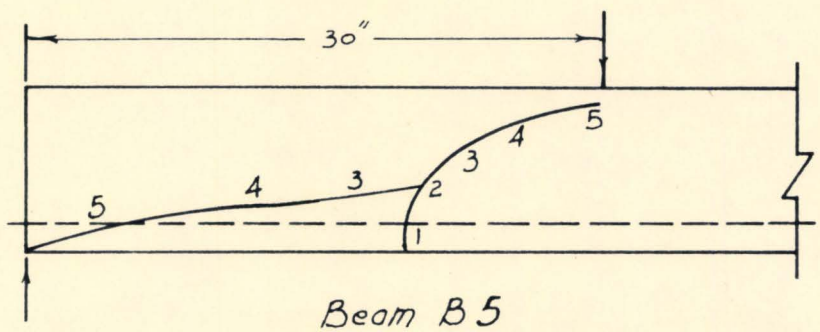

Beam B5

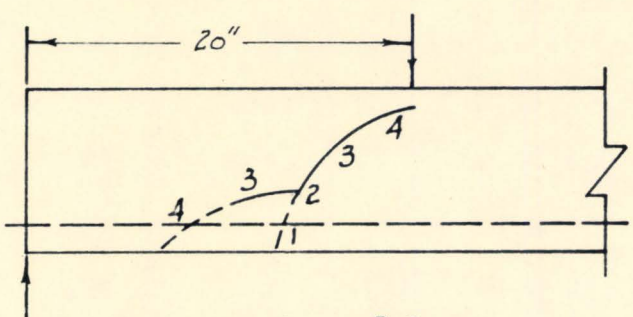

Beam B6

Figure 4.9 Schematic Representation of the Development of Cracks in Test Beams

Table 4-1

Summary of Test Results

Beam No.	a/d	Design Load (lb)	Maximum Capacity (lb)	Reinforcement	M Design (in-lb)	M measured at failure (in-lb)	Load at which 1st crack occurred in shear span	Load at which crack began to incline	Ultimate failure
B1	4.3	2575	8640	5/8" diameter plain bar	38625	129,600	3000	——	Flexural
B2	4.3	2575	8540	5/8" diameter plain bar	38625	128,100	3000	——	Flexural
B3	4.3	2575	9040	5/8" d. plain bar + 5 washers	38625	135,600	3000	5500	Diagonal
B4	4.3	2575	9100	5/8" dia. plain bar + 5 washers	38625	136,500	3250	6000	Diagonal
B5	4.3	2575	9640	5/8" diameter galvanized bar	38625	144,600	3000	6500	Diagonal (Anchorage)
B6	2.9	3680	13240	5/8" diameter galvanized bar	36800	132400	4000	7000	Diagonal

In the comparison of the crack profiles of beams B1 and B2, there is no noticeable difference observed.

Both beams B3 and B4 showed a diagonal failure. The flexural crack lengths and widths under the load points were comparatively smaller than those observed in beam B1 and B2, owing to the presence of the welded washers. These washers did produce a resistance to slip in the reinforcement (or the relative movement of the concrete and the steel). This in turn indicated that there was a better bond quality along the reinforcement, resulting in the diagonal failure of the member.

It is believed that, for beams reinforced with deformed bars, an initial diagonal crack forms somewhere near the mid-depth of a section in the shear span. This diagonal crack proceeds upward into the compression zone with a slight inclination and backward in the tension zone. Under increasing load, it extends further into the compression zone and flattens towards the applied load. At the same instant, owing to the increased bar tension and increased bond, this diagonal crack propagates downward into the zone around the steel. Finally, a sudden failure by the extension of the crack close to the load point and the splitting of concrete because of bond causes the mature diagonal failure of the member. Figure (4-10) shows the diagonal failure of beams reinforced with deformed bars reported by Leonhardt and Walther[8].

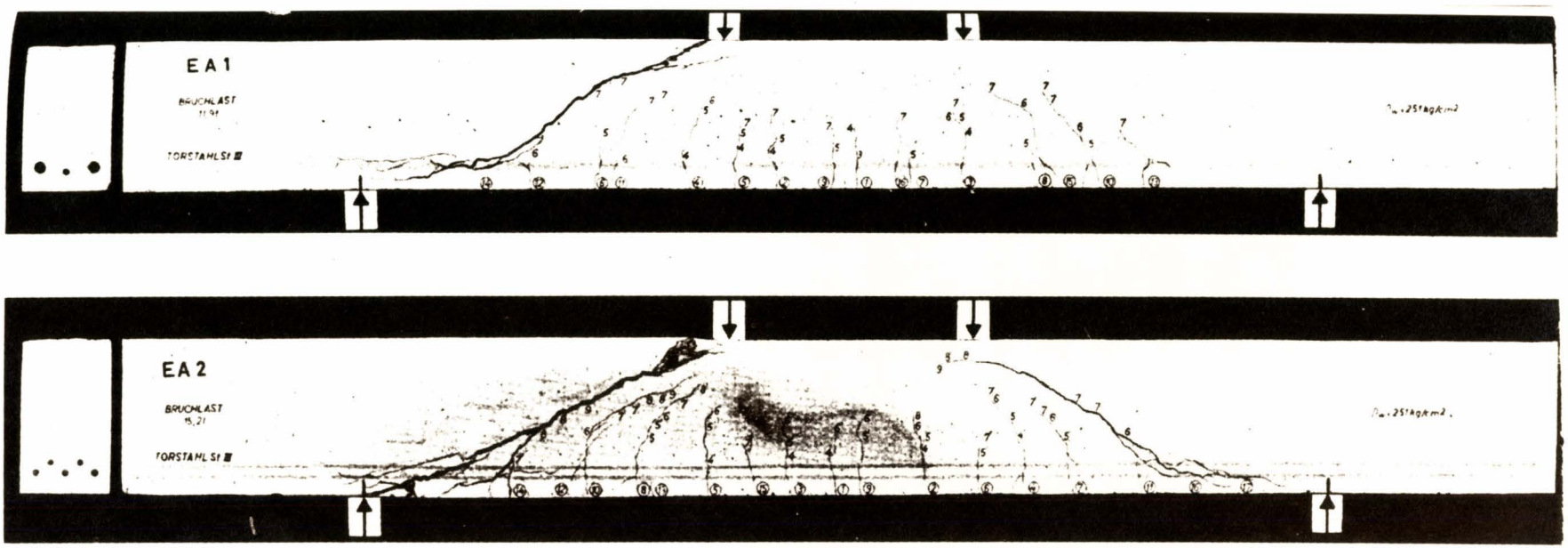

Figure 4.10
Crack Profiles of Beams with Deformed Bars, due to Leonhardt and Walther

The diagonal crack pattern observed in figures (4-5) and (4-6) differ from most of the tested beams performed by other investigators. It is thought that the behaviour and effect of different bond quality in the tensile reinforcement account for the major difference. Up to the present time, deformed bars are used by investigators in order to achieve a better adhesion between steel and concrete (or a better bond), resulting in the general diagonal crack pattern so often observed in test beams. However, it is thought that the upset perimeter of these deformed bars merely serves as a mechanical resistance to slip. In beams reinforced with plain bars and welded washers, the slip would be reduced considerably under the load point. These washers were large in size. If smaller washers were used and they were evenly distributed along the steel, it would behave in a similar manner as the upset bar which provides a mechanical slip resistance.

In the comparison of figures (4-5) and (4-6), it is noticed that the spacing of washers in the shear spans did not appear to affect the crack profile very much. It is thought that once the slip had been reduced by the washers under the load points, the washers inside the shear spans would serve as anchors. These washers were rather large and their distribution in the shear spans would be ineffective.

By comparing beams B1 and B2 with B5 and B6, it is noted that beams reinforced with galvanized steel did produce a better adhesion between steel and concrete, resulting in the diagonal failure of the

members. The final shear failure of beams resulting from the better adhesion between steel and concrete (or better bond) could be further observed in other tested beams[8] as shown in figure (4-11). EB1 was reported to have failed in bending while EB2 failed in shear. The maximum carrying capacity of EB1 was about 15 percent higher than EB2. It is suggested[8] that some adhesion between steel and concrete had developed which led to the final shear failure of the member. If this adhesion had been completely avoided, then failure under bending would surely have occurred.

In the comparison of beams B5 and B6 tested with different "shear arm ratio", the moment carrying capacity of beam B5 (a/d = 4.3) is about 9 percent higher than beam B6 (a/d = 2.9). This shows qualitative agreement with the test results obtained by other research workers[7].

4.7 Summary

The significant observations of the tested beams are summarized below:

1. For beams reinforced with plain bars, less adhesion occurred between concrete and steel (or poor bond), resulting in the final flexural failure of the members.
2. Steel washers welded along the reinforcement reduced the major slip occurrence; especially under the load point. These washers

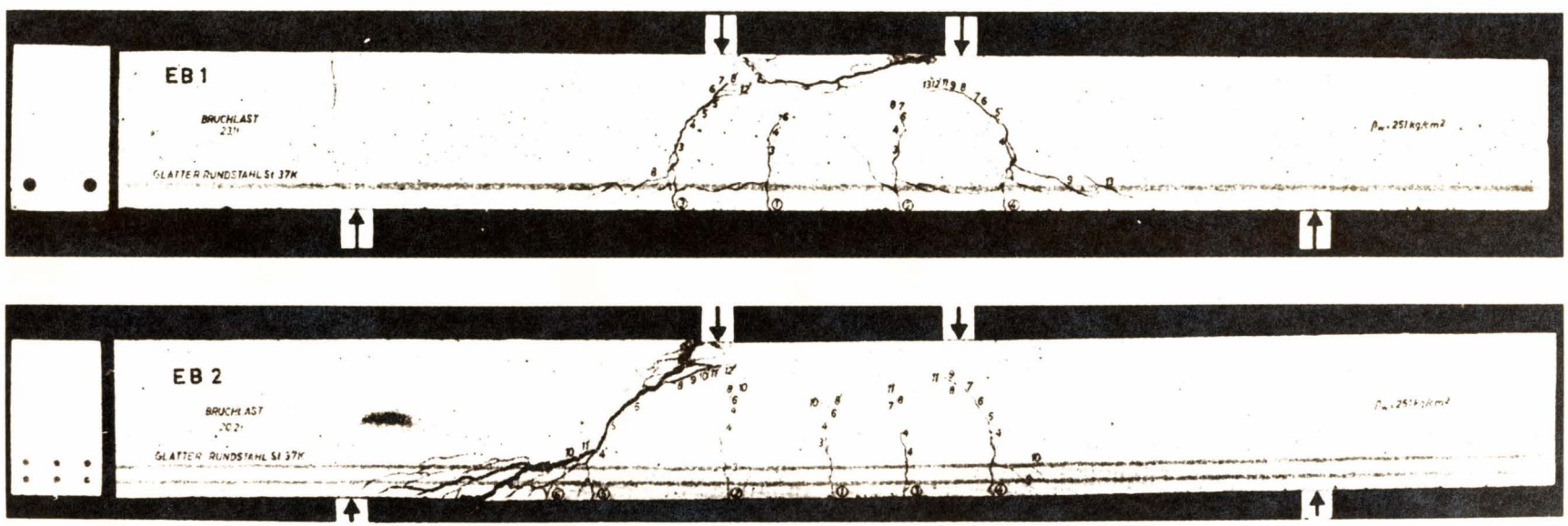

Figure 4.11

Crack Profiles of Beams with Plain Bars, Due to Leonhardt and Walther

insured better bond quality between the steel and the concrete, and led to the ultimate diagonal failure (or the so-called shear failure) of the members at a higher cracking load.

3. With galvanized steel, protection from corrosion afforded by the coating produces better adhesion between steel and concrete (or a better bond) than the plain bars. Diagonal failure occurred, in these beams reinforced with steel of better bond quality, at a higher load.

CHAPTER 5

Summary and Suggestions for Future Studies

The failure mechanism of a reinforced concrete beam has been studied both analytically and experimentally. The analysis was made on the basis of complete and incomplete interaction between the composite elements, the concrete and the steel.

Consideration of the strain trajectories did not appear to give much insight into the problem of the diagonal crack, the investigation was then extended to the study of the principal tensile strains, resulting from strain redistributions in the remaining uncracked zone. It is the author's opinion that the principal tensile strains alone do not provide a rational explanation of the diagonal cracking behaviour.

In the comparison of the potential crack profile with the visible crack profile, a probable range of visible concrete cracking strain has been suggested. This cracking strain will provide a visible crack profile similar to that observed in test beams. Furthermore, it was reasoned that micro cracks are likely to occur between two major cracks, resulting from the effect of breakdown of interaction.

On the basis of the experimental load-slip characteristics, the degree of interaction along the length of the beam from supports to load points was investigated. It has been found that the interaction

coefficient is likely to vary in a curvilinear manner. The degree of breakdown of interaction at any section depends upon the load slip characteristic of the reinforcement.

The bond quality which is thought to affect the failure mechanism of reinforced concrete beams was further demonstrated by tests on beam specimens with different types of reinforcement.

The diagonal failure mechanism of a reinforced concrete beam is dependent upon a number of parameters. Further experimental works are needed to investigate the problem in this respect. The writer wishes to make the following suggestions:

1. Obtain experimentally the slip distribution along the beam. The slip magnitude at any visible crack section should be measured.

2. The localized breakdown of interaction effect close to the load point could be further demonstrated by using thinner and smaller washers welded along the reinforcement, and by varying the distribution of these washers.

CHAPTER 6

Conclusions

The conclusions from this study are as follows:

1. The estimated shear stress resultant carried by the remaining uncracked concrete in the case of high degree of breakdown of interaction is very small.
2. The study of the strain trajectories, the principal strain magnitudes and their directions in the remaining uncracked zone does not appear to give much insight into the nature of the development of the diagonal crack.
3. The estimated steel strain and slip distribution between two cracks show qualitative agreement with those measured by other experimenters. Assuming that loss of interaction occurs, it is reasoned that micro cracks must occur between two major cracks.
4. Consideration of a reinforced concrete beam as a composite beam with incomplete interaction, the reduced bond brought on by breakdown of interaction close to the load point causes the crack to extend rapidly into the compression zone.
5. Tests on reinforced concrete beams showed that diagonal cracks occurred in beams reinforced with steel of better bond quality than that of uncoated plain bars.

APPENDIX 1

List of Symbols

a	Distant from the support to the applied load.
A_c	Effective cross-sectional area of the concrete
A_s	Cross-sectional area of the steel
b	Width of the concrete beam
C	Interaction coefficient
d	Effective depth of the reinforced concrete beam
E_c, E_s	Moduli of Elasticity of concrete and steel respectively
$\frac{1}{\overline{EA}}$	$\frac{1}{E_c A_c} + \frac{1}{E_s A_c}$
ΣEI	$E_c I_c + E_s I_s$
$\overline{EI}$	$\Sigma EI + \overline{EA}\, Z^2$
F, F'	Horizontal direct forces acting at the centroids of the concrete and the steel
I_c, I_s	Second moments of area of concrete and steel respectively
k	Modulus of the shear connection (in. lb/in.)
L	Span length of the beam
M_t	External moment applied to the beam
q, q'	Horizontal shear per unit length
Q	Load on connection
Q_s	Force in the bar
s	Spacing of discrete connection
Sc	$\frac{Yc}{\Sigma EI}$

v	Unit shear stress
V	Vertical shear
Yc	Vertical distance from the centroidal axis of the concrete
Z	Distance between the centroidal axes of the concrete cross-section and the steel
ε_c	Strain of the concrete
ε_p	The tensile cracking strain of concrete
τ_1, τ_2	Maximum and minimum principal stresses respectively
σ_x	Bending stress
τ_{xy}	Shearing stress
γ	Slip between the concrete and the steel

APPENDIX 2

Sample Calculations of the iteration process for the determination of 1/c from the load-slip characteristics

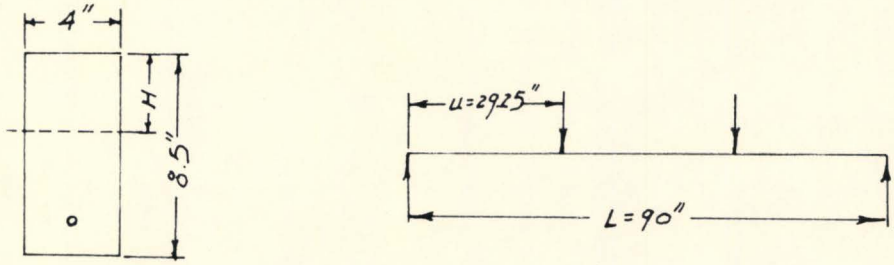

For a cracked section at the location under the load point

First iteration (Complete interaction)

$H = 3.28$ in.

$Z = 5.36$ in.

$A_c = 4 \times H = 13.12$ in.^{2}

$E_s = 30 \times 10^6$ psi

$E_c = 3.5 \times 10^6$ psi

$A_s = 0.31$ in.^{2}

$M_t = 36200$ in-lb

$V = 1237.6$ lb.

$$\frac{1}{\overline{EA}} = \frac{1}{E_s A_s} + \frac{1}{E_c A_c}$$

$$= \frac{1}{30 \times 10^6 \times .31} + \frac{1}{3.5 \times 10^6 \times 13.12}$$

$$= 0.126 \times 10^{-6}$$

$$\overline{EA} = 7.93 \times 10^6$$

$$\Sigma EI = E_c I_c + E_s I_s = E_c I_c = 3.5 \times 10^6 \times \frac{4(3.28)^3}{12} = 41.2 \times 10^6$$

$$\overline{EI} = \Sigma EI + \overline{EA} \cdot Z^2 = 41.2 \times 10^6 + 7.93 \times 10^6 \times 5.36^2 = 268.2 \times 10^6$$

$$F' = \frac{\overline{EA}}{\overline{EI}} Z M_t = \frac{7.93 \times 10^6}{268.2 \times 10^6} \times 5.36 \times 36200 = 5703$$

$$q' = \frac{\overline{EA}}{\overline{EI}} Z V = \frac{7.93 \times 10^6}{268.2 \times 10^6} \times 5.36 \times 1237.6 = 195.8$$

2nd Iteration

With the value of F' from the 1st iteration, a corresponding value of slip (γ) is obtained from the load-slip curve.

$$k = \frac{q's}{\gamma} = \frac{195.8}{.00073} = 267000$$

$$c = \frac{\overline{EA} \cdot \Sigma EI \cdot \pi^2}{k \cdot L^2 \cdot \overline{EI}}$$

$$= \frac{7.93 \times 10^6 \times 41.2 \times 10^6 \times 3.1416^2}{267000 \times 90^2 \times 268.2 \times 10^6}$$

$$= .00565$$

$$F = V\frac{\overline{EA}}{\overline{EI}} ZL \left[\frac{x}{L} - \frac{\sqrt{c}}{\pi} \frac{\cosh \frac{\pi}{\sqrt{c}} \left(\frac{1}{2} - \frac{u}{L}\right)}{\cosh \left(\frac{\pi}{\sqrt{c}} \frac{1}{2}\right)} \sinh \frac{x}{L} \frac{\pi}{\sqrt{c}} \right.$$

$$= 1237.6 \frac{7.93 \times 10^6}{268.2 \times 10^6} \times 5.36 \times 90 \left[\frac{29.25}{90} - \frac{\sqrt{.00565}}{3.1416} \right.$$

$$\left. \left. \frac{\cosh \frac{3.1416}{\sqrt{.00565}} (.5-.375)}{\cosh \left(.5 \times \frac{3.1416}{\sqrt{.00565}}\right)} \sinh \left(.375 \times \frac{3.1416}{\sqrt{.00565}}\right) \right] \right]$$

$$= 5560$$

$$q = V\sqrt{\frac{EA}{EI}}\,Z\left[1 - \frac{\cosh\frac{\pi}{\sqrt{c}}\left(\frac{1}{2} - \frac{u}{L}\right)}{\cosh\left(\frac{\pi}{\sqrt{c}}\,\frac{1}{2}\right)}\cosh\left(\frac{\pi}{\sqrt{c}}\,\frac{x}{L}\right)\right]$$

$$= 1237.6 \times \frac{7.93 \times 10^{6}}{268.2 \times 10^{6}} \times 5.36 \times \left[1 - \frac{\cosh\frac{3.1416}{\sqrt{.00565}}\,(.5 - .375)}{\cosh\left(.5 \times \frac{3.1416}{\sqrt{.00565}}\right)}\right.$$

$$\left.\cosh\left(.375 \times \frac{3.1416}{\sqrt{.00565}}\right)\right]$$

$$= 98.41$$

After six iterations, 1/c = 25.8

BIBLIOGRAPHY

1. Robinson, H., Preliminary investigation of a composite beam with ribbed slab formed by cellular steel decking, 1963.

2. Plowman, J.M., "Measurement of stress in Concrete Beam Reinforcement" The Institution of Civil Engineers, June 1963, Proceedings, Vol. 25.

3. ACI-ASCE Committee 326, "Shear and Diagonal Tension" Journal of the ACI, Jan. 1962, Proceedings, V.59, No. 1

4. Ferguson, P.M., "Some Implications of Recent Diagonal Tension Tests", Journal of the ACI, V.28 No. 2, Aug. 1956 Proceedings V.53.

5. ACI-ASCE Committee 326, "Shear and Diagonal Tension", Journal of the ACI, Feb. 1962, Proceedings V.59, No.2

6. Kani, G.N.J., "The Mechanism of So-Called Shear Failure", Tran. Engng. Inst. Canada, April 1963.

7. Kani, G.N.J., "The Riddle of Shear Failure and its Solution", Journal of the ACI, April 1964, Proceedings, V.61, No. 4.

8. Leonhardt, F. and Walther, R., Contribution to the Treatment of Shear in Reinforced Concrete, National Research Council of Canada, Technical Translation 1172, Ottawa, 1965.

9. Robinson, H., "Discussion of Paper Measurement of Stress in Concrete Beam Reinforcement", the Institution of Civil Engineers, Proceedings, July 1964, V.28.

10. Moe, J., "Shear and Diagonal Tension, Discussion of a paper by ACI-ASCE Committee 326" Journal of the ACI, Sept. 1962, Proceedings, V.59, No. 9.

11. Wong, A.C.C., Loss of Bond in the Reinforced Concrete Beam, M. of Eng. Thesis, McMaster University, Oct. 1964.

12. Seiss, C.P., Viest, I.M., Newmark, N.M., Studies of Slab and Beam Highway Bridges, Part III, University of Illinois Engineering experiment Station Bulletin Series No. 396.

13. Manning, J.T., "Discussion of Paper Measurement of Stress in Concrete Beam Reinforcement", The Institution of Civil Engineers, Proceedings, July 1964, V.28.

14. Evans, R.H. and Robinson, G.W., "Bond Stresses in Prestressed Concrete from X-Ray Photographs", The Institution of Civil Engineers, Proceedings Pt. 1, 1955, No. 4.

15. Mathey, R.G. and Watstein, D., "Investigation of Bond in Beam and Pull-out Specimens with High-Yield-Strength Deformed Bars," Journal of the ACI, March 1961, No. 9, V.32, Proceedings V.57.

16. Broms, B.B., "Stress Distribution, Crack Patterns, and Failure Mechanisms of Reinforced Concrete Members", Journal of the A.C.I. Proceedings V.61, No.12 Dec. 1964.

17. Watstein, D. and Mathey, R.G., "Strains in Beams Having Diagonal Cracks", Journal of the A.C.I., V. 30, No.6, Dec. 1958.

18. Acharya, D.N. and Kemp, K.O., "Significance of Dowel Forces on the Shear Failure of Rectangular Reinforced Concrete Beams Without Web Reinforcement", Journal of the A.C.I., V.62, No. 10, Oct. 1965.

19. Ferguson, P.M. and Thompson, J.N., "Development Length for Large High Strength Reinforcing Bars", Journal of the A.C.I., Proceedings V.62, No. 1, Jan. 1965.

20. Frocht, M.M., Photoelasticity, Volume 1, 1960, John Wiley and Sons, Inc., New York.